REPORT NO.
UC SESM 71-10

STRUCTURES AND MATERIALS RESEARCH
DEPARTMENT OF CIVIL ENGINEERING

ANALYTICAL STUDIES OF THE SOUTHERN CROSSING CABLE STAYED GIRDER BRIDGE

VOL. 1 - THEORY AND DETERMINATION OF RESULTS FOR VARIOUS LOAD CONDITIONS

by

FRANK BARON

and

SHEN-YING LIEN

Report to the Sponsors: Division of Bay Toll Crossings, Department of Public Works; State of California

JUNE 1971

STRUCTURAL ENGINEERING LABORATORY
UNIVERSITY OF CALIFORNIA
BERKELEY CALIFORNIA

Structures and Materials Research
Department of Civil Engineering
Division of Structural Engineering
and
Structural Mechanics

UC-SESM Report No. 71-10

ANALYTICAL STUDIES OF THE SOUTHERN CROSSING CABLE STAYED GIRDER BRIDGE

Vol. I - THEORY AND DETERMINATION OF RESULTS FOR VARIOUS LOAD CONDITIONS

by

Frank Baron
Professor of Civil Engineering

and

Shen-Ying Lien
Research Assistant

to

The Division of Bay Toll Crossings
Department of Public Works
State of California
Under Standard Agreement
No. TC-1432

College of Engineering
Office of Research Services
University of California
Berkeley, California

June 1971

TABLE OF CONTENTS

Page

LIST OF TABLES

LIST OF FIGURES
(VOLUME 1)

LIST OF FIGURES
(VOLUME II)

Figure | Page

ACKNOWLEDGMENTS

This investigation was carried out under the terms of State of California Standard Agreement No. TC-1432, between the University of California and the sponsor, the Division of Bay Toll Crossings, State of California.

Close liaison and support from the Division of Bay Toll Crossings, State of California, was provided by Messrs. Charles Seim, Assistant Design Engineer; Stanford Larsen, Senior Bridge Engineer; and Arthur Dang, Associate Bridge Engineer. Their assistance is gratefully acknowledged. The assistance of Mr. John Kozak, Deputy Chief Engineer of the Division of Bay Toll Crossings, during various stages of the investigation also is gratefully acknowledged.

The senior writer served as the faculty investigator for the University of California. The junior writer participated in every phase of this investigation as Research Assistant, and in pursuit of a suitable dissertation topic for the degree of Doctor of Philosophy. Acknowledgments are given to several graduate students (Messrs. Arain, U. R., Chopelin, P., Franklin, C. M., Galdi, P. J., Ghosh, S., Habibullah, A., and Mazumder, T. L.) who assisted the writers in the different aspects of this study.

Grateful acknowledgments also are given to the University of California for its support of graduate research, and specifically to the Computer Center University of California, Berkeley, for the use of the CDC-6400 digital computer in performing the numerical calculations reported herein.

1. PURPOSES AND SCOPE

A comprehensive investigation of the behavior of the Southern Crossing Bridge is planned. The purposes of the investigation are to provide an independent check of the calculations made by the designers, and to inspect matters that are ordinarily not considered in design. The investigation is necessary because of the innovations which are being considered by the Division of Bay Toll Crossings (the designers) in bridge type, design, and erection sequence.

The bridge type being considered is a cable stayed girder. The latter type has been used in Europe and elsewhere, but as yet has not been introduced in the United States. The central span length of the Southern Crossing Bridge is greater than that of any cable stayed girder constructed elsewhere. The articulation of the roadway, cables, and towers of the Southern Crossing differs appreciably from that of any other bridge. Further, the requirement of maintaining at all times a 1,200 foot navigable waterway in the main channel of San Francisco Bay imposes certain restrictions on the erection sequence to be selected by the designers and constructors of the bridge. Also, the conditions of traffic, wind, soils, and seismic disturbances are unique to the site, and need be taken into account in the design of the Southern Crossing Bridge.

The entire investigation is to include studies of the linear and nonlinear behavior of the cable stayed girder bridge subjected to static and dynamic conditions of load. Aerodynamic and seismic effects are to be considered. For budgetary reasons, this report deals only with the linear and nonlinear behavior of the bridge subjected to static

loads. The structural behavior is three dimensional although for convenience it is called the planar behavior of the bridge. This is because the loads considered herein are symmetrical with respect to the central longitudinal axis of the bridge. It is assumed that plane right-sections of the roadway girder before loading remain plane and right after loading. The linear displacements of the roadway girder are in a vertical plane and the angular displacements are about axes normal to the plane. The effects of localized distributions of stress, localized buckling, shear lag, and other three dimensional aspects of the roadway girder are not included in this study. The orientations of the cables and towers in three dimensional space, however, are taken into account. For all members, the properties of materials are assumed to be linear; that is, Hooke's Law is assumed.

A brief description of the Southern Crossing and the cable stayed girder bridge is given in the report. An analytical model of the bridge is described for determining the linear and nonlinear behavior of the bridge. A linear theory and a nonlinear theory are presented for determining the effects of various load conditions on the bridge. The linear theory is employed in determining influence lines for various parameters of the bridge, and in determining the maximum effects caused by specified live loads, temperature changes, and differential movements. The influence lines are based on the direct application of Muller-Breslau's principle to structures composed of finite elastic elements. The linear theory also is employed for obtaining the effects of ten selected cases of live load distributions. The latter distributions are of interest in assessing the overall safety and behavior of the bridge. Special attention is given to the distributions of forces and moments

in the towers for various load conditions. Included are those conditions associated with a tower immediately after the tower is erected, and after the tower is subjected to the full dead load of the bridge.

The nonlinear theory is general and was developed by the writers for other structures besides cable stayed girder bridges. Among the former group of structures are suspension bridges, pipe lines, guyed towers, reticulated domes, cable nets, suspended roofs, and high-rise buildings. The theory is employed herein for determining (1) the camber of the girder and the dimensions of each unstressed segment of the Southern Crossing Bridge, (2) the displacements, forces, and moments at each section of the bridge for various stages of erection, and (3) the influences of possible overloads of vehicular traffic on the nonlinear response of the bridge. The dimensions of the unstressed segments of the bridge are required for fabrication and to determine camber. The camber is required to insure that all conditions at dead load, prescribed by the designers, are obtained after erection. The other studies of nonlinear behavior are needed to determine possible modes of failure during and after erection. The latter studies are related to the selection of suitable factors of safety, and load factors, in the design of the bridge.

For use in the nonlinear theory, nonlinear force-deformation relations and tangent stiffnesses are presented for the kinds of members encountered in the analytical model. The kinds of members are (1) axial-flexural members which lie in two or three dimensional space, and (2) cables composed of straight or catenary segments. For the axial-flexural members, the influences of eccentricities are taken into account in both the linear and nonlinear theories.

The quantitative results reported in this study are obtained by means of special and general purpose computer programs. The programs were developed by the writers.

The text and the theory employed in determining the results for the various load conditions on the bridge are given in Volume 1 of this report. Quantitative results are summarized in Volumes 1 and 2. The Figures of Volume 1 are restricted to those needed to illustrate the text. The Figures of Volume 2 are restricted to summaries of results which pertain to the bridge.

2. DESCRIPTION OF THE SOUTHERN CROSSING BAY BRIDGE

A detailed description of the Southern Crossing Bay Bridge is given in the design drawings of the Division of Bay Toll Crossings, State of California and in Refs. 10 and 11. A brief description of the bridge is given herein for convenience and for understanding of this report.

The Southern Crossing will bridge the lower arm of San Francisco Bay and link the southern peninsula of the Bay region to Alameda, Oakland, and San Leandro on the eastern shore (see Figure 2.1). From the southern peninsula near Hunters Point, the approach leads into an eight lane, four and one-half mile main bay crossing of which two and one-half miles is a series of high level structures. Near the eastern shore the roadway splits into two six-lane approaches. One approach heads north through Alameda to join the Oakland freeway system, and the other heads south through Bay Farm Island to link with the freeway system in San Leandro.

About one and one-half miles east of the San Francisco shoreline, a high level structure is to cross the main shipping channel. Navigation requirements dictated clearances of 1200 feet horizontally and 220 feet vertically above MHHW. The latter requirement limited the number of structural types that could be considered by the designers as possible choices for the main span. Extensive studies were made by the Division of Bay Toll Crossings of several types of bridges that are practical for this span length. Among the types studied are the tied-arch, suspension, cantilever truss, and cable-stayed girder. Based on these studies and architectural considerations, a cable-stayed girder bridge, with the girder continuous for three spans, was selected for the location.

The cable-stayed girder bridge is the subject of this investigation. Actually, an intermediate selection made by the Division of Bay Toll Crossings of the final dimensions and make-up of the bridge is considered in this report. For reference only, a brief description is given of the various changes that were made in design during the investigation. In the beginning, a six-lane bridge supported by two end-bents and two towers of concrete was considered by the designers and the writers. Calculations of the six-lane bridge ceased when the Division of Bay Toll Crossings widened the bridge to eight lanes with the bents and towers remaining of concrete. The calculations reported herein are for the latter design, as agreed upon by the designers and writers. Modifications which occurred in design of the latter structure are incorporated in the report. Subsequently, a final design was made by the Division in which the bridge was widened an additional ten feet with the accompanying towers designed of steel.

The overall dimensions of the cable-stayed girder bridge are given in Figure 2.2. The roadway girder has a constant depth of 18 feet, an out-to-out width of 107 feet, and a length of 2305 feet. It is continuous for its entire length and is supported at two end-bents (or anchorage piers), two towers, and eight cable anchorage points along each side of the roadway. At each end-bent, the girder is held down against uplift from the cables by a pair of tie-down assemblies that allow for temperature movement. The tie-down assemblies are axial members with pins at their ends. At the east tower (Tower 2), the girder is supported by a pair of pinned bearings, and at the west tower (Tower 1) by a pair of rocker and buffer systems. The buffers yield under slow temperature movement but act as pinned bearings under wind and seismic loads.

The roadway girder is composed of twin trapezoidal box girders which are interconnected at their tops by an orthotropic steel deck. See Figure 2.3 for the make-up of two typical cross-sections of the roadway girder. The steel deck of the girder is stiffened in the longitudinal direction by closed trapezoidal ribs, and in the transverse direction by 42 inch depth beams spaced longitudinally at 20 feet on centers. In the longitudinal direction, the webs of the trapezoidal box girders are stiffened by plate stiffeners and the lower flanges are stiffened by trapezoidal ribs. Transversely both the webs and bottom flanges are stiffened at 20 foot centers by cross frames that coincide with the floor beams to form diaphragms. At each cable anchorage along the roadway, the trapezoidal box girders are interconnected by rectangular transverse anchorage beams. The latter beams are 18 feet in depth and house the cable anchorages at their ends. The orthotropic deck serves as the top flange of the roadway girder, and also as the top flange of the transverse anchorage beams.

The steel deck is paved with a two-inch skid resistant smooth riding wearing surface. A central median barrier divides the deck into two four-lane roadways, each roadway sloping transversely downward from the barrier at a slope of 1-1/2 percent. The longitudinal profile of the roadway lies along a parabola which goes through a specified work-point and is tangent to a specified grade line at each end of the girder (see the design drawings). For purposes of fabrication and erection, the girder is segmented into 80 segments along its length. Each segment has a constant cross-section and constant properties along its length. The lengths, cross-sectional areas, weights per foot, centroidal distances from the top of the roadway, and moments of

inertias of the different segments along the roadway are given in the design drawings. In this study, the number, lengths, and properties of the segments are the same as those selected by the designers. It need be mentioned that changes in the latter and in other properties of the bridge continued to occur as the design proceeded. The same changes in computer input data were made by the writers as the investigation proceeded.

For the highly stressed areas of the girders, the designers selected structural steel of ASTM-A588 designation for plates thicker than 3/4 inches and of ASTM-A441 designation for plates 3/4 inch and under. They selected structural carbon steel of ASTM-A36 designation for the remainder of the structure.

The overall dimensions of the tower are given in Figure 2.4 and typical section views in Figure 2.5. Each tower is composed of two single cell legs, a top strut and an intermediate strut to which the roadway bearings are attached. Two pairs of saddles, each pair symmetrical about the longitudinal center-line of the tower, are anchored to the top strut. The cables pass continuously over these saddles and are firmly clamped to the saddles. In the longitudinal elevation, the legs are straight and taper from an outside width of 25 feet at the base to 12.5 feet at the top. In the transverse elevation, the towers are termed diamond shaped. In this elevation, the two legs of a tower splay outward from an out-to-out width of 79.33 feet at the base to an out-to-out width of 150 feet at the roadway level. From the roadway level, the two legs are inclined toward the center-line of the tower to an out-to-out width of 38 feet at the top of the tower. Each leg is composed of two straight segments, with the segments being tapered and the thicknesses of the outside walls decreasing from the bottom to the top. The

legs are stiffened with horizontal diaphrams and are reinforced with longitudinal and horizontal steel. The longitudinal steel is distributed between the inside and outside faces of the legs, with a greater proportion being distributed to the outside faces. The selected shape of each tower was based on architectural considerations, and the designers' objectives to gather the cables closely together at the top and to minimize the cost of foundations. The latter objective is bounded by stability requirements of the bridge for lateral loads.

For the concrete of the towers, the designers specify a strength of 3250 pounds per square inch at the end of 28 days. They specify ASTM-A15 designation for the longitudinal reinforcing steel.

The cables are arranged in a pattern commonly called "RADIATING" (see Figure 2.2). From the top of each tower, four pairs of cables (each pair symmetrical about the longitudinal center-line of the bridge) radiate to the respective anchorages at the sides of the roadway. As described elsewhere, the cables pass continuously over the saddles at the top of a tower and are firmly clamped to the saddles. At a girder anchorage, the strands of a cable splay out from a splay saddle and pass through bushings arranged in a hexagonal pattern on a splay frame (See the design drawings). The splay frame forms the entrance to the cable anchorage housing at the end of the anchorage beam. The strands terminate at the cable anchorage frame in tensile type sockets.

Each cable consists of 19 structural strands of ASTM-A586 steel with Class "A" galvanized coatings on the interior wires and Class "C" coatings on the exterior wires. The strands are prestressed to produce a minimum modulus of elasticity of 22,000,000 psi. The long

cables (see Figure 2.2) are made up of 3-1/8 inch diameter strands and the short cables are made up of 2-1/4 inch diameter strands. A summary of the cable properties is given in Table 2.1.

TABLE 2.1 : PROPERTIES OF CABLES

CABLES	AREA (FT. ^{2})	YOUNG'S MODULUS, E (10^7 KIPS/FT ^{2})	WEIGHT (With Wrapping) (KIPS/FT.)
A, D, E, H (LONG)	0.65400	0.31680	0.34510
B, C, F, G (SHORT)	0.40100	0.33120	0.21410

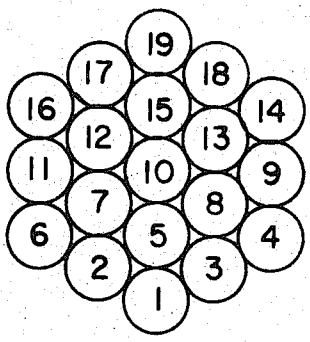

CABLE SECTION

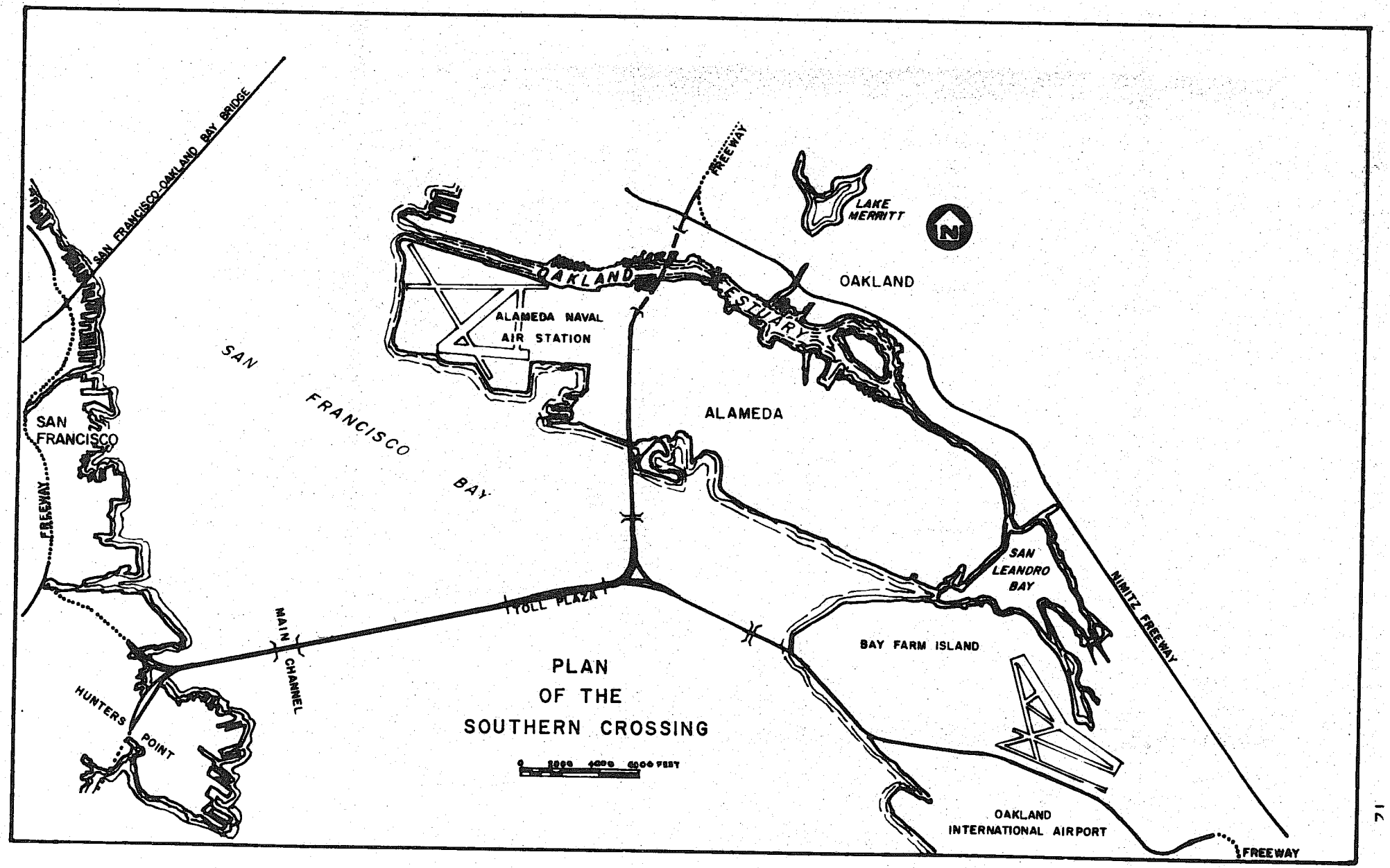
SAN FRANCISCO-OAKLAND BAY BRIDGE
U.S.
FREEWAY
LAKE MERRITT
N
OAKLAND
OAKLAND
ESTUARY
ALAMEDA NAVAL AIR STATION
SAN FRANCISCO BAY
ALAMEDA
SAN FRANCISCO
FREEWAY
TOLL PLAZA
MAIN CHANNEL
SAN LEANDRO BAY
NIMITZ FREEWAY
BAY FARM ISLAND
HUNTERS POINT
PLAN
OF THE
SOUTHERN CROSSING
0 2000 4000 6000 FEET
OAKLAND
INTERNATIONAL AIRPORT
FREEWAY

FIG. 2.1

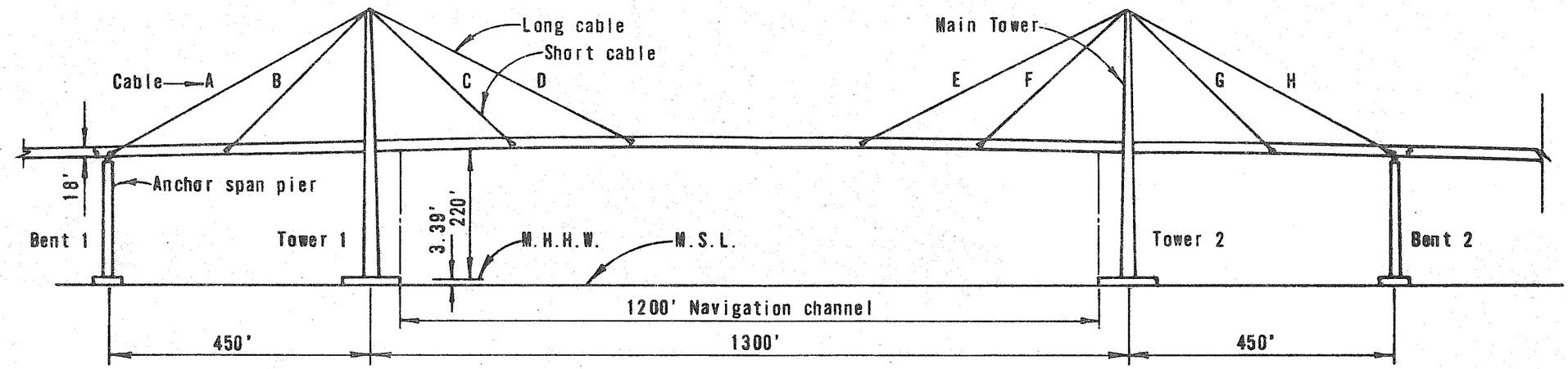

ELEVATION

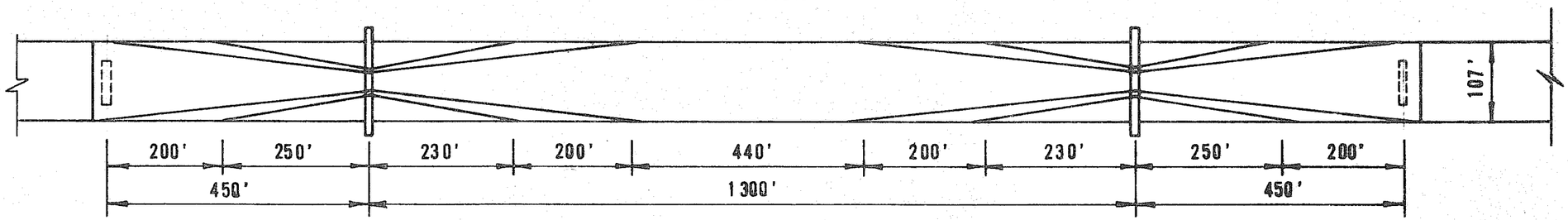

PLAN

MAIN CHANNEL STRUCTURE

THE CABLE STAYED GIRDER BRIDGE

FIG. 2.2

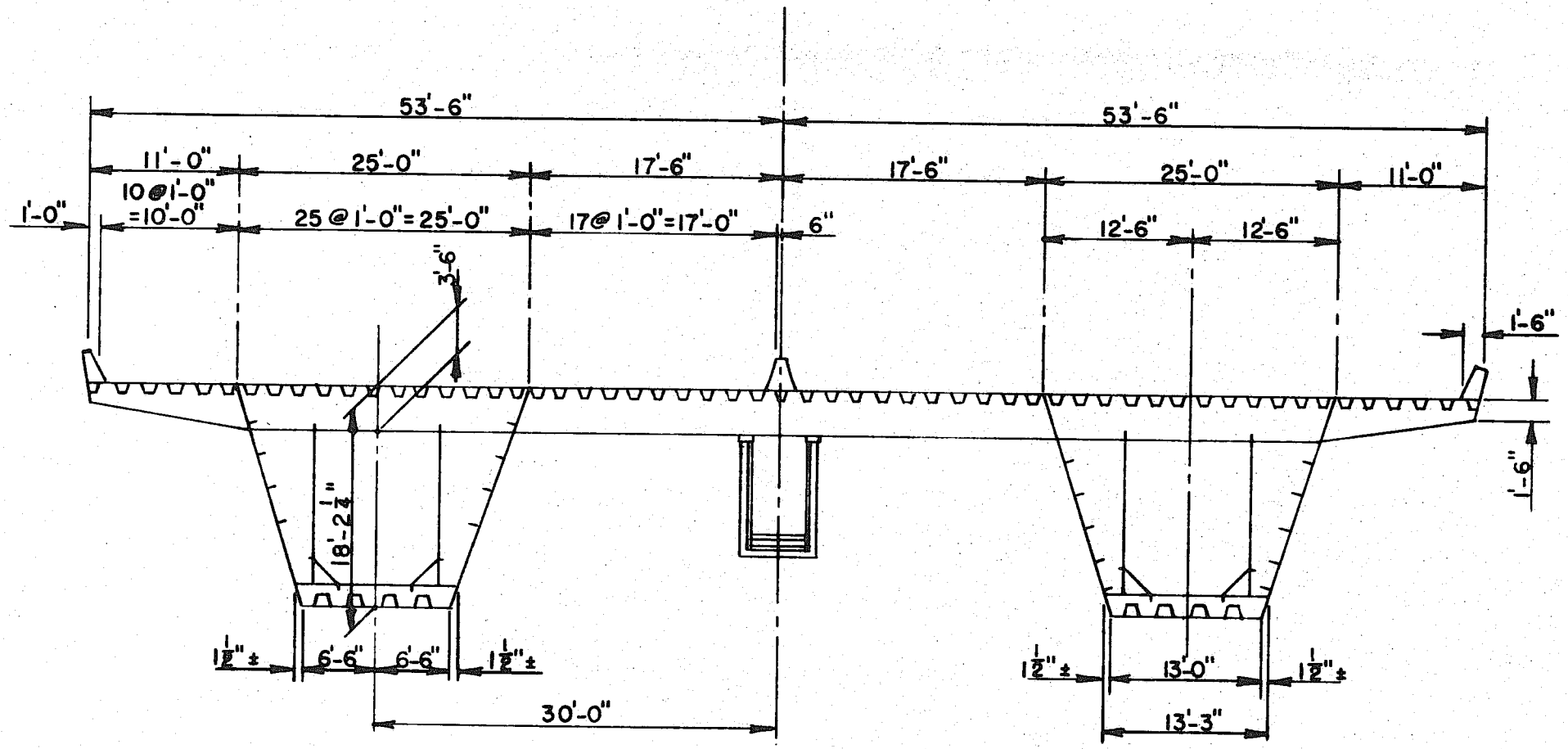

SECTION NEAR CENTER OF SPAN

SECTION NEAR SUPPORT

SECTIONS OF ROADWAY GIRDER

FIG. 2.3

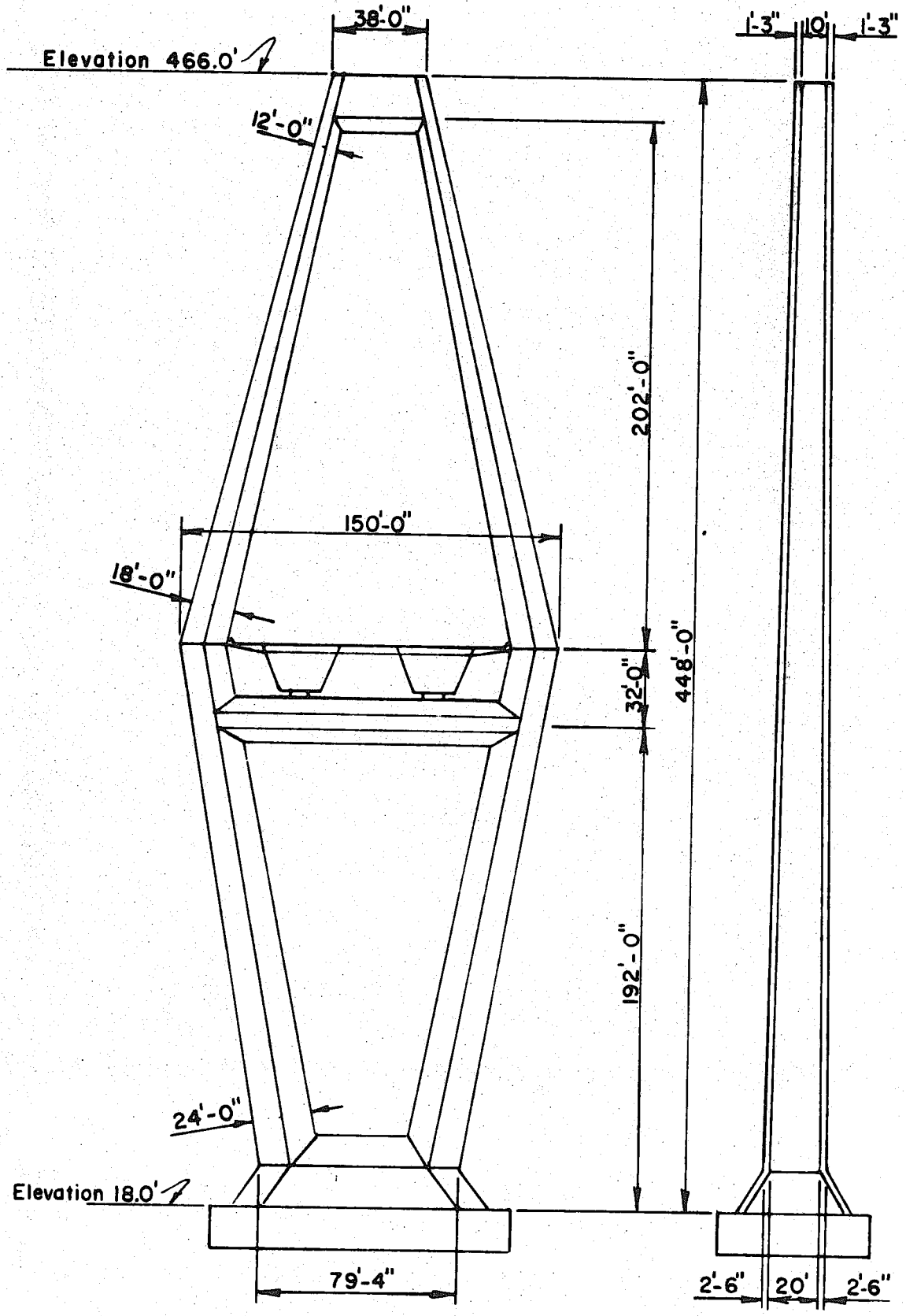

ELEVATIONS OF DIAMOND TOWERS

FIG. 2.4

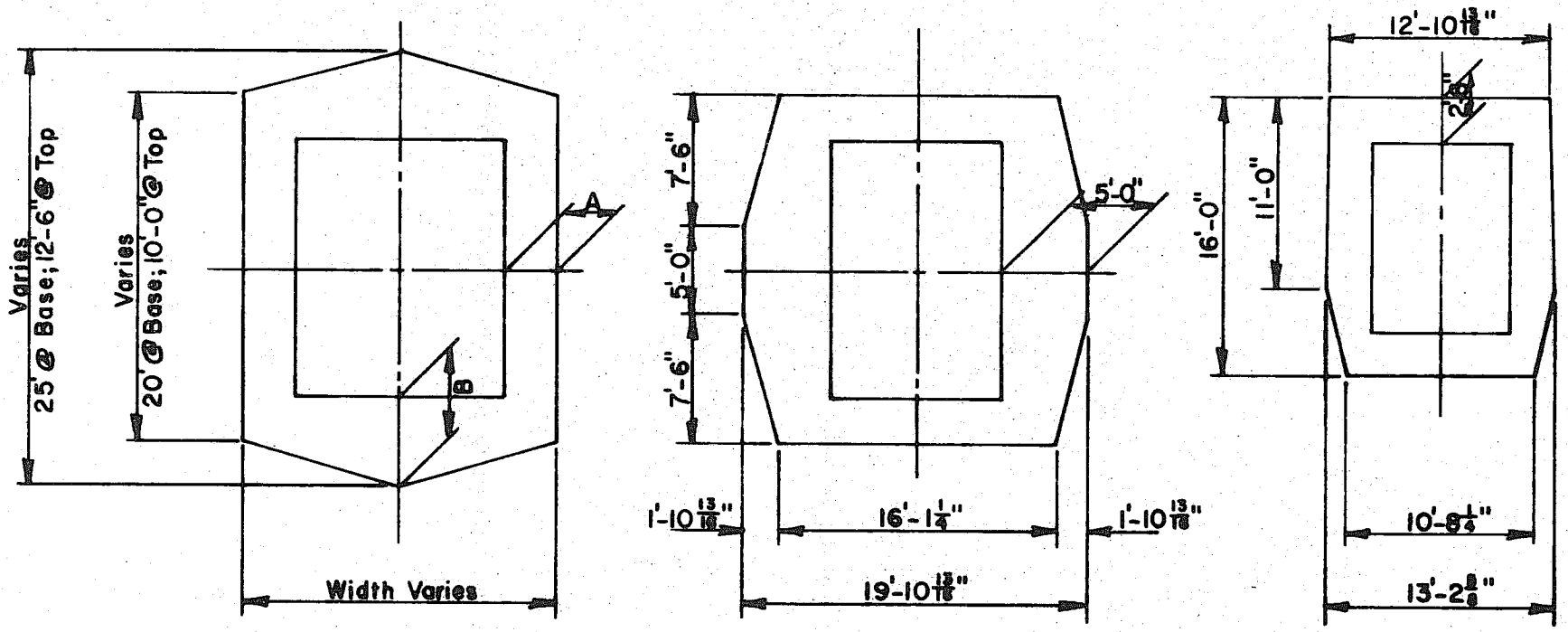

A & B Vary

TOWER LEGS

INTERMEDIATE STRUT

TOP STRUT

CROSS-SECTIONS OF EACH TOWER

FIG. 2.8

3. THE ANALYTICAL MODEL OF THE CABLE STAYED GIRDER BRIDGE

The analytical model employed in this investigation is briefly described. It is represented in Figures 3.1 and 3.2. The model is three-dimensional and symmetrical about a vertical plane. The longitudinal center-line of the roadway lies in this plane. The model is composed of 271 members and 264 nodal points. Each member is identified by a number (see Figure 3.1) and lies between identifying node-points I and J. Also, each node-point is identified by a number (see Figure 3.2).

The box-girders of the bridge are represented by twin longitudinal girders which in plan and elevation exactly follow the longitudinal centroidal axes of the box-girders. Each girder of the model is composed of the same number of members as in the prototype, and each member of the model has the same properties as the corresponding member of the prototype. Eccentricities of the longitudinal centroidal axis along the girder, which occur because of the differences of the properties of the members, are taken into account. They are taken into account as follows: In Figure 3.3, three consecutive members are shown, each member having different properties from the others. The following assumptions are made concerning the prototype: (1) for full dead load, the profile of the roadway lies along a parabola as defined by the designers. (2) for full dead load, a transverse section common to any two adjacent members is normal to a line which is tangent to the parabolic curve at the section. (3) plane cross-sections before loading remain plane after loading. To meet these assumptions for the model, a rigid arm is introduced at each cross-section which is common to the

deformable members lying to each side of the section (see Figure 3.3). The rigid arm connects the ends of the deformable members and its length is equal to the distance between the centroidal axes of the two members. A node point is introduced for reference at the mid-point of the rigid arm. Consequently, each member of the actual girder is represented in the model by a deformable segment and two rigid arms. The arms are attached to ends I and J of the deformable member and extend to the respective node points. (If desired, this expedient can be explained in terms of master and slave nodes, although not necessary nor innovative except in terminology). It is noted that the behavior of the model meets the assumptions listed above. Also, the preceding defines the coordinates of the node points, the orientations of the sections at the ends of each member, and the properties of the deformable members with respect to their principal axes. The latter observations are important in determining camber and in the non-linear theory developed by the writers.

In Figure 3.1, members transverse to the longitudinal axis of the bridge are used to interconnect the longitudinal girders at the node-points of the girders. At the anchorage beams, the transverse members extend to the work-points of the cable anchorages. In this way, the eccentricities of the cable anchorages are taken into account. In this study, the properties of the transverse beams and of the girder are defined to be consistent with the assumption that the plane cross-sections across the width of the roadway remain plane. The transverse beams, however, are useful for obtaining an estimate of the possible influences of the three-dimensional behavior of the deck. The latter has been partially pursued by the writers but the results are not

reported herein. Suffice it to state that the results show that the three-dimensional behavior of the deck has little influence on the magnitudes of the total forces and moments acting on the different sections of the roadway. The localized distributions of these totals, across the width and through the depth of the roadway, are fit subjects for further study.

Each long cable of the model is divided into six axial members between cable anchorage and cable saddle, and each short cable into four. In the linear analysis, each cable is assumed to be straight. For the effects of dead load and in the nonlinear studies conducted herein, each cable is considered to be a catenary supporting its own dead weight. For dynamic studies, the node points along the cables will serve as places for concentrating the masses of the cable segments.

Each tower of the model, see Figures 3.4 and 3.5, is divided into 28 members which lie between 29 node points. The members of the model lie along the centroidal axes of the prototype. Their properties are obtained as follows: The properties of the members in the prototype firstly, are calculated at each node point shown in the model. Properties associated with axial and flexural effects are based on the theory of uncracked sections with the longitudinal steel transformed to an equivalent amount of concrete. The torsional resistance of each section is calculated by approximating each section by an elliptical tube having about the same lateral dimensions as the actual section. The longitudinal steel on each face of the section is transformed to an equivalent thin-walled tube of concrete and its torsional resistance added to that of the actual concrete. The area resisting a shear is obtained by considering 5/6 of the areas of the walls of the

cross-section which are in the direction of the shear. In the model, each member between adjacent node points is of constant cross-section and has properties which are the averages of those calculated at the corresponding node points of the prototype. Because of the changes occurring in design, the calculations for the dimensions, coordinates, and properties of the tower are made by means of a subroutine, called CONTOW. A similar subroutine, called METTOW, is defined for steel or other metal towers.

Other members are included in the model to represent the cable saddles, bearings, end-anchorages, and reaction devices (see Figures 3.1 and 3.2).

The properties and dimensions of the analytical model are summarized in Table 2.1A (see Appendix). These properties and dimensions were employed in the initial phases of the study. Because of the changes which occurred in design, other properties were employed in the later phases of the study. The latter properties are not given herein.

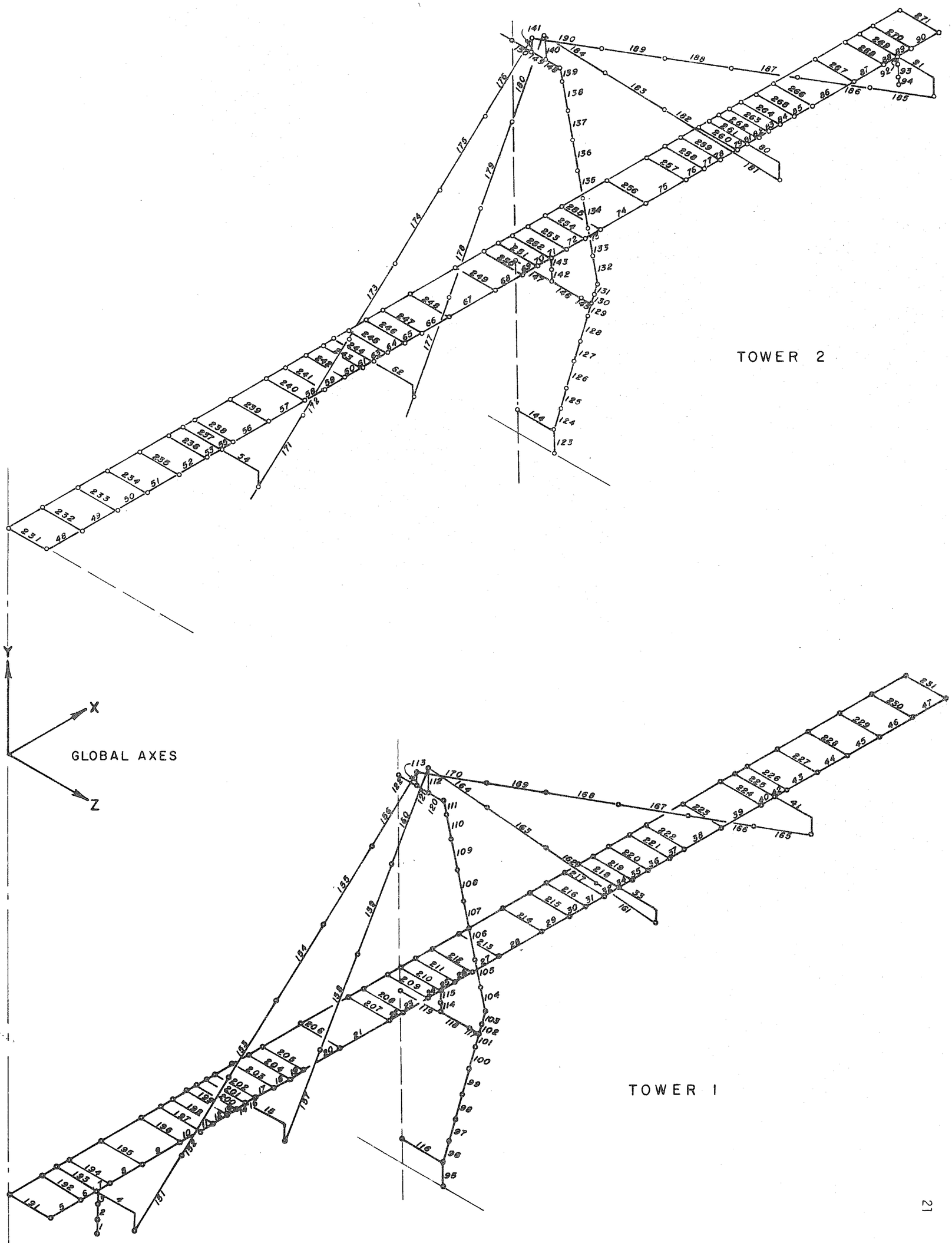

MEMBER NUMBERS FOR THE ANALYTICAL MODEL

FIG. 3.1

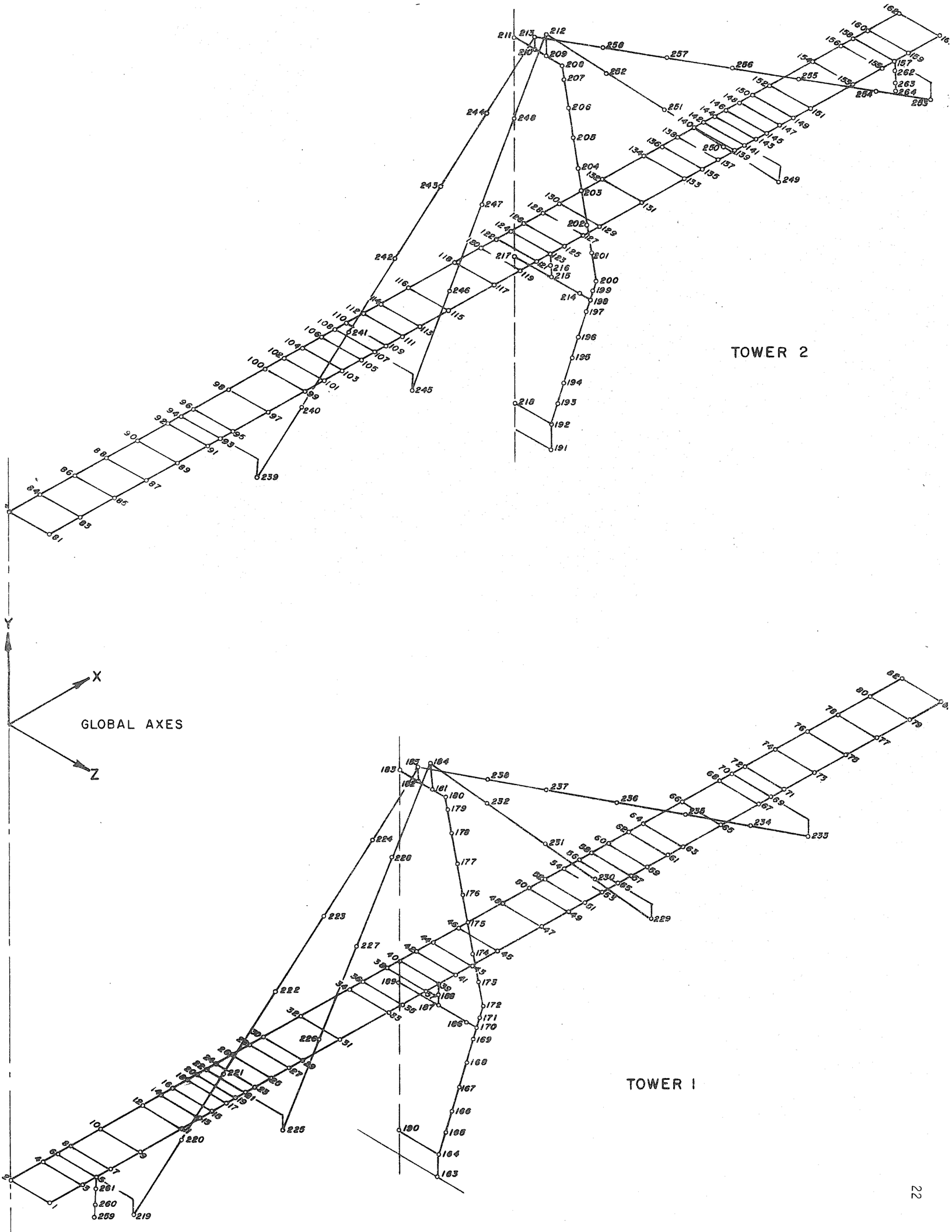

NODE POINT NUMBERS FOR THE ANALYTICAL MODEL

FIG. 3.2

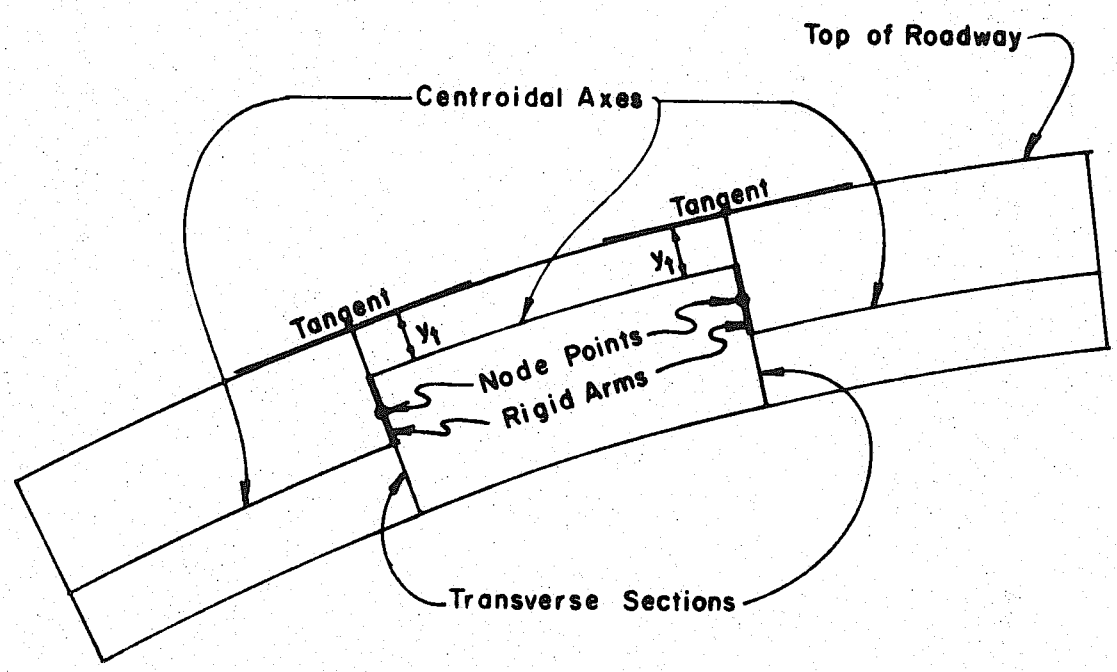

THREE CONSECUTIVE MEMBERS ALONG THE GIRDER

FIG. 3.3

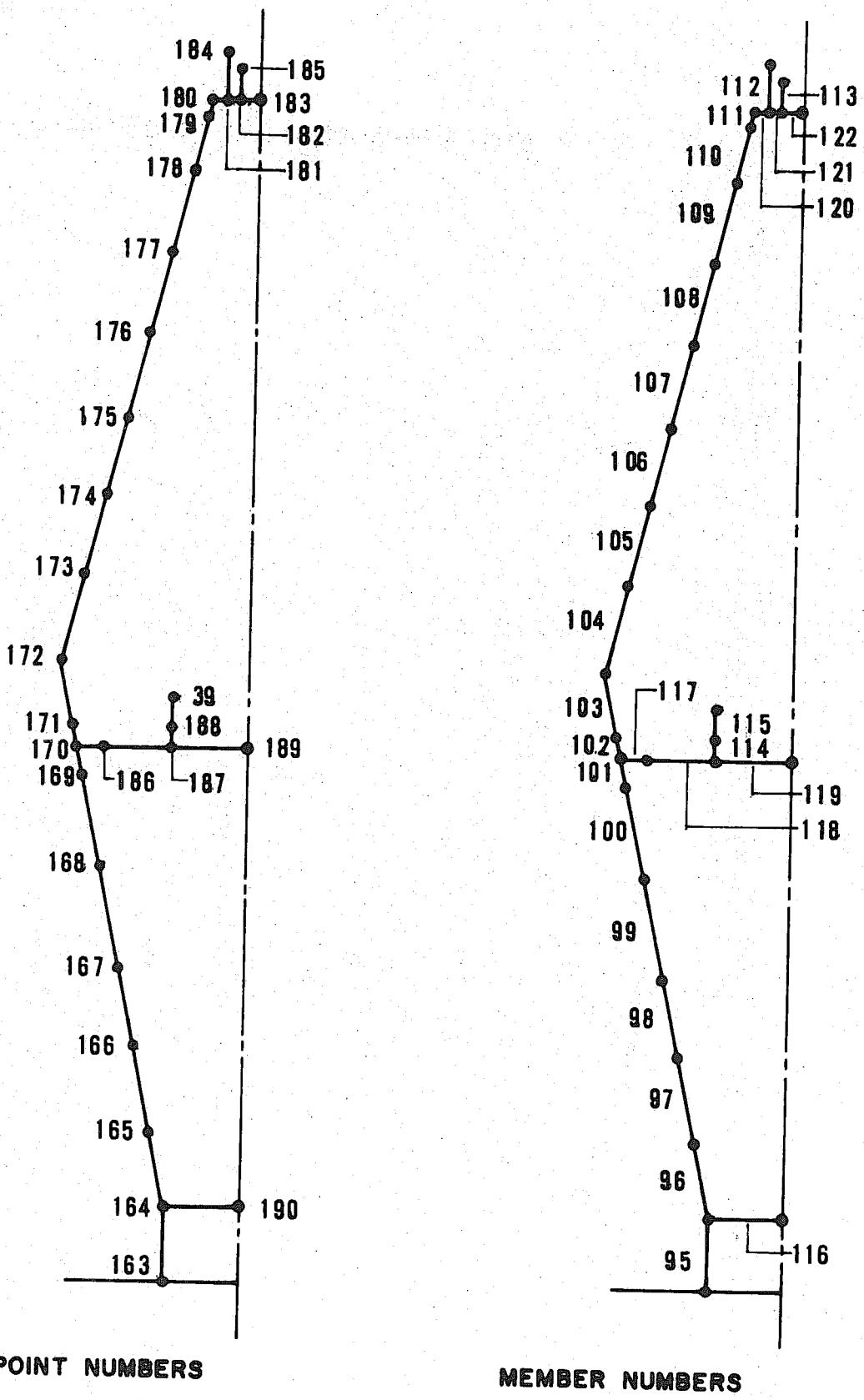

NODE POINT NUMBERS

MEMBER NUMBERS

NODE POINT AND MEMBER DESIGNATIONS FOR TOWER I

FIG. 3.4

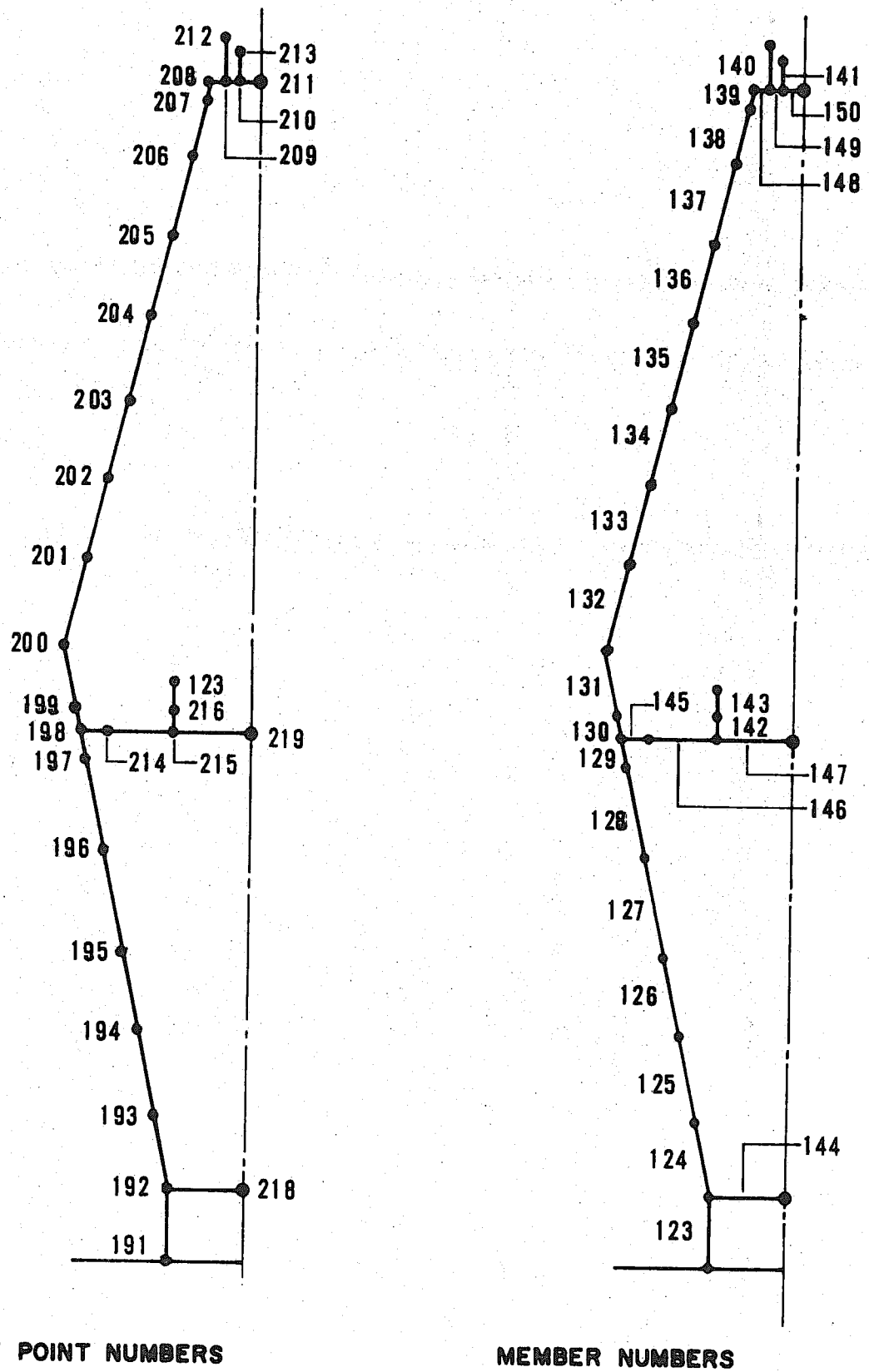

NODE POINT NUMBERS

MEMBER NUMBERS

NODE POINT AND MEMBER DESIGNATIONS FOR TOWER 2

FIG. 3.5

4. LINEAR AND NONLINEAR THEORIES OF STRUCTURAL BEHAVIOR

Two kinds of analytical procedures are used in this study. One kind is based on the classical theory of linear elastic structures (7, 9)* in which the displacements are considered small, and the contributions of the member forces to the balance of the external loads are stated in terms of the initial geometry of the structure. The other kind is based on a nonlinear theory of structures (1, 3, 7, 8, 9, 12) in which (1) the strain-displacement relations of members are non-linear, and (2) the equations of joint equilibrium are written in terms of the final geometries of the structures.

4.1 The Linear (or classical) Theory

In the linear (or classical) theory, the relations between the external loads P and the joint displacements U are given in matrix form by

$$P = K_E U \tag{4.1}$$

in which K_E is the stiffness matrix of the structure. The stiffness matrix K_E is formed by assembling the contributions of each member which lies between joints I and J to the balance of the external loads at joints I and J. Eq. 4.1 is an equation of equilibrium, stated in matrix form, and is referred to a global set of axes. For the bridge, a right-handed rectangular system of axes (X, Y, Z) is selected for the global system as shown in Figs. 3.1 and 3.2. The coordinates of node-points and the direction cosines of members are referred to the global

* Numbers in parantheses refer to References.

system of axes. External force and linear displacement components are positive in the directions of the axes, and at each node are identified by subscripts 1, 2, and 3. External moments and angular displacement components are positive about the axes, using a right handed rule of signs. At each node, the moments and angular displacement components are identified by subscripts 4, 5, and 6.

For a member loaded only at its ends, the force-deformation relationships are given in matrix form by

$$\{p\} = [k]\{u\} \qquad (4.2)$$

in which $\{p\}$ is a column vector of the force components at the ends, $\{u\}$ is a column vector of the displacement components, and $[k]$ is the stiffness matrix of the member. For the full array of force-components at both ends of a member, Eq. 4.2 includes the requirements of equilibrium.

In the classical theory, the relationship between $\{p\}$ and $\{u\}$ is linear and is in terms of the initial geometry of the member. Hooke's Law is assumed and strains are considered small. For the bridge, three types of straight prismatic members are used although only one type is required. The three are used for the efficiency of the computer program developed by the writers. They are (1) axial members as for the end-anchorages and the straight segments of the cables, (2) axial-flexural members which lie in a plane as for the members of the roadway girder, and (3) axial-flexural members which lie in space as for the members of the towers. For each of these members, the directions and designations of the forces and deformations at the ends are referred to a set of local axes. For example, the set for type (3)

is a right-handed rectangular set (x, y, z) with the x-axis coinciding with the longitudinal axis of the member, the y and z axes coinciding with the principal axes of the sections, and the origin of the set at end I of the member. See Fig. 4.1 for the designations and signs of the force and displacement components at ends I and J of each of the three types of members.

In forming the structural stiffness matrix, K_E of Eq. 4.1, the stiffness matrix of each member firstly is transformed from the local to the global set of axes. This transformation is associated with a rotation matrix. Because of the eccentricities of the centroidal axes of the members along the roadway girder, an adjustment is made in the force-deformation relationships of type (2) and type (3) members. For these members, the global force and displacement components at the ends of each deformable segment are transformed to global axes at the ends of the rigid arms. Eq. 4.2 then becomes

$$\{p\}_g = [k]_g \{u\}_g \tag{4.3}$$

in which the subscript g designates the global set of axes at the node points of the eccentric members. The structural stiffness matrix K_E is formed by assembling the elements of each $[k]_g$ in the proper rows and columns of K_E.

For use in the studies of the linear behavior of the bridge, a general computer program is employed. The program is called GENLIN and incorporates the types of members used in the bridge. For a given case of load or thermal effect on a structure, Eq. 4.1 is solved for U,

and the internal forces and moments, p, at the ends of the members are obtained by means of Eq. 4.2. Multiple cases of loadings can be solved in a single computer run.

4.2 The Nonlinear Theory

The nonlinear theory (1, 7) employed by the writers is based on the direct stiffness method. The theory is stated in terms of an estimate plus a correction to account for the nonlinear effects of changes in the geometry of a given structure. In this study, the concept of a tangent stiffness matrix is employed in obtaining the estimate. Then, the stiffness matrix and the forces and displacements are successively adjusted to obtain a set of results compatible with the final dimensions of the structure. A solution technique, based on the Newton--Raphson method, is used. It is not based on the incremental step technique for problems of large displacements as presented elsewhere (12). It is based on a one step technique for large increments of load. In those cases when an increment is too large the increment is subdivided.

In the nonlinear theory of structures, when displacements are large, Eq. 4.1 is no longer valid because: (1) The strain-displacement relations of members are nonlinear. Consequently, K_E is not applicable; and (2) the equations of joint equilibrium are written in terms of the final geometries of the structures.

Consider two deformed states, 1 and 2, of a structure. If the changes between the two deformed states are considered, an incremental equation of joint equilibrium can be written in matrix form as follows:

$$P_{12} = K_{12} U_{12} \tag{4.4}$$

in which P_{12} = a column vector of the change in loads from state 1 to state 2, and U_{12} = a column vector of the increment of displacements. The matrix K_{12} is a function of U_{12};

$$K_{12} = K_{12} (U_{12}) \tag{4.5}$$

and of state 1 understood. It can be interpreted as a secant stiffness for the given increment of load P_{12}.

Solutions to Eq. 4.4 can be obtained by means of various techniques. The technique used in this study is that in which the final solution for the response of a structure is obtained by means of successive estimates and corrections. For this purpose, Eq. 4.4 is rewritten as:

$$P = P_{est} + P_{cor} = [K_{est} + K_{cor}] \; [U_{est} + U_{cor}] \tag{4.6}$$

in which the subscripts 12 are suppressed. Particular use is made herein of a tangent stiffness matrix or of a linearized version of the nonlinear stiffness matrix for obtaining such estimates. For this purpose, Eq. 4.6 is rewritten as:

$$P = [K_L + K_{NL}] \; [U_L + U_{NL}] \tag{4.7}$$

in which K_L = a constant matrix and K_{NL} = a nonlinear function of the displacements U_{12}. Both matrixes, K_L and K_{NL}, are assembled

in exactly the same way as K_E of the classical theory of linear elastic structures. For this purpose, the contributions of each member of a structure to K_L and K_{NL} are required.

In the nonlinear studies of the bridge, four types of members are used although only two are needed. The four are used to obtain the maximum efficiency of a general computer program for the nonlinear effects of elastic structures. The four types are (1) axial members as for the end-anchorages, (2) axial-flexural members which lie in a plane as for the members of the roadway girder, (3) axial-flexural members which lie in space as for the members of the towers, and (4) cables which are shaped in the form of catenaries. See Fig. 4.1 for the designations and signs of the local force and displacement components at ends I and J of the first three types of members, and Fig. 4.2 of cable members in the shapes of catenaries.

In Ref. 1, five techniques are given for solving the nonlinear equation,

$$P = K U \tag{4.8}$$

for the displacement vector U when the loads P are known. One of these, the tangent stiffness technique, is used for the bridge. It is illustrated by a schematic diagram (see Fig. 4.3) which shows a nonlinear relation between the loads P and the displacement U of a given structure. The diagram is abstract because P and U are N-dimensional vectors for a structure with N-degrees of freedom. In the iterative scheme, an estimate, U_{est}, is constantly sought for the displacement vector U. The tangent stiffness matrix K_T is used to

obtain the estimate for U during each cycle of iteration. The iterative scheme is as follows:

$$P_R^{(i-1)} = K_T^{(i-1)} \; U_{12}^{(i)} \quad i = 1, 2, 3... \tag{4.9}$$

in which $P_R^{(i)}$ = the remaining load vector after i cycles of iteration, and $K_T^{(i)}$ = the tangent stiffness matrix formed by using the joint coordinates and member forces at the end of i cycles of iteration. For the case when $i = 1$, $P_R^{(o)} = P_{12}$.

Inspect the sequence of calculations indicated by Eq. 4.9. Assume that at the end of (i-1) cycles of iteration, $P_R^{(i-1)}$, $K_T^{(i-1)}$, and the joint coordinates of a structure are known. Now solve Eq. 4.9 for $U_{12}^{(i)}$. Then determine the new coordinates of the joints and the deformations, $u^{(i)}$, at the ends of the members. Assuming that the force-deformation relations, $k^{(i)}$, for each member are known, solve

$$p^{(i)} = k^{(i)} \; u^{(i)} \tag{4.10}$$

for $p^{(i)}$. In this study, the force-deformation relations are obtained for each of the four types of members. The latter relations are non-linear; that is, $k^{(i)}$, is a function of $u^{(i)}$. For each type of member, $k^{(i)}$ is composed of two parts;

$$k^{(i)} = k_E + k_G^{(i)} \tag{4.11}$$

in which k_E is the ordinary elastic stiffness matrix of the member, and $k_G^{(i)}$ (called the geometric stiffness) is a function of $u^{(i)}$. Knowing $p^{(i)}$ for each member, transform it to global coordinates at

the respective nodes and by means of statics determine the external loads, $P_{EQ}^{(i)}$, which are in balance with the internal forces. Calculate the remaining load vector $P_R^{(i)}$ from

$$P_R^{(i)} = P - P_{EQ}^{(i)} \tag{4.12}$$

Now form the tangent stiffness matrix $K_T^{(i)}$ using the current values of the geometry and member forces. Continue the iteration and stop when the remaining load vector, $P_R^{(i)}$, either vanishes or is within a specified tolerance.

Note that in the solution technique just described two sets of relations (k and K_T) are required for each of the four types of members used in this study. One set consists of the force-deformation relations which exist between a stressed state and the unstressed state of the member. The other set consists of the relations which exist between the local stiffness of a member and the tangent stiffness of the structure for a given state of stress. In this report, the force-deformation relations for each of the four types of members are given. The procedure for obtaining the tangent stiffness is described.

4.2a Force-Deformation Relations

Summaries are given in Figs. 4.4 to 4.6 of the force-deformation relations for axial and axial-flexural members. The relations for cable members in the shapes of catenaries are given in Chapter 5. In each of the preceding Figures, the relations are for reference forces and deformations at the ends of the member; that is, $[k]_r$ of

$$\{p\}_r = [k]_r \{u\}_r \tag{4.13}$$

is given in each Figure for the respective member. For example: In Fig. 4.5, vectors $\{p\}_r$ and $\{u\}_r$ are for a two dimensional axial-flexural member and are given by

$$\{p\}_r = \begin{Bmatrix} p_3 \\ p_6 \\ p_4 \end{Bmatrix} ; \quad \{u\}_r = \begin{Bmatrix} u_3 \\ u_6 \\ u_4 \end{Bmatrix} \tag{4.14}$$

in which the subscripts 3, 6, and 4 designate the reference components of force and deformation. The reference stiffness, $[k]_r$, is given by

$$[k]_r = \begin{bmatrix} k_{3,3} & k_{3,6} & k_{3,4} \\ k_{6,3} & k_{6,6} & k_{6,4} \\ k_{4,3} & k_{4,6} & k_{4,4} \end{bmatrix} \tag{4.15}$$

The complete set of forces and deformations at both ends of the member is obtained by means of a matrix transformation.

In Ref. 2, several consistent formulations are given of the force-deformation relations for members of two dimensional framed structures. The relations are obtained as follows: Assume a linear variation of displacement ξ along the member,

$$\xi = ax \tag{4.16}$$

and a third-degree polynomial for displacement η along the member

$$\eta = c_1 x + c_2 x^2 + c_3 x^3 \tag{4.17}$$

From the boundary conditions at ends I and J, determine the coefficients a, c_1, c_2, and c_3. Form the strain energy of the member,

$$U = U_a + U_b \tag{4.18}$$

in which

$$U_a = \frac{AE}{2} \int_0^L \varepsilon_a^2 \, dx \tag{4.19}$$

and

$$U_b = \frac{EI}{2} \int_0^L \varepsilon_b^2 \, dx \tag{4.20}$$

Terms U_a and U_b respectively are the strain energy associated with axial and flexural deformations. The influences of shear deformations are neglected. The potential energy, E_p, for the member is given by

$$E_p = U - P\delta \tag{4.21}$$

in which

$$P\delta = p_3 u_3 + p_6 u_6 + p_4 u_4 \tag{4.22}$$

From a well known principle, a minimum of E_p by variation of the parameters u_3, u_6, and u_4 corresponds to stable equilibrium. Then, differentiate E_p with respect to u_3, u_6, and u_4, and set the resulting equations to zero. Solve the latter equations for $\{p\}_r$ in terms of $\{u\}_r$ and obtain the resulting equation for $[k]_r$ as given in Fig. 4.5.

For this study, the force-deformation relations given in Fig. 4.6 for three dimensional axial-flexural members are obtained in almost exactly the same way as those for two dimensional members. Assume (1) a linear variation of displacement ξ along the member,

$$\xi = ax \tag{4.23}$$

(2) a linear variation of the rotational displacements β_x along the member,

$$\beta_x = bx \tag{4.24}$$

(3) a third-degree polynomial for displacements η along the member,

$$\eta = c_1x + c_2x^2 + c_3x^3 \tag{4.25}$$

and (4) a third-degree polynomial for displacements ζ along the member,

$$\zeta = d_1x + d_2x^2 + d_3x^3 \tag{4.26}$$

From the boundary conditions at ends I and J, determine the coefficients a, b, c, and d of Eqs. 4.23 to 4.26. Form the strain energy of the member,

$$U = U_a + U_t + U_{bx} + U_{by} \tag{4.27}$$

in which

$$U_a = \frac{AE}{2} \int_0^L \varepsilon_a^2 \, dx \tag{4.28}$$

$$U_t = \frac{GJ}{2} \int_0^L \varepsilon_{tx}^2 \, dx \tag{4.29}$$

$$U_{by} = \frac{EIy}{2} \int_0^L \varepsilon_{by}^2 \, dx \tag{4.30}$$

and

$$U_{bz} = \frac{EIz}{2} \int_0^L \varepsilon_{bz}^2 \, dx \tag{4.31}$$

Terms U_a, U_t, U_{by}, and U_{bz} respectively are the strain energies associated with axial, torsional, and flexural deformations. Again, the influences of shear deformations are neglected. It need be mentioned that the expressions for the strains ε_a, ε_{tx}, ε_{by}, and ε_{bz} in Eqs. 4.27 to 4.31 are associated with the deflected shape of the deformed member in three dimensional space and not with the deflected shape projected separately into the xy and the xz planes.

The potential energy, E_p, for the three dimensional member is given by Eq. 4.21 in which

$$P\delta = p_5u_5 + p_6u_6 + p_7u_7 + p_{10}u_{10} + p_{11}u_{11} + p_{12}u_{12} \tag{4.32}$$

Then, differentiate E_p with respect to the parameters u, and set the resulting equations to zero. Solve the latter equations for $\{p\}_r$ in terms of $\{u\}_r$ and obtain the resulting equations for $[k]_r$ as given in Fig. 4.6. As a check on this expression, $[k]_r$ of Fig. 4.6

can be degenerated into two expressions of $[k]_r$, each similar to that given in Fig. 4.5. Each of the latter expressions is associated with a two dimensional member lying in a plane.

4.2b Tangent Stiffness

In Ref. 1, the tangent stiffness of a structure composed only of axial members is obtained on the basis of physical considerations. The contribution of an axial member to the total tangent stiffness of such a structure is given in Fig. 4.4.

For the bridge composed of the four types of members, the tangent stiffness, K_T, is obtained by means of the calculus of variations. In the calculus, a change in P from one state to another is related to a change in U, and in the functions of U, as U is permitted to approach zero in the limit. The latter statement is the classical definition of a tangent plane to an N-dimensional surface.

The contribution of each member to the tangent stiffness, K_T, of the structure is explained as follows: The force deformation relations of a member, when stated in terms of local coordinates, are given by

$$p = k\,u \tag{4.33}$$

The change of p as u is varied is given by

$$d_p = k\,du + dk\,u \tag{4.34}$$

in which k is a function of u, and dk is a function of u and du. Consequently, Eq. 4.34 can be written in the form of

$$dp = k_t \, du \tag{4.35}$$

in which k_t is the tangent stiffness of the member, stated in terms of local coordinates.

However, the contribution of each member to the tangent stiffness, K_T, of the structure is required in global coordinates. Then, transform the forces p of Eq. 4.33 to global coordinates and obtain

$$p_g = T\,p = T\,k\,u \tag{4.36}$$

in which T is the transformation matrix. The change in p_g as U is varied is given by

$$dp_g = dT\,k\,u + T\,k\,du + T\,dk\,u \tag{4.37}$$

which is rewritten as

$$dp_g = dT\,ku + T\,(k\,du + dk\,u) \tag{4.38}$$

Because dT is a function of dU, the first term on the right side of Eq. 4.38 can be written as

$$dT\,ku = A\,dU \tag{4.39}$$

From Eqs. 4.34 and 4.35, the remaining terms on the right side of Eq. 4.38 can be written as

$$T\,[k\,du + dk\,u] = T\,k_t\,du \tag{4.40}$$

But note

$$du = T^* dU \tag{4.41}$$

in which T^* is the transpose of T. Consequently, Eq. 4.38 is rewritten as

$$dp_g = [A + T\, k_t\, T^*]\, du \tag{4.42}$$

or

$$dp_g = k_T\, dU \tag{4.43}$$

in which

$$k_T = [A + T\, k_t\, T^*] \tag{4.44}$$

In Eqs. 4.43 and 4.44, k_T is referred to global coordinates and is the desired contribution of each member to the tangent stiffness, K_T, of the structure. The contribution consists of two parts: Term $T\, k_t\, T^*$ is the conventional transformation of a stiffness matrix in local coordinates to a stiffness matrix in global coordinates. Term A is the contribution to k_T due to the change in the direction cosines of the member.

Then, the tangent stiffness, K_T, of the structure is assembled in exactly the same way as K_E of the classical theory of linear elastic structures.

Based on the preceding, a general computer program called NONLIN is employed for studying the nonlinear behavior of the bridge.

Type 1: Axial Member

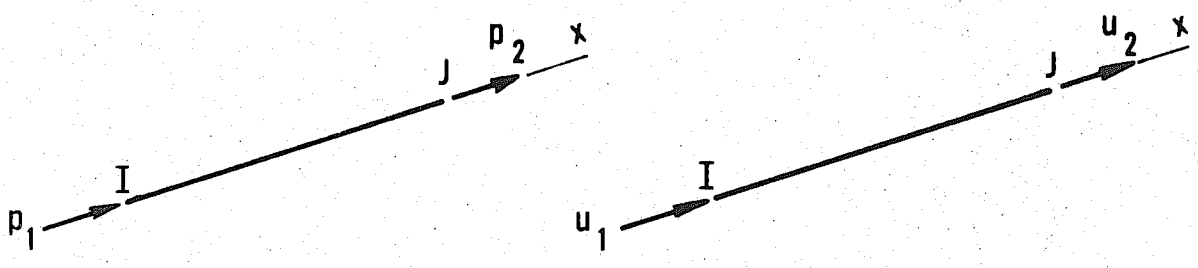

Type 2: 2D Axial-Flexural Member

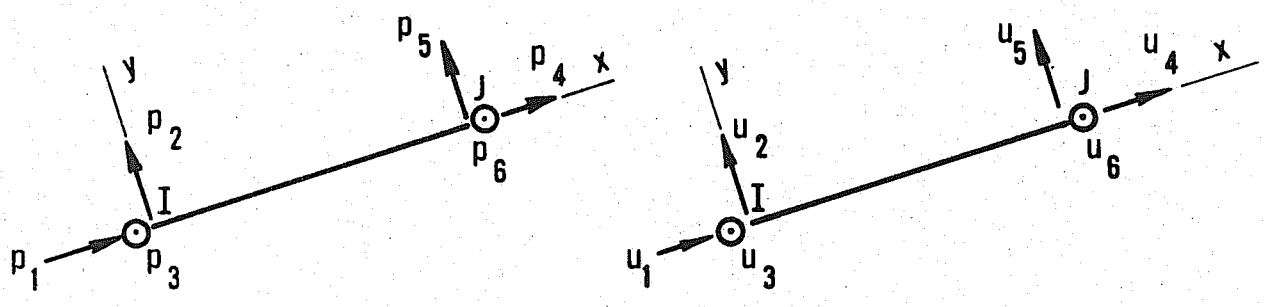

Type 3: 3D Axial-Flexural Member

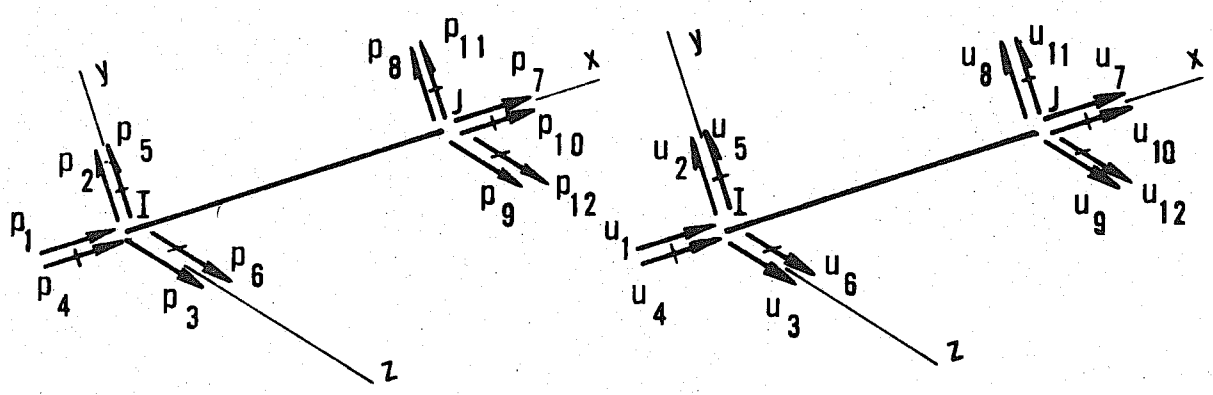

Local Forces

Local Displacements

FORCE AND DISPLACEMENT COMPONENTS OF AXIAL-FLEXURAL MEMBERS

FIG. 4.1

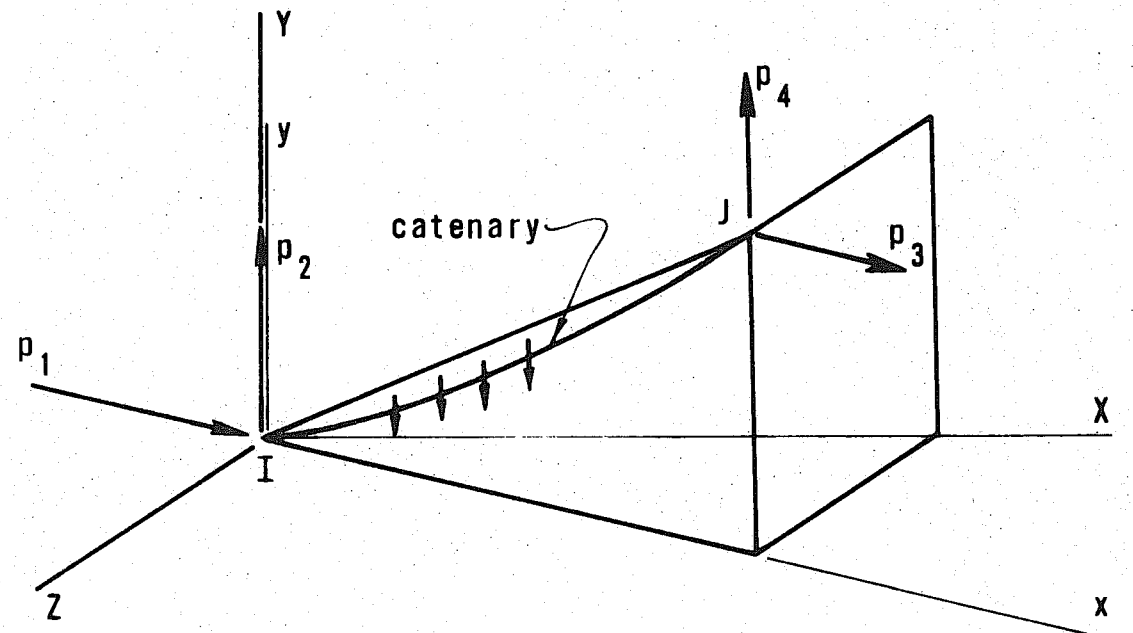

Local Forces

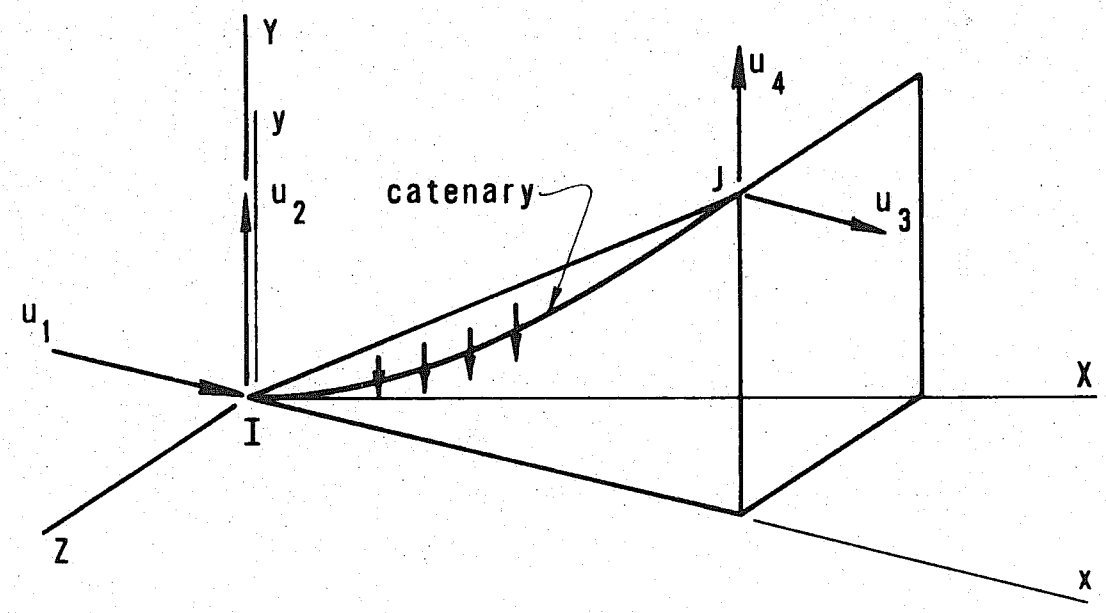

Local Displacements

FORCE AND DISPLACEMENT COMPONENTS OF CATENARIES

FIG. 4.2

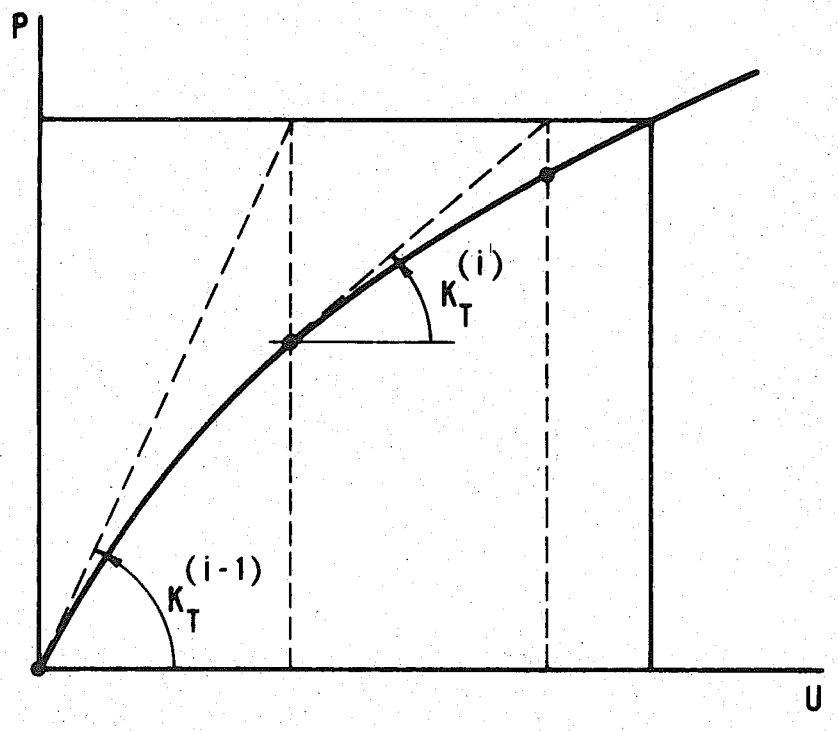

- Shift to deformed geometry associated with this point and use the remaining load vector as the applied load vector.

SCHEMATIC DIAGRAM FOR TANGENT STIFFNESS TECHNIQUE

FIG. 4.3

Force – Deformation Relations:

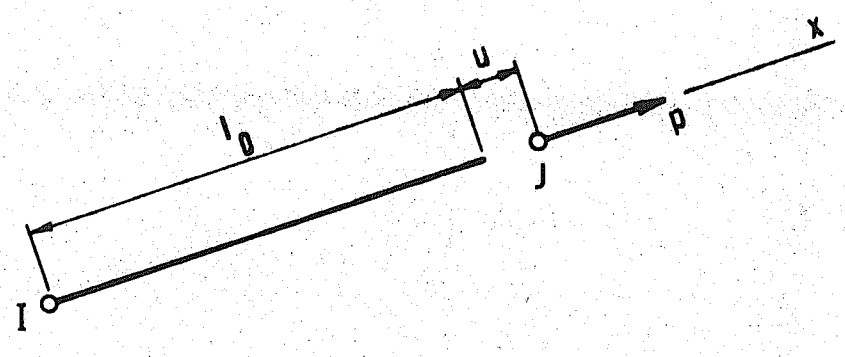

$$\{p\}_r = \{k\}_r \{u\}_r$$

in which

$$\{p\}_r = \{p\}; \quad \{u\}_r = \{u\}; \quad \{k\}_r = \left[\frac{AE}{l_0}\right]$$

Tangent Stiffness:

$$k_T = \frac{AE}{l_0}\left[\frac{LL^*}{l^2}\right] + \frac{p}{l}\left[I - \frac{LL^*}{l^2}\right]$$

in which

$$L = \begin{Bmatrix} L_x \\ L_y \\ L_z \end{Bmatrix}; \qquad I = \begin{bmatrix} 1 & 0 & 0 \\ 0 & 1 & 0 \\ 0 & 0 & 1 \end{bmatrix}$$

FORCE - DEFORMATION RELATIONS FOR AXIAL MEMBERS

FIG. 4.4

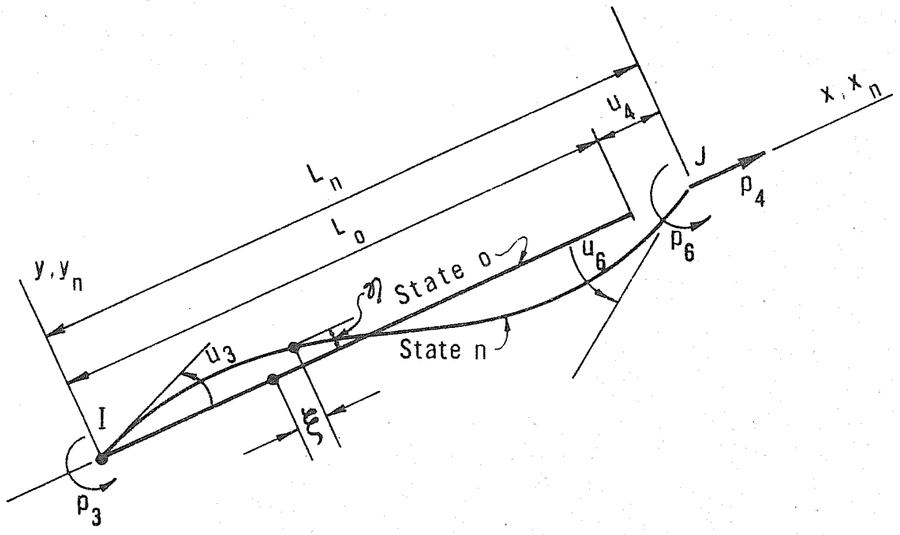

$$\{p\}_r = [k]_r \{u\}_r$$

in which

$$\{p\}_r = \begin{Bmatrix} p_3 \\ p_6 \\ p_4 \end{Bmatrix}; \quad \{u\}_r = \begin{Bmatrix} u_3 \\ u_6 \\ u_4 \end{Bmatrix}; \quad [k]_r = \begin{bmatrix} k_{3,3} & k_{3,6} & k_{3,4} \\ & k_{6,6} & k_{6,4} \\ \text{SYM.} & & k_{4,4} \end{bmatrix}$$

$$k_{3,3} = \frac{4EI}{L} - \frac{EI}{105L}\left\{512u_3^2 + 128u_3u_6 + 24u_6^2\right\}$$
$$+\frac{EAL}{280}\left\{\left(1+\frac{u_4}{L}\right)\left(8u_3^2 - 2u_3u_6 + 2u_6^2\right)\right\} + \frac{EA}{15}u_4\left(1+\frac{u_4}{L}\right)$$
$$-\frac{EA}{560}u_4\left\{4u_3^2 - 2u_3u_6 + u_6^2\right\}$$

$$k_{3,6} = \frac{2EI}{L} - \frac{64}{105}\frac{EI}{L}\left(u_3^2 + u_6^2\right) - \frac{EA}{60}u_4\left(1+\frac{u_4}{L}\right)$$
$$-\frac{EAL}{280}\left(1+\frac{u_4}{L}\right)\left(u_3^2 + u_6^2\right)$$

$$k_{3,4} = \frac{EA}{60}\left(1+\frac{u_4}{L}\right)\left(4u_3 - u_6\right) + \frac{EA}{560}\left\{4u_3^3 - 2u_3^2u_6 + u_3u_6^2\right\}$$

$$k_{6,6} = \frac{4EI}{L} - \frac{EI}{105L}\left\{512u_6^2 + 128u_3u_6 + 24u_3^2\right\}$$
$$+\frac{EAL}{280}\left\{\left(1+\frac{u_4}{L}\right)\left(8u_6^2 - 2u_3u_6 + 2u_3^2\right)\right\} + \frac{EA}{15}u_4\left(1+\frac{u_4}{L}\right)$$
$$-\frac{EA}{560}u_4\left\{4u_6^2 - 2u_3u_6 + u_3^2\right\}$$

$$k_{6,4} = \frac{EA}{60}\left(1+\frac{u_4}{L}\right)\left(-u_3 + 4u_6\right) + \frac{EA}{560}\left\{4u_6^3 - 2u_6^2u_3 + u_6u_3^2\right\}$$

$$k_{4,4} = \frac{EA}{L} + \frac{EA}{30L}\left\{2u_3^2 - u_3u_6 + 2u_6^2\right\}$$

FORCE-DEFORMATION RELATIONS OF 2D AXIAL-FLEXURAL MEMBERS

FIG. 4.5

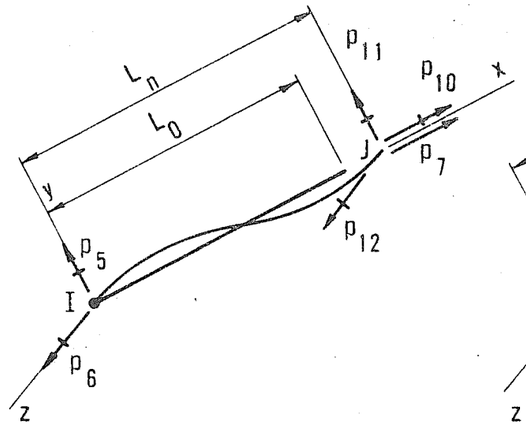

Reference Forces

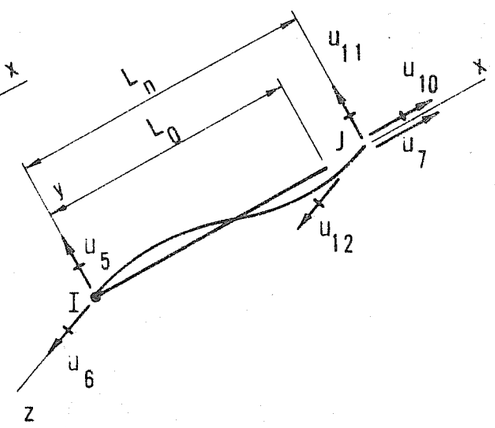

Reference Deformations

$$\{p\}_r = [k]_r \{u\}_r$$

in which

$$\{p\}_r = \begin{Bmatrix} p_5 \\ p_6 \\ p_7 \\ p_{10} \\ p_{11} \\ p_{12} \end{Bmatrix}; \quad \{u\}_r = \begin{Bmatrix} u_5 \\ u_6 \\ u_7 \\ u_{10} \\ u_{11} \\ u_{12} \end{Bmatrix}; \quad [k]_r = \begin{bmatrix} k_{5,5} & k_{5,6} & k_{5,7} & k_{5,10} & k_{5,11} & k_{5,12} \\ \bullet & k_{6,6} & k_{6,7} & k_{6,10} & k_{6,11} & k_{6,12} \\ \bullet & \bullet & k_{7,7} & k_{7,10} & k_{7,11} & k_{7,12} \\ \bullet & \bullet & \bullet & k_{10,10} & k_{10,11} & k_{10,12} \\ \bullet & \bullet & \bullet & \bullet & k_{11,11} & k_{11,12} \\ \bullet & \bullet & \bullet & \bullet & \bullet & k_{12,12} \end{bmatrix}$$

SYM.

and

$$k_{5,5} = \frac{4EI_y}{L_0} - \frac{EI_y}{105L_0}\left[\left(512u_5^2 + 128u_5u_{11} + 24u_{11}^2\right) + \left(256u_6^2 - 104u_6u_{12} + 88u_{12}^2\right)\right]$$
$$- \frac{EI_z}{105L_0}\left[256u_6^2 + 232u_6u_{12} + 88u_{12}^2\right] + \frac{EA}{15}u_7\left(1 + \frac{u_7}{L_0}\right)$$
$$+ \frac{EAL_0}{420}\left[\left(12u_5^2 - 3u_5u_{11} + 3u_{11}^2\right) + \left(12u_6^2 - 3u_6u_{12} + u_{12}^2\right)\right]$$
$$+ \frac{EA}{560}u_7\left[\left(12u_5^2 - 2u_5u_{11} + 3u_{11}^2\right) + \left(12u_6^2 - 2u_6u_{12} + u_{12}^2\right)\right]$$

$$k_{5,6} = 0$$

$$k_{5,7} = \frac{EA}{60}\left(1 + \frac{u_7}{L_0}\right)\left(4u_5 - u_{11}\right)$$
$$+ \frac{EA}{1680}\left[\left(12u_5^3 - 6u_5^2u_{11} + 3u_5u_{11}^2\right) + \left(12u_5u_6^2 + u_5u_{12}^2 - 6u_5u_6u_{12} + 2u_6u_{11}u_{12}\right)\right]$$

$$k_{5,10} = 0$$

$$k_{5,11} = \frac{2EI_y}{L_0} - \frac{4EI_y}{105L_0}\left[16\left(u_5^2 + u_{11}^2\right) + \left(29u_6^2 - 19u_6u_{12} + 29u_{12}^2\right)\right]$$
$$+ \frac{4EI_z}{105L_0}\left[13u_6^2 + 19u_6u_{12} + 13u_{12}^2\right] - \frac{EA}{60}u_7\left(1 + \frac{u_7}{L_0}\right)$$
$$- \frac{EAL_0}{840}\left[3\left(u_5^2 + u_{11}^2\right) + \left(3u_6^2 - 4u_6u_{12} + 3u_{12}^2\right)\right]$$
$$- \frac{EA}{840}u_7\left[3\left(u_5^2 + u_{11}^2\right) + 3\left(u_6^2 - u_6u_{12} + u_{12}^2\right)\right]$$

$$k_{5,12} = 0$$

$$k_{6,6} = \frac{4EI_z}{L_0} - \frac{EI_z}{105L_0}\left[\left(512u_6^2 + 128u_6u_{12} + 24u_{12}^2\right) + \left(256u_5^2 - 104u_5u_{11} + 88u_{11}^2\right)\right]$$
$$- \frac{EI_y}{105L_0}\left[256u_5^2 + 232u_5u_{11} + 88u_{11}^2\right] + \frac{EA}{15}u_7\left(1 + \frac{u_7}{L_0}\right)$$
$$+ \frac{EAL_0}{420}\left[\left(12u_6^2 - 3u_6u_{12} + 3u_{12}^2\right) + \left(12u_5^2 - 3u_5u_{11} + u_{11}^2\right)\right]$$
$$+ \frac{EA}{560}u_7\left[\left(12u_6^2 - 2u_6u_{12} + 3u_{12}^2\right) + \left(12u_5^2 - 2u_5u_{11} + u_{11}^2\right)\right]$$

$$k_{6,7} = \frac{EA}{60}\left(1 + \frac{u_7}{L_0}\right)\left(4u_6 - u_{12}\right)$$
$$+ \frac{EA}{1680}\left[\left(12u_6^3 - 6u_6^2u_{12} + 3u_6u_{12}^2\right) + \left(12u_5^2u_6 + u_6u_{11}^2 - 6u_6u_5u_{11} + 2u_5u_{11}u_{12}\right)\right]$$

FORCE - DEFORMATION RELATIONS OF 3D AXIAL-FLEXURAL MEMBERS

(Sheet 1 of 2)

FIG. 4.6

$$k_{6,10} = 0.$$

$$k_{6,11} = 0.$$

$$k_{6,12} = \frac{2EI_z}{L_0} - \frac{4EI_z}{105L_0}\left[16\left(u_6^2 + u_{12}^2\right) + \left(29u_5^2 - 19u_5u_{11} + 29u_{11}^2\right)\right]$$
$$+ \frac{4EI_y}{105L_0}\left[13u_5^2 + 19u_5u_{11} + 13u_{11}^2\right] - \frac{EA}{60}u_7\left(1 + \frac{u_7}{L_0}\right)$$
$$- \frac{EAL_0}{840}\left[3\left(u_6^2 + u_{12}^2\right) + \left(3u_5^2 - 4u_5u_{11} + 3u_{11}^2\right)\right]$$
$$- \frac{EA}{840}u_7\left[3\left(u_6^2 + u_{12}^2\right) + 3\left(u_5^2 - u_5u_{11} + u_{11}^2\right)\right]$$

$$k_{7,7} = \frac{EA}{L_0} + \frac{EA}{30L_0}\left[\left(2u_5^2 - u_5u_{11} + 2u_{11}^2\right) + \left(2u_6^2 - u_6u_{12} + 2u_{12}^2\right)\right]$$

$$k_{7,10} = 0.$$

$$k_{7,11} = \frac{EA}{60}\left(1 + \frac{u_7}{L_0}\right)\left(4u_{11} - u_5\right)$$
$$+ \frac{EA}{1680}\left[\left(12u_{11}^3 - 6u_{11}^2u_5 + 3u_{11}u_5^2\right) + \left(12u_{11}u_{12}^2 + u_{11}u_6^2 - 6u_6u_{12}u_{11} + 2u_5u_6u_{12}\right)\right]$$

$$k_{7,12} = \frac{EA}{60}\left(1 + \frac{u_7}{L_0}\right)\left(4u_{12} - u_6\right)$$
$$+ \frac{EA}{1680}\left[\left(12u_{12}^3 - 6u_{12}^2u_6 + 3u_{12}u_6^2\right) + \left(12u_{12}u_{11}^2 + u_{12}u_5^2 - 6u_5u_{11}u_{12} + 2u_5u_6u_{11}\right)\right]$$

$$k_{10,10} = \frac{GJ}{L_0}$$

$$k_{10,11} = 0.$$

$$k_{10,12} = 0.$$

$$k_{11,11} = \frac{4EI_y}{L_0} - \frac{EI_y}{105L_0}\left[\left(512u_{11}^2 + 128u_5u_{11} + 24u_5^2\right) + \left(256u_{12}^2 - 104u_6u_{12} + 88u_6^2\right)\right]$$
$$- \frac{EI_z}{105L_0}\left(256u_{12}^2 + 232u_6u_{12} + 88u_6^2\right) + \frac{EA}{15}u_7\left(1 + \frac{u_7}{L_0}\right)$$
$$+ \frac{EAL_0}{420}\left[\left(12u_{11}^2 - 3u_5u_{11} + 3u_5^2\right) + \left(12u_{12}^2 - 3u_6u_{12} + u_6^2\right)\right]$$
$$+ \frac{EA}{560}u_7\left[\left(12u_{11}^2 - 2u_5u_{11} + 3u_5^2\right) + \left(12u_{12}^2 - 2u_6u_{12} + u_6^2\right)\right]$$

$$k_{11,12} = 0.0$$

$$k_{12,12} = \frac{4EI_z}{L_0} - \frac{EI_z}{105L_0}\left[\left(512u_{12}^2 + 128u_6u_{12} + 24u_6^2\right) + \left(256u_{11}^2 - 104u_5u_{11} + 88u_5^2\right)\right]$$
$$- \frac{EI_y}{105L_0}\left[256u_{11}^2 + 232u_5u_{11} + 88u_5^2\right] + \frac{EA}{15}u_7\left(1 + \frac{u_7}{L_0}\right)$$
$$+ \frac{EAL_0}{420}\left[\left(12u_{12}^2 - 3u_6u_{12} + 3u_6^2\right) + \left(12u_{11}^2 - 3u_5u_{11} + u_5^2\right)\right]$$
$$+ \frac{EA}{560}u_7\left[\left(12u_{12}^2 - 2u_6u_{12} + 3u_6^2\right) + \left(12u_{11}^2 - 2u_5u_{11} + u_5^2\right)\right]$$

FORCE-DEFORMATION RELATIONS OF 3D AXIAL-FLEXURAL MEMBERS

(Sheet 2 of 2)

FIG. 4.6

5. CONDITIONS AT DEAD LOAD AND CAMBER

A structure is said to be cambered when so constructed that it assumes a desired theoretical form for a defined condition of load. For the Southern Crossing Bridge, the requirements of camber are intimately related to several matters. They are related to the desired shape of the structure at full dead load, and also to the safety and response of the structure for subsequent conditions of load. They are exceedingly important to observe and obtain during fabrication of each element of the bridge, and during the erection sequence being proposed. If the requirements of camber are not closely obtained during fabrication and erection, the resulting bridge at full dead load can have severe residual stresses not taken into account in the analysis and in design. Such residuals can affect expected standards of maintenance, the stability, reserve strength, and response of the bridge for subsequent conditions of load; namely live load, wind load, temperature changes, subsidences, and seismic movements. Consequently, an accurate determination of camber is required for each element of the bridge.

The desired conditions at dead load serve as the bases for determining the unstressed dimensions of each element. The unstressed dimensions are required for fabrication, and for the analysis of the different load cases of the bridge. The Division of Bay Toll Crossings, the designers, supplied the desired conditions at dead load. The desired conditions were stated as follows: (A) The profile of the roadway lies along a parabola, with the coordinates and slopes at the end-points as specified. (B) The coordinates of work-points, make-up of members and details, dimensions and properties of sections (including

their eccentricities) and the distributions of dead load along the girder are in accordance with the design drawings. (C) In addition, the X, Y, Z,-components of the cable forces at the roadway level, the reactions at the end bents, and the displacements at the tops of the towers are as shown in Fig. 5.1.

Based on this information, a statical check was made of the distributions of loads along the girder considered by the writers and by the Division of Bay Toll Crossings. Comparisons are given in Fig. 5.2 of (1) the rections at the tower bearings, and (2) the moments at selected sections of the roadway girder as calculated by each group. Accepting the very slight differences in the results obtained by each group, the writers proceeded with the subsequent studies of the bridge subjected to full dead load.

5.1 Roadway Girder

The distribution of moments, axial forces, and shear along the girder are as shown in Fig. 5.1 (II)*. These are calculated by means of the general computer program (GENLIN) for linear elastic structures. It is observed that with the preceding information supplied by the designers, the internal forces and moments along the girder are a direct consequence of statics. The calculations of statics are in accordance with the geometry of the girder at full dead load. In brief; for the given conditions at full dead load the roadway girder is statically determinate.

To obtain the dimensions of each member in its unstressed state, the nonlinear stiffness matrix developed for 2D axial-flexural members

---

* The Roman numeral II designates that the Figure is given in Volume II.

(see Fig. 4.5) is employed. The stiffness matrix relates the forces with the deformations at the ends of each member as follows:

$$\{p\} = [k] \{u\} \tag{5.1}$$

For each member, the values of $\{p\}$ and the stressed length at full dead load are known. A subroutine called RELAX is employed to solve Eq. 5.1 for the deformations, $\{u\}$. Because $[k]$ is a function of $\{u\}$, the equation is solved by iteration. From the values of $\{u\}$ and the dimensions of the member at full dead load, the unstressed length and the cutting angles at the ends of the member are determined. This information is required for fabrication and is summarized in Table 5.1.

5.1a Camber of the Roadway Girder

The camber of the girder is obtained through elementary considerations of geometry. Because the distances, y_t, of the centroidal axes of the members measured from the top of the roadway vary along the girder, we describe only the determination of the top surface of the girder. The girder is weightless and unstressed. See Fig. 5.3 for the geometry of two adjacent members of the unstressed girder, and Fig. 5.4 for the polygon (shown as a curve in the Figure) which represents the top surface of the girder. It is required to obtain the x, y-coordinates and the angle-break, ψ, at each node point, with reference to selected axes. The selected x-axis is parallel to the horizontal axis which goes through both bearings of the roadway, and the origin of the selected x, y axes is at the hinged bearing. The calculations for the required coordinates and angle-breaks are as follows:

(1) For each member, calculate the unstressed length at the top of the member. (See Fig. 5.5)

(2) At each station N, calculate the angle break ψ_N, between the adjacent members. (See Fig. 5.3)

(3) Guess at the x, y coordinates of node point 1, and at the slope of the first member at the left end of the girder. (See Fig. 5.4). Then sequentially calculate from left to right the x, y coordinates of each node point, and the slope of each segment of the polygon.

The unstressed segments of the girder in step (3) are placed end to end with the transverse section at end j of a segment m in contact with the transverse section at end i of segment n. (See Fig. 5.3). Note that the calculations in this step are conducted in exactly the same way as those conducted in surveying when a polygon with given angles between segments of given lengths is traversed. Also note that the shape of the unstressed girder is independent of the set of coordinate axes selected in step (3). The selected axes merely serve for reference.

(4) In step (4), select a set of references axes for the camber diagram which is more convenient than that arbitrarily selected in step (3). Select the horizontal line which goes through the roller bearing at A and the pinned bearing at B. Also, select point B of the unstressed girder (i.e. the camber diagram) to coincide with point B of the girder subjected to dead load. (See Fig. 5.4) Now transform the coordinates of the camber diagram in step (3) to the coordinate axes of step (4). The latter transformation consists of a coordinate translation in the X, Y-plane and a coordinate rotation about the Z-axis.

Essentially, the camber diagram in step (3) is translated and rotated as a rigid body in the X, Y-plane; until points B of the stressed and the unstressed girders coincide, and points A of both girders are on a horizontal line.

The camber diagrams for the roadway girder are given in Fig. 5.2 (II). Included is a diagram called the X-camber. The diagram shows the difference between the X-coordinates of corresponding node points of the unstressed and the stressed girder. The diagrams in Fig. 5.2 (II) are obtained by means of a subroutine, called CAMBER. It is emphasized that the subroutine is based on considerations of nonlinear force-deformation relations for each member, and on the geometry of large displacements; that is, the calculations are in accordance with a non-linear theory. Both axial and flexural deformations and eccentricities of the centroidal axes of the girder are taken into account.

An independent check of the camber diagram was made by means of the computer program called NONLIN. The unstressed girder was loaded with the external dead load forces and reactions as specified by the designers. The shape of the stressed girder at full dead load was calculated to be the same as that specified by the designers, and the distributions of the internal forces and moments along the stressed girder were the same as those given in Fig. 5.1 (II). They were the same within acceptable tolerances of round-off error. The differences between the given and the calculated values were at most in the sixth bit of a ten-bit output.

A further check was made by means of the program called CAMBER, in which the camber diagram was calculated for the case of the member forces of the girder equal to zero. The camber diagram then coincided with the profile of the girder as specified by the designers.

5.1b Approximations of Camber

Another set of camber diagrams is given in Fig. 5.2 (II). The diagrams are approximations of the true camber diagrams given in the same Figure. They are exact, however, if the assumptions of the classical linear theory in regard to calculations of geometry are accepted. The approximate diagrams of Fig. 5.2 (II) are obtained as follows:

Analyze the girder by means of the classical linear theory. The girder is loaded with the external set of dead loads, cable forces, and anchorage pier reactions as specified by the designers. It is supported on a hinged bearing at B and a roller bearing at A. The shape of the roadway profile and the makeup of the members are the same as those shown in the design drawings. In the analysis, form K_E and solve

$$P = K_E U \tag{5.2}$$

for U. Then determine u from U, and p from

$$p = k_E u \tag{5.3}$$

Now review the assumptions of the linear theory and observe the following: (1) The internal forces and moments along the girder (see Fig. 5.1 (II) are statically determinate for the given conditions of load. The equations of statics are in accordance with the dimensions of the girder at full dead load. (2) The magnitudes of the deformations u are linearly related to p and are based on Hooke's Law (see Eq. 5.3). (3) The calculations of the node point displacements are based on the following assumptions of geometry: The deformations, rotations,

and displacements are small, and the usual definition of a small angle-change is accepted. In the analysis, the contributions of a deformation $\{u\}$ at a point i to displacements $\{U\}$ at a point j are given in global form by

$$\begin{bmatrix} 1 & 0 & -(Y_j - Y_i) \\ 0 & 1 & (X_j - X_i) \\ 0 & 0 & 1 \end{bmatrix} \begin{Bmatrix} u_X \\ u_Y \\ u_Z \end{Bmatrix} = \begin{Bmatrix} U_X \\ U_Y \\ U_Z \end{Bmatrix} \tag{5.4}$$

The positions and directions of the member deformations are assumed to be in accordance with the given profile of the roadway at full dead load.

Based on the preceding assumptions, displacement diagrams of the girder are given in Fig. 5.3 (II).

A common expedient in obtaining the coordinates of a camber diagram of a girder is to deduct the calculated displacements caused by dead load from the coordinates of the girder at conditions of dead load. The approximate camber diagrams given in Fig. 5.2 (II) are calculated in this way.

A comparison of the approximate and the true camber diagram shown in Fig. 5.2 (II) yields the following: The approximate Y-diagram differs but little from the true. The difference between the two Y-diagrams is 0.004 ft. at the center of the bridge and 0.009 ft. at each end bent. More important differences exist between the approximate and the true X-diagrams. They are of sufficient importance to require an accurate determination of camber for the final design of the girder. The writers prefer to obtain the camber requirements of the roadway girder by relaxing each member of the girder of its dead load stress and then

simply conducting a traverse of the unstressed girder; or else, to obtain the camber requirements by unloading the girder of its dead load forces and conducting an analysis based on the nonlinear theory of elastic structures.

5.2 Cables

The shape of each cable under its own weight is a catenary, assuming that flexural deformations are neglected. In Fig. 5.6, a catenary is shown which lies in a local x, y-plane. The origin of the x, y-axes is at end i of the cable, and the y-axis is parallel to the force of gravity. In terms of these axes the shape of the catenary (4) is given by

$$y = \frac{H}{w} \cosh \left(\frac{w}{H} x + a_1\right) + a_2 \tag{5.5}$$

in which

$$a_2 = - \frac{H}{w} \cosh a_1 \tag{5.6}$$

$$a_1 = \sinh^{-1} \left[\frac{wh}{2H \cdot \sinh r} \right] - r \tag{5.7}$$

and

$$r = \frac{w}{2} \frac{L}{H} \tag{5.8}$$

Term H in these equations is the horizontal component of the cable tension, w is the weight per unit of length, L is the base length, and h is the vertical distance between ends i and j of the cable. The slope of the cable as a function of x may be desired as a check during erection. It is given by

$$\frac{dy}{dx} = \sinh \left(\frac{w}{H} x + a_1 \right) \tag{5.9}$$

from which the end slopes at ends i and j, respectively are given by

$$\tan \theta_i = \sinh a_1 = \frac{w}{H} \left[h \cdot \coth r - L_s \right] \tag{5.10}$$

and

$$\tan \theta_j = \sinh (2r + a_1) = \frac{w}{2H} \left[h \cdot \coth r + L_s \right] \tag{5.11}$$

in which L_s is the length of the stressed cable. The vertical components of cable tension at ends i and j are given by

$$V_i = \frac{w}{2} \left[h \cdot \coth r - L_s \right] \tag{5.12}$$

$$V_j = \frac{w}{2} \left[h \cdot \coth r + L_s \right] \tag{5.13}$$

The length of the stressed cable is defined by

$$L_s = \int_i^j ds = \int_0^L \left[1 + \left(\frac{dy}{dx} \right)^2 \right]^{\frac{1}{2}} \cdot dx \tag{5.14}$$

or

$$L_s = \int_0^L \cosh \left(\frac{wx}{H} + a_1 \right) \cdot dx \tag{5.15}$$

which yields

$$L_s = \frac{H}{w} \left[\sinh \left(\frac{wL}{H} + a_1 \right) - \sinh a_1 \right] \tag{5.16}$$

Eq. 5.16 can be rewritten as

$$L_s = \left[h^2 + \frac{4H^2}{w^2} \sinh^2 r \right]^{\frac{1}{2}} \tag{5.17}$$

or

$$\left[L_s^2 - h^2 \right]^{\frac{1}{2}} = \frac{2H}{w} \sinh r \tag{5.18}$$

For checks during erection, the maximum sag, s, measured perpendicular to the chord between ends i and j may be desired. At x_s, the horizontal distance to the point of maximum sag, the slope equals $\frac{h}{L}$. Consequently,

$$x_s = \frac{H}{w} \left[\sinh^{-1} \frac{h}{L} - a_1 \right] \tag{5.19}$$

and

$$y_{(x_s)} = \frac{H}{w} \left[\sec \theta_c - \cosh a_1 \right] \tag{5.20}$$

in which θ_c is the angle measured from the x-axis to the chord between ends i and j. The magnitude of the maximum sag is given by

$$s = x_s \cdot \sin \theta_c - y_{(x_s)} \cdot \cos \theta_c \tag{5.21}$$

The length of the unstressed cable, L_u, is required as information for provisions to be made at the ends of the cable during fabrication and erection. Also, it specifically is required in the nonlinear theory of structures developed by the writers. It is

obtained as follows: Consider a differential length, ds, of the cable as shown in Fig. 5.7 subjected to a tension force, T. From Hooke's Law, we have

$$\frac{T}{AE} = \frac{ds - ds_u}{ds_u} \tag{5.22}$$

in which ds_u is the unstressed length of the differential element. Eq. 5.22 can be rewritten as

$$ds_u = \frac{ds}{1 + \frac{T}{AE}} \tag{5.23}$$

Because $\frac{T}{AE}$ is small relative to 1.0, ds_u is approximated by

$$ds_u \cong \left(1 - \frac{T}{AE}\right) ds \tag{5.24}$$

However, T as a function of x is given by

$$T = H \frac{ds}{dx} = H \cdot \cosh\left(\frac{wx}{H} + a_1\right) \tag{5.25}$$

and ds by

$$ds = \cosh\left(\frac{wx}{H} + a_1\right) dx \tag{5.26}$$

Eqs. 5.24 to 5.26 yield

$$ds_u = \left[1 - \frac{H}{AE} \cosh\left(\frac{wx}{H} + a_1\right)\right] \cosh\left(\frac{wx}{H} + a_1\right) dx \tag{5.27}$$

From the relation

$$L_u = \int_0^{L_u} ds_u \tag{5.28}$$

the unstressed length, L_u, of the cable is obtained; namely,

$$L_u = \frac{H}{w}\left\{\sinh\left(\frac{wL}{H} + a_1\right) - \sinh a_1\right\} - \frac{H^2}{2AEw}\left\{\begin{array}{l}\left[\left(\frac{wL}{H} + a_1\right) + \sinh\left(\frac{wL}{H} + a_1\right)\cosh\left(\frac{wL}{H} + a_1\right)\right] \\ -\left[a_1 + \sinh a_1 \cdot \cosh a_1\right]\end{array}\right\} \tag{5.29}$$

in which a_1 is given by Eq. 5.7. An inspection of Eq. 5.29 shows that the first term within the brackets is equal to the length of the stressed cable; that is,

$$L_s = \frac{H}{w}\left\{\sinh\left(\frac{wL}{H} + a_1\right) - \sinh a_1\right\} \tag{5.30}$$

Then, the change in length from the unstressed state to the stressed state is given by

$$\Delta L_{us} = \frac{H^2}{2AEw}\left\{\begin{array}{l}\left[\left(\frac{WL}{H} + a_1\right) + \sinh\left(\frac{wL}{H} + a_1\right)\cosh\left(\frac{wL}{H} + a_1\right)\right] \\ -\left[a_1 + \sinh a_1 \cdot \cosh a_1\right]\end{array}\right\} \tag{5.31}$$

For the magnitudes of the force components at end i of each cable as specified for the condition of dead load, the values of the remaining parameters for the bridge are determined as follows: (1) The unbalanced force components, P_x, at the top of each tower and at each

roadway bearing are calculated from statics. (2) For these values of force components, the displacements, U_X, at the top and intermediate struts of each tower are calculated by means of the general program for linearly elastic structures. (3) The coordinates of the hinged bearing and of end j of each cable are determined by considerations of geometry. In the same way, the coordinates of the work points (W. P) along the roadway and of end i of each cable are determined from the profile requirements of the roadway and the coordinates at the hinged bearing. We now have all the information required to calculate the unstressed lengths of the various cables, and the values of any additional parameters of the cables that may be desired for the condition of dead load.

Summaries are given in Tables 5.2 to 5.9 for the values of certain parameters for each cable of the bridge (see Fig. 5.8). Dead load conditions are considered and are based on the weight of each cable given in Table 2.1. Among the various parameters listed are the stressed and unstressed lengths, the slopes of the chord and of the tangents at ends i and j, the sag, the horizontal cable tension, and the resultant force and its global components at ends i and j. The values of these parameters are required for provisions to be made during fabrication and erection. The values of other parameters, if desired, are easily calculated. A subroutine, called CABLE, is employed in making the calculations. The subroutine is based on the properties of a catenary as given in Eqs. 5.1 through 5.31.

5.3 Towers

The distributions of forces and moments along the various members of each tower are considered for two conditions of dead load.

The two conditions are (1) dead load of the tower alone after the tower is erected, and (2) full dead load of the tower and bridge after the entire bridge is erected. Condition (1) is referred to as stage (T) of the tower, and condition (2) as stage (B).

Let ϕ represent a function of interest for either stage.

For stage (B), the value of a function is given by

$$\phi^{(B)} = \phi_o^{(B)} + \phi_R^{(B)} \tag{5.32}$$

in which

$$\phi_o^{(B)} = \phi_1^{(B)} + \phi_2^{(B)} \tag{5.33}$$

In Eqs. 5.32 and 5.33, the subscripts o, 1, 2, and R designate installments to the final value of the function, and superscript (B) designates that the function is associated with the full dead load of the bridge. The term without a subscript designates the final value of the function.

In the succeeding discussion, functions of interest are the axial force and moment at a section of a tower. Let

$$\bar{p} = \begin{Bmatrix} p \\ m \end{Bmatrix} \tag{5.34}$$

in which p is the axial force at the centroid and m is the moment about the centroidal axis of the section. The centroidal axis is parallel to the global X-axis. Other functions of interest are the stresses at a section. Let

$$\bar{\sigma} = \begin{Bmatrix} \sigma_a \\ \sigma_b \end{Bmatrix} = \begin{bmatrix} 1/A & o \\ o & c/I \end{bmatrix} \begin{Bmatrix} p \\ m \end{Bmatrix} \tag{5.35}$$

in which σ_a is the axial stress at the centroid and σ_b is the bending stress at the extreme fiber of the section. In Eq. 5.35, A and I are properties of the transformed section, and c is the transverse distance measured from the centroidal axis to the extreme fiber of the section. It is assumed in this study that cracking of a section does not occur, and that Eq. 5.35 is applicable for the concrete and the steel towers. The total stress in the extreme fibers of a section then is given by

$$\sigma = \sigma_a \pm \sigma_b \tag{5.36}$$

For further purposes, let

$$e = \frac{m}{p} \tag{5.37}$$

in which e designates the eccentricity of the pressure line, or of the resultant force acting on the section, measured from the centroidal axis of the section. Also, let

$$e_m = \frac{I}{Ac} = \frac{r^2}{c} \tag{5.38}$$

in which e_m designates the limiting lateral dimension of the kern of the section, measured in the same direction as e. It remains to explain the various installments to the functions of stage (B), the final values of the functions, and how they are obtained.

Installments 1 and 2 of (B), see Fig. 5.9, are for an imaginary structure and are introduced for computation purposes only. Installment 1 is for the dead load of the tower only, and installment 2 for the dead load reactions of the cables at the saddle tops and of the roadway at the bearings. Each of these installments is calculated as if the dead load is suddenly flashed onto an imaginary weightless tower with properties and dimensions as selected by the designers. Obviously the real dead load will not be applied as imagined for these installments. The final condition of the tower, for stages (T) and (B) will depend on the erection sequence to be selected and on the provisions to be made during erection. Included among these provisions may be temporary braces, struts, prestressing, cambering, falsework, and erection equipment. The writers have not been supplied with the erection sequence to be selected for either the concrete or the steel towers. The erection sequence is to be selected by the contractor and is to be approved by the designers. The writers in need of the dead load condition of the tower and bridge for subsequent calculations of the nonlinear behavior of the bridge, present a procedure for the determination of the condition of the tower at stage (B). (The condition of the tower at stage (T) is obtained from stage (B) by means of the nonlinear theory developed by the writers. In the latter study, the tower is unloaded from stage (B) to stage (T) by removing the dead load reactions at the saddle tops and at the roadway bearings.)

The procedure for the determination of the tower at stage (B) is independent of the erection sequence selected. It is applicable to the concrete and to the steel tower; assuming for the concrete tower that sections are not severely cracked during intermediate stages of

erection, and for the steel tower that buckling or yielding does not occur during the same stages. The procedure is illustrated for Tower 1 only. The results for Tower 2 are almost the same. For purposes of achieving definiteness, the following assumptions and objectives of design are selected by the writers:

(1) For every stage of erection, including stages (T) and (B), the resultant pressure line at each section of a tower leg is to be within the kern of the section. Because of the big values of saddle and roadway reactions for stage (B), tension in the struts is allowed; or else prestressing of the legs and struts need be considered. In this study, prestressing is precluded.

(2) For stage (B), the camber of each member is to be such that the final coordinates and geometry of the tower are as prescribed by the Division of Bay Toll Crossings in the design drawings.

(3) Also for stage (B), the distributions of forces and moments in the tower are to meet a specified optimum condition. A possible optimum condition is selected by the writers for illustration only. Other optimum conditions are possible and are briefly discussed. If specified, they can be studied further.

Installments 1 and 2 of (B) are analyzed in accordance with the linear theory of elastic structures, and installment 0 of (B) is obtained by superposition (see Eq. 5.33). The results for these installments are given in Fig. 5.4 (II). In Table 5.10, summaries are given of axial forces and moments associated with installment 0. The axial forces and moments are at 7 selected sections of the tower legs. The properties of the selected sections are given in Table 5.11. A summary is given in Table 5.12 of calculated stresses at these sections

for installment 0. Tension exists in the extreme fibers of member 103. Consequently, the distributions of forces and moments in the legs of the tower for installment 0 doe not meet the objectives in design selected by the writers.

In any case, the internal forces and moments of installment 0 of (B) are in equilibrium with the dead loads of stage (B). The equations of equilibrium are with reference to the geometry of the tower for stage (B), as prescribed by the Division of Bay Toll Crossings in the design drawings. However, the set of internal forces and moments as calculated in accordance with the linear theory of elastic structures is but one of an infinite number of statically possible distributions of forces and moments for the given stage. To the latter installment, installment R of (B) is added which does not disturb the requirements of equilibrium (see Fig. 5.9). Installment R of (B) is internally self-balancing, that is, the external loads of the installment are zero. For reference, the magnitudes of the axial forces and moments at the mid-points of the two horizontal struts are selected as redundants. Only four are selected, although if prestressing of the struts only is permissible at least six can be selected. The four that are selected to illustrate the procedure are designated by $X_1^{(B)}$ to $X_4^{(B)}$. Based on statics, the axial force, $p_{nR}^{(B)}$, at a section n of the tower is given by

$$p_{nR}^{(B)} = p_{n1}^{(B)}X_1^{(B)} + p_{n2}^{(B)}X_2^{(B)} + p_{n3}^{(B)}X_3^{(B)} + p_{n4}^{(B)}X_4^{(B)} = \sum_{i=1}^{4} p_{ni}^{(B)}X_i^{(B)} \quad (5.39)$$

and the moment, $m_{nR}^{(B)}$, by

$$m_{nr}^{(B)} = m_{n1}^{(B)}X_1^{(B)} + m_{n2}^{(B)}X_2^{(B)} + m_{n3}^{(B)}X_3^{(B)} + m_{n4}^{(B)}X_4^{(B)} = \sum_{i=1}^{4} m_{ni}^{(B)}X_i^{(B)} \quad (5.40)$$

in which the coefficients $p_{ni}^{(B)}$ and $m_{ni}^{(B)}$ are calculated in accordance with the geometry of the tower for stage (B). From Eq. 5.32, the final values of the axial force and moment at section n respectively are given by

$$p_n^{(B)} = p_{no}^{(B)} + \Sigma\ p_{ni}^{(B)} X_i^{(B)} \tag{5.41}$$

$$m_n^{(B)} = m_{no}^{(B)} + \Sigma\ m_{ni}^{(B)} X_i^{(B)} \tag{5.42}$$

We are reminded that the values of $X_i^{(B)}$ are independent of the selected erection procedure. Then, the question arises as to what values of $X_i^{(B)}$ are deemed most desirable for the condition of full dead load of the bridge. Various criteria can be established for the determination of the most suitable set of $X_i^{(B)}$. For example, the criterion can be that the final pressure line for full dead-load approximates most closely the center-lines of the legs of the tower. In this case, the distribution of stress across each section of a leg is approximately uniform, and all material of the leg is used to its best advantage in resisting dead load. But in addition, each portion of the tower has the greatest reserve strength for resisting cracking (buckling or yielding of the steel tower) caused by subsequent loads or effects; for example, seismic effects. For another example, the criterion can be that the final values of axial forces and moments and of the associated deformations must meet the requirement of minimum strain energy to resist full dead load. If desired, the criterion can be based on achieving a minimum weight of tower.

Again, for achieving definiteness and for simplicity of obtaining a solution, the writers specified the following criteria for obtaining the optimum values of $X_i^{(B)}$:

(1) For the 7 sections listed in Table 5.10, each extreme fiber stress at sections n shall be in compression; that is,

$$\sigma_n = (p_{no} + \Sigma\, p_{ni} X_i)\frac{1}{A_n} - (m_{no} + \Sigma\, m_{ni} X_i)\frac{cn}{I_n} \geqq 0 \qquad (5.43)$$

(2) The selected values of X_i shall meet the requirement,

$$\Sigma\ |X_i| = \text{minimum} \qquad (5.44)$$

Note that Eq. 5.43 and each inequality of Eq. 5.44 are linear in terms of X_i. Consequently, a solution to Eqs. 5.43 and 5.44 is obtained by means of linear programming (5). A standard computer program on file in the Computer Center Library of the University of California, Berkeley was employed to obtain a solution to Eqs. 5.43 and 5.44. The calculated values of $X_1^{(B)}$ to $X_4^{(B)}$ were adjusted after an inspection was made of the results obtained for additional sections of the tower. The final values of $X_1^{(B)}$ to $X_4^{(B)}$ selected for this study are

$$X_1^{(B)} = -100.0 \text{ Kips} \qquad (5.45)$$

$$X_2^{(B)} = 0. \qquad (5.46)$$

$$X_3^{(B)} = 93.1 \text{ kips} \qquad (5.47)$$

$$X_4^{(B)} = 12035.3 \text{ kip-ft} \qquad (5.48)$$

The final distributions of axial forces and moments in the tower for stage (B) are calculated by means of Eqs. 5.41 and 5.42. Summaries are given in Table 5.10 of axial forces and moments associated with installment R and with stage (B). The axial forces and moments are at the 7 selected sections of the tower legs. A summary is given in Table 5.12 of the calculated stresses at these sections for stage (B). Now note that the resultant pressure line at each section of the tower legs is within the kern of the section.

For stage (B), the distributions of axial forces and moments given in Fig. 5.5 (II) are used to determine the dimensions of each unstressed member of the tower. The latter dimensions are required in the subsequent studies of the nonlinear behavior of the bridge.

For each member of the tower, the values of $\{p\}$ and the stressed length for stage (B) now are known. As for the members of the roadway girder, the subroutine called RELAX is employed to solve

$$\{p\} = [k] \{u\} \tag{5.49}$$

for the deformations $\{u\}$. A nonlinear relation between $\{p\}$ and $\{u\}$ is used. The dimensions of each unstressed member of the tower are given in Table 5.13.

TABLE 5.1

INITIAL LENGTHS AND ANGLES AT THE ENDS OF EACH MEMBER OF THE GIRDER

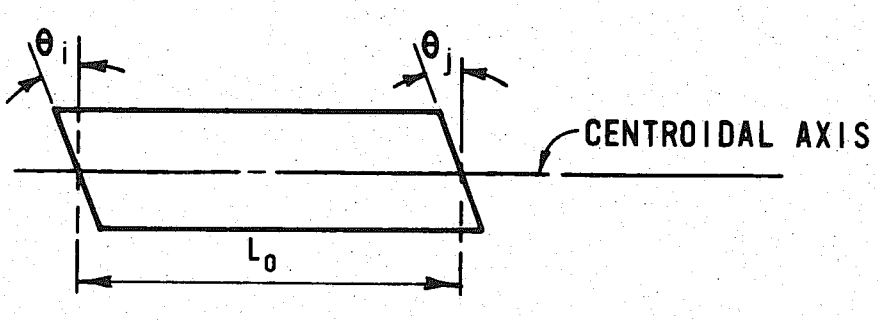

MEMBER	UNSTRESSED LENGTH, L_0 (IN FEET)	INITIAL ANGLES θ (IN 1/1000 RADIANS)	
		θ_i	θ_j
1	41.510	−.20572	+.41144
2	11.003	−.11028	+.12113
3	11.004	−.15884	+.15532
4	24.008	−.38110	+.37007
5	40.012	−.65373	+.65383
6	40.011	−.69686	+.73980
7	20.005	−.36229	+.37943
8	20.004	−.37704	+.39753
9	20.004	−.40550	+.42906
10	14.002	−.30591	+.35855
11	11.002	−.21031	+.21708
12	11.002	−.22272	+.21579
13	24.005	−.47452	+.44058
14	20.004	−.35613	+.33558
15	20.004	−.32968	+.31234
16	30.006	−.46676	+.43819
17	40.009	−.60494	+.58480
18	40.008	−.58396	+.60327
19	20.003	−.28327	+.29462
20	24.003	−.31474	+.33573
21	21.002	−.29835	+.31831
22	21.002	−.32255	+.30684
23	34.003	−.50056	+.47349
24	20.002	−.28743	+.28355
25	50.005	−.80989	+.53516

TABLE 5.1 (CONTINUED)
INITIAL LENGTHS AND ANGLES AT THE ENDS OF EACH MEMBER OF THE GIRDER

MEMBER	UNSTRESSED LENGTH, L_o (IN FEET)	INITIAL ANGLES θ (IN 1/1000 RADIANS)	
		θ_i	θ_j
26	20.001	−.31940	+.33082
27	20.001	−.32555	+.34054
28	30.001	−.53362	+.57709
29	24.000	−.48700	+.52075
30	11.000	−.22988	+.23671
31	11.000	−.23379	+.22840
32	23.999	−.59582	+.56879
33	19.999	−.46854	+.45352
34	19.999	−.46257	+.45114
35	44.999	−1.05840	+1.03530
36	44.998	−1.04250	+1.07280
37	23.999	−.54322	+.56090
38	11.000	−.22817	+.23264
39	10.999	−.20346	+.19300
40	13.998	−.34073	+.31703
41	29.995	−.58416	+.47822
42	39.994	−.38674	+.21817
43	39.993	+.07137	−.19234
44	39.994	+.40625	−.48412
45	44.993	+.66628	−.70032
46	44.993	+.70007	−.66578
47	39.994	+.48326	−.40518
48	39.993	+.19095	−.06979
49	39.994	−.22014	+.38890
50	29.995	−.47989	+.58592
51	13.998	−.31784	+.34156
52	10.999	−.19343	+.20399
53	11.000	−.23311	+.22861
54	23.999	−.56178	+.54394
55	44.998	−1.07320	+1.04220
56	44.999	−1.03360	+1.05600
57	19.999	−.44970	+.46100
58	19.999	−.45177	+.46667
59	23.999	−.56634	+.59321
60	11.000	−.22746	+.23284

TABLE 5.1 (CONTINUED)
INITIAL LENGTHS AND ANGLES AT THE ENDS OF EACH MEMBER OF THE GIRDER

MEMBER	UNSTRESSED LENGTH, L_0 (IN FEET)	INITIAL ANGLES θ (IN 1/1000 RADIANS)	
		θ_i	θ_j
61	11.000	−.23570	+.22886
62	24.000	−.51768	+.48381
63	30.001	−.57256	+.52892
64	20.001	−.33704	+.32199
65	20.001	−.32688	+.31537
66	50.001	−.82361	+.79778
67	20.002	−.27871	+.28250
68	34.003	−.46520	+.49205
69	21.002	−.30172	+.31735
70	21.002	−.31304	+.29311
71	24.003	−.32929	+.30833
72	20.003	−.28848	+.27716
73	40.008	−.59008	+.57089
74	40.004	−.57197	+.59223
75	30.006	−.42965	+.45829
76	20.004	−.30720	+.32456
77	20.004	−.33087	+.35144
78	24.004	−.43549	+.46946
79	11.002	−.21387	+.22081
80	11.002	−.21522	+.20848
81	14.002	−.31564	+.30306
82	20.004	−.42497	+.40157
83	20.004	−.39362	+.37330
84	20.005	−.37569	+.35873
85	40.011	−.73308	+.69096
86	40.012	−.64958	+.65031
87	24.008	−.36886	+.38013
88	11.004	−.15506	+.15862
89	11.003	−.12113	+.11028
90	41.510	−.41144	+.20572

TABLE 5.2: REFERENCE COORDINATES, LENGTHS, AND FORCES OF CABLE A.
SEE FIG 5.8 FOR NOTATIONS

CABLE	GLOBAL COORDINATES (FEET)					
	END I			END J		
	X	Y	Z	X	Y	Z
	-1100.3	224.46	58.000	-650.11	457.93	10.330
	LOCAL COORDINATES AND SLOPES					
	SLOPES (RADIANS)			COORDINATES (FEET)		
	CHORD, θ_C	END I, θ_I	END J, θ_J	SAG	X-SAG	Y-SAG
	.51572	.49479	.53677	2.1113	226.68	114.53
	LENGTHS (FEET)					
	BASE BL	CHORD CL	STRESSED L	UNSTRESSED L_0	CHANGE ΔL	
(A)	452.71	509.36	509.39	508.23	1.1584	
	FORCES AT END I (KIPS)					
	RESULTANT T	HOR. COMP. H	GLOBAL COMPONENTS F_X	F_Y	F_Z	
	4674.4	4187.4	-4164.1	-2077.3	440.91	
	FORCES AT END J (KIPS)					
	RESULTANT T	HOR. COMP. H	GLOBAL COMPONENTS F_X	F_Y	F_Z	
	4752.5	4187.4	4164.2	2247.7	-440.94	

TABLE 5.3: REFERENCE COORDINATES, LENGTHS, AND FORCES OF CABLE B.
SEE FIG. 5.8 FOR NOTATIONS

CABLE	GLOBAL COORDINATES (FEET)						
	END I			END J			
	X	Y	Z	X	Y	Z	
	-900.01	229.46	58.000	-650.11	459.76	12.250	
	LOCAL COORDINATES AND SLOPES						
	SLOPES (RADIANS)			COORDINATES (FEET)			
	CHORD, θ_C	END I, θ_I	END J, θ_J	SAG	X-SAG	Y-SAG	
	.90650	.89175	.92133	.69579	127.18	114.35	
	LENGTHS (FEET)						
(B)	BASE BL	CHORD CL	STRESSED L	UNSTRESSED L_0	CHANGE ΔL		
	254.05	342.90	342.90	342.04	.86515		
	FORCES AT END I (KIPS)						
	RESULTANT T	HOR. COMP. H	GLOBAL COMPONENTS F_X	F_Y	F_Z		
	3326.8	2482.5	-2442.0	-2214.6	447.06		
	FORCES AT END J (KIPS)						
	RESULTANT T	HOR. COMP. H	GLOBAL COMPONENTS F_X	F_Y	F_Z		
	3375.6	2482.5	2442.0	2287.2	-447.06		

TABLE 5.4: REFERENCE COORDINATES, LENGTHS, AND FORCES OF CABLE C.
SEE FIG. 5.8 FOR NOTATIONS

CABLE	GLOBAL COORDINATES (FEET)						
	END I			END J			
	X	Y	Z	X	Y	Z	
	-419.94	237.38	58.000	-650.11	459.76	12.250	
	LOCAL COORDINATES AND SLOPES						
	SLOPES (RADIANS)			COORDINATES (FEET)			
	CHORD, θ_C	END I, θ_I	END J, θ_J	SAG	X-SAG	Y-SAG	
	.94762	.93170	.96362	.67982	117.49	110.40	
	LENGTHS (FEET)						
	BASE BL	CHORD CL	STRESSED L	UNSTRESSED L_0	CHANGE ΔL		
(C)	234.67	323.30	323.31	322.58	.72711		
	FORCES AT END I (KIPS)						
	RESULTANT T	HOR. COMP. H	GLOBAL COMPONENTS F_X	F_Y	F_Z		
	2964.7	2186.0	2126.4	-2022.2	422.66		
	FORCES AT END J (KIPS)						
	RESULTANT T	HOR. COMP. H	GLOBAL COMPONENTS F_X	F_Y	F_Z		
	3010.8	2186.0	-2126.4	2089.1	-422.66		

TABLE 5.5: REFERENCE COORDINATES, LENGTHS, AND FORCES OF CABLE D.
SEE FIG. 5.8 FOR NOTATIONS

CABLE	GLOBAL COORDINATES (FEET)					
	END I			END J		
	X	Y	Z	X	Y	Z
	-219.88	238.98	58.000	-650.11	457.93	10.330
	LOCAL COORDINATES AND SLOPES					
	SLOPES (RADIANS)			COORDINATES (FEET)		
	CHORD, θ_C	END I, θ_I	END J, θ_J	SAG	X-SAG	Y-SAG
	.50582	.48720	.52453	1.8026	216.70	107.59
	LENGTHS (FEET)					
	BASE BL	CHORD CL	STRESSED L	UNSTRESSED L_0	CHANGE ΔL	
(D)	432.86	485.09	485.10	483.93	1.1766	
	FORCES AT END I (KIPS)					
	RESULTANT T	HOR. COMP. H	GLOBAL COMPONENTS F_X	F_Y	F_Z	
	4989.8	4483.9	4456.6	-2189.3	493.76	
	FORCES AT END J (KIPS)					
	RESULTANT T	HOR. COMP. H	GLOBAL COMPONENTS F_X	F_Y	F_Z	
	5063.2	4483.9	-4456.6	2351.9	493.79	

TABLE 5.6: REFERENCE COORDINATES, LENGTHS, AND FORCES OF CABLE E.
SEE FIG. 5.8 FOR NOTATIONS

CABLE	GLOBAL COORDINATES (FEET)						
	END I			END J			
	X	Y	Z	X	Y	Z	
	219.88	238.98	58.000	649.98	457.93	10.330	
	LOCAL COORDINATES AND SLOPES						
	SLOPES (RADIANS)			COORDINATES (FEET)			
	CHORD, θ_C	END I, θ_I	END J, θ_J	SAG	X-SAG	Y-SAG	
	.50597	.48739	.52464	1.7976	216.64	107.60	
	LENGTHS (FEET)						
	BASE BL	CHORD CL	STRESSED L	UNSTRESSED L_0	CHANGE ΔL		
(E)	432.73	484.97	484.99	483.81	1.1789		
	FORCES AT END I (KIPS)						
	RESULTANT T	HOR. COMP. H	GLOBAL COMPONENTS				
			F_X	F_Y	F_Z		
	5000.7	4493.7	-4466.3	-2194.1	494.99		
	FORCES AT END J (KIPS)						
	RESULTANT T	HOR. COMP. H	GLOBAL COMPONENTS				
			F_X	F_Y	F_Z		
	5074.6	4493.7	4466.3	2357.6	-495.03		

TABLE 5.7: REFERENCE COORDINATES, LENGTHS, AND FORCES OF CABLE F.
SEE FIG. 5.8 FOR NOTATIONS

CABLE	GLOBAL COORDINATES (FEET)					
	END I			END J		
	X	Y	Z	X	Y	Z
	419.94	2373.8	58.000	649.98	459.76	12.250
	LOCAL COORDINATES AND SLOPES					
	SLOPES (RADIANS)			COORDINATES (FEET)		
	CHORD, θ_C	END I, θ_I	END J, θ_J	SAG	X-SAG	Y-SAG
	.94813	.93221	.96414	.67952	117.43	110.40
	LENGTHS (FEET)					
	BASE BL	CHORD CL	STRESSED L	UNSTRESSED L_0	CHANGE ΔL	
(F)	234.55	323.21	323.21	322.49	.72661	
	FORCES AT END I (KIPS)					
	RESULTANT T	HOR. COMP. H	GLOBAL COMPONENTS F_X	F_Y	F_Z	
	2962.8	2166.6	-2125.0	-2020.9	422.61	
	FORCES AT END J (KIPS)					
	RESULTANT T	HOR. COMP. H	GLOBAL COMPONENTS F_X	F_Y	F_Z	
	3009.6	2166.6	2125.0	2088.9	-422.61	

TABLE 5.8: REFERENCE COORDINATES, LENGTHS, AND FORCES OF CABLE G
SEE FIG. 5.8 FOR NOTATIONS

CABLE	GLOBAL COORDINATES (FEET)					
	END I			END J		
	X	Y	Z	X	Y	Z
	900.01	229.46	58.000	649.98	459.76	12.250
	LOCAL COORDINATES AND SLOPES					
	SLOPES (RADIANS)			COORDINATES (FEET)		
	CHORD, θ_C	END I, θ_I	END J, θ_J	SAG	X-SAG	Y-SAG
	.90605	.89127	.92090	.69776	127.25	114.35
	LENGTHS (FEET)					
	BASE BL	CHORD CL	STRESSED L	UNSTRESSED L_0	CHANGE ΔL	
(G)	254.18	343.00	343.00	343.14	.86363	
	FORCES AT END I (KIPS)					
	RESULTANT T	HOR. COMP. H	GLOBAL COMPONENTS F_X	F_Y	F_Z	
	3320.8	2478.1	2437.6	-2210.6	446.02	
	FORCES AT END J (KIPS)					
	RESULTANT T	HOR. COMP. H	GLOBAL COMPONENTS F_X	F_Y	F_Z	
	3368.7	2478.1	-2437.6	2282.0	-446.02	

TABLE 5.9: REFERENCE COORDINATES, LENGTHS, AND FORCES OF CABLE H.
SEE FIG. 5.8 FOR NOTATIONS

CABLE	GLOBAL COORDINATES (FEET)					
	END I			END J		
	X	Y	Z	X	Y	Z
	1100.3	224.46	58.000	649.98	457.93	10.330
	LOCAL COORDINATES AND SLOPES					
	SLOPES (RADIANS)			COORDINATES (FEET)		
	CHORD, θ_C	END I, θ_I	END J, θ_J	SAG	X-SAG	Y-SAG
	.51557	.49451	.53675	2.1251	226.74	114.51
	LENGTHS (FEET)					
	BASE BL	CHORD CL	STRESSED L	UNSTRESSED L_0	CHANGE ΔL	
(H)	452.84	509.48	509.50	508.35	1.1518	
	FORCES AT END I (KIPS)					
	RESULTANT T	HOR. COMP. H	GLOBAL COMPONENTS F_X	F_Y	F_Z	
	4646.5	4162.6	4139.5	-2064.5	438.17	
	FORCES AT END J (KIPS)					
	RESULTANT T	HOR. COMP. H	GLOBAL COMPONENTS F_X	F_Y	F_Z	
	4724.4	4162.6	-4139.5	2234.3	-438.20	

TABLE 5.10

FORCES AND MOMENTS OF TOWER 1 FOR STAGE (B).

MEM. NO.	NODE PT.NO.	INSTALLMENT O		INSTALLMENT R		STAGE B	
		P KIPS	M KIP-FT.	P KIPS	M KIP-FT.	P KIPS	M KIP-FT.
96	164	27720.0	-30569.0	0.0	+12635.0	27720.0	-17934.0
98	167	22869.0	-6097.0	0.0	-11922.0	22869.0	-18019.0
100	169	20316.0	+13480.0	1.0	-11468.0	20317.0	+2012.0
103	171	14371.0	-77420.0	17.0	+22126.0	14388.0	-55294.0
104	172	14462.0	+36770.0	-24.0	+20209.0	14438.0	+56979.0
107	175	12045.0	-1930.9	-24.0	+11889.9	12021.0	+9959.0
110	179	9641.3	-10244.0	-23.3	-800.0	9618.0	-11044.0

TABLE 5.11

PROPERTIES OF TOWER 1

MEM. NO.	NODE PT. NO.	A_x FT^2	A_y FT^2	A_z FT^2	I_x FT^4	I_y FT^4	I_z FT^4	C FT.
96	164	381.9	180.7	190.7	31575.8	21368.1	23220.1	11.756
98	167	282.8	139.8	120.3	21378.0	14758.8	15539.2	10.780
100	169	255.0	130.9	109.9	15407.2	10757.6	11350.5	9.804
103	171	253.4	139.7	115.4	12195.7	8638.7	9192.7	9.18
104	172	232.6	128.9	102.8	10459.4	7446.1	7883.3	8.757
107	175	167.1	95.4	64.6	5918.3	4306.0	4455.4	7.54
110	179	142.1	83.9	63.9	3236.5	2415.1	2577.8	6.33

TABLE 5.12

STRESSES IN TOWER 1 FOR INSTALLMENT 0 AND FOR STAGE (B).
(STRESSES ARE IN PSI.)

MEM. NO.	NODE PT.NO.	INSTALLMENT 0				STAGE B			
		P/A	Mc/I	σ_1 *	σ_2 *	P/A	Mc/I	σ_1 *	σ_2 *
96	164	504	-107	397	611	504	-63	441	567
98	167	562	-29	533	591	562	-87	475	649
100	169	553	81	634	472	553	12	565	541
103	171	394	-537	-143	931	394	-383	11	777
104	172	432	284	716	148	435	434	69	1
107	175	501	-23	478	524	500	117	617	383
110	179	471	67	538	404	470	-188	282	658

$$*\sigma_1 = \frac{P}{A} + \frac{Mc}{I} \; ; \; \sigma_2 = \frac{P}{A} - \frac{Mc}{I}$$

TABLE 5.13

INITIAL LENGTHS AND ANGLES AT THE ENDS OF EACH MEMBER OF TOWER 1

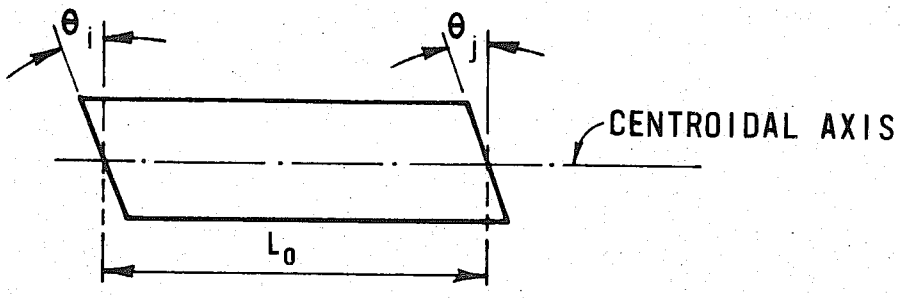

MEMBER	UNSTRESSED LENGTH, L_0 (IN FEET)	INITIAL ANGLES θ (IN 1/1000 RADIANS)	
		θ_i	θ_j
95	12.000	−.00017	−.00001
96	34.546	+.01357	−.00304
97	34.547	−.01553	+.02215
98	34.547	−.03660	+.03818
99	34.547	−.04127	+.03626
100	34.547	−.02304	+.00953
101	10.159	+.00004	−.00006
102	10.159	+.00087	−.00070
103	22.353	+.04085	+.04599
104	28.483	−.17043	+.14614
105	28.464	−.12734	+.10563
106	28.474	−.08450	+.06673
107	28.474	−.04661	+.03470
108	28.474	−.02343	+.01950
109	28.474	−.02602	+.03302
110	28.476	−.06979	+.09149
111	8.218	−.00009	+.00009
112	15.760	+.00014	−.00007
113.	13.930	+.00010	−.00005
114	12.000	−.00000	−.00000
115	12.393	−.00000	−.00000
116	27.500	−.00000	−.00000
117	9.704	−.00080	+.00068
118	20.059	−.05648	+.01966
119	29.999	+.05501	−.07607
120	5.747	+.00002	−.00012
121	1.917	+.00005	−.00006
122	10.333	+.06231	−.06313

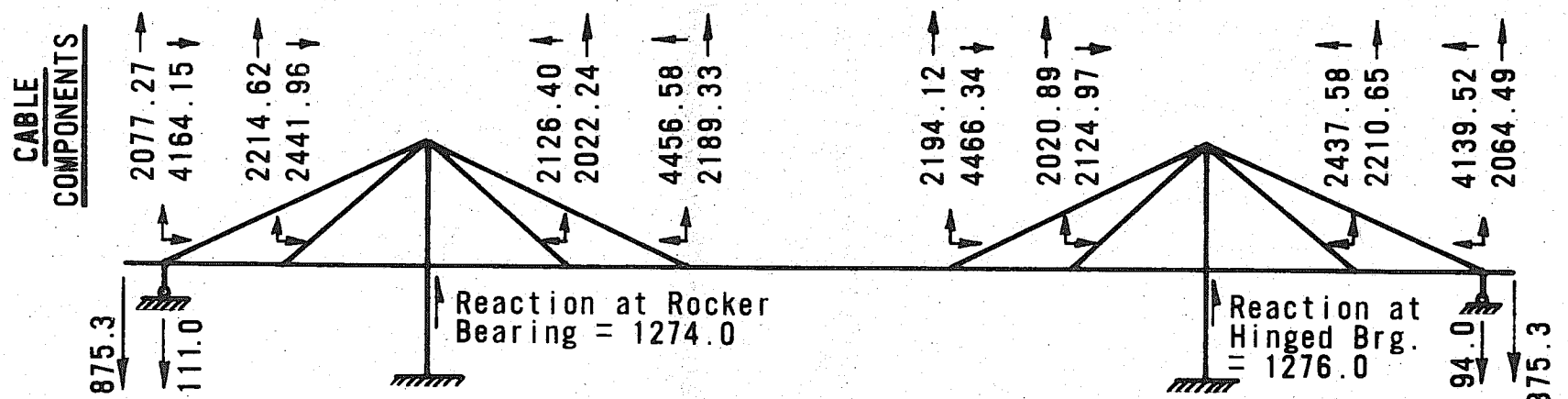

CABLE COMPONENTS (GLOBAL) AND VERTICAL REACTIONS

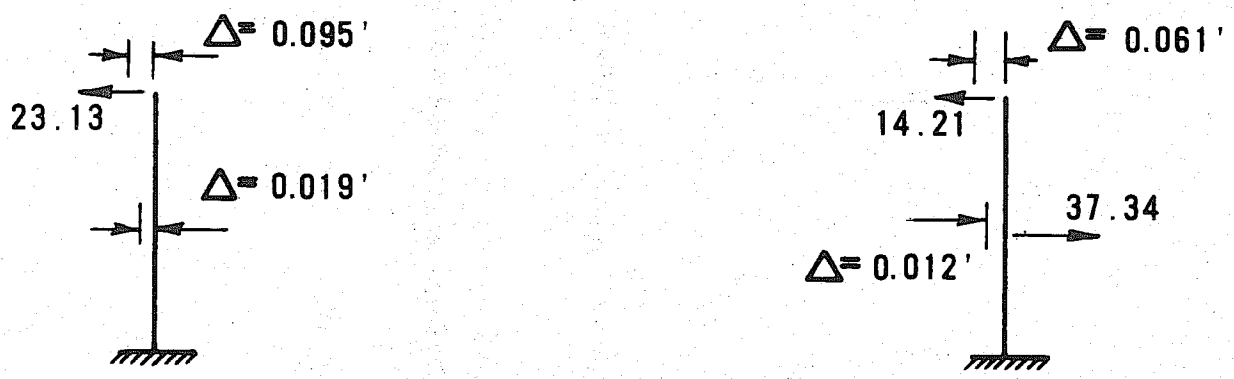

HORIZONTAL X-COMPONENTS ON TOWERS

(ALL FORCES IN KIPS ON 1/2 BRIDGE)

MAGNITUDES OF CABLE FORCES AND REACTIONS ON GIRDER AT FULL DEAD LOAD

(INFORMATION SUPPLIED BY THE DIVISION OF BAY TOLL CROSSINGS)

FIG. 5.1

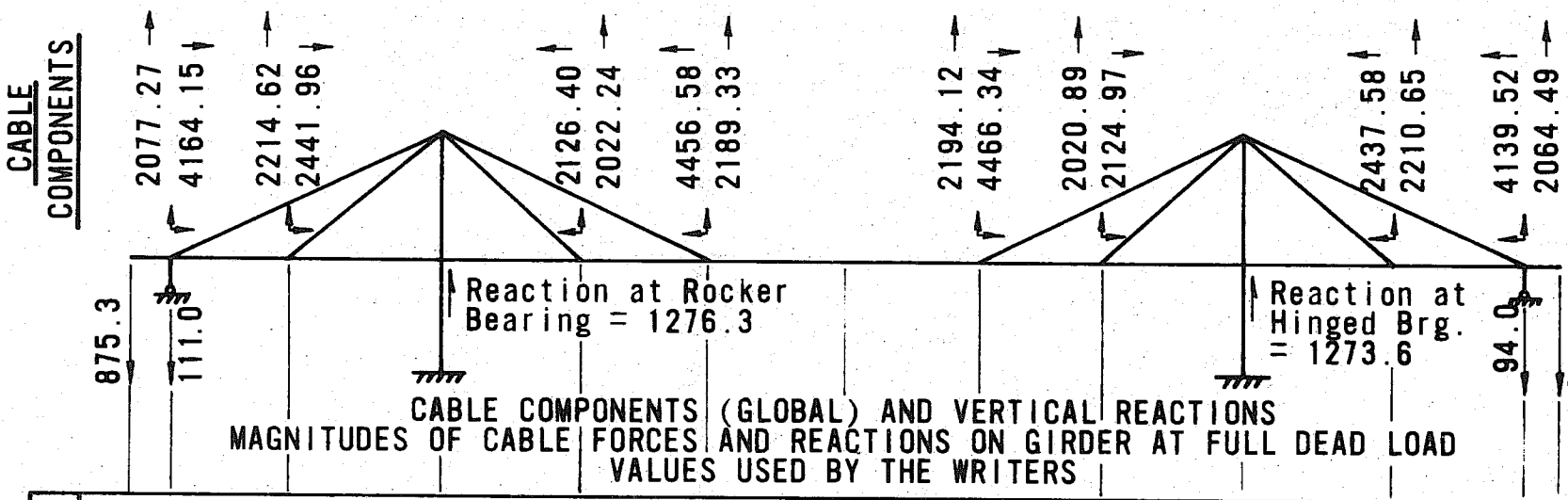

CABLE COMPONENTS (GLOBAL) AND VERTICAL REACTIONS

MAGNITUDES OF CABLE FORCES AND REACTIONS ON GIRDER AT FULL DEAD LOAD

VALUES USED BY THE WRITERS

CALCULATED BY	COMPARISON OF MOMENTS AT SELECTED SECTIONS (IN KIP-FT.)																			
UNIV. OF CAL.	55,314.8	68,042.6	117,378.0	120,413.7	73,493.8	73,493.8	134,640.2	132,245.8	116,524.1	105,136.4	-43,681.5	-43,681.5	105,355.3	116,768.0	131,700.7	134,093.6	72,345.6	73,432.6	119,412.2	116,382.1	67,967.5	55,314.8
DIV. OF BTC	55,710	67,710	118,294	122,087	75,833	74,748	132,534	130,600	113,287	103,811	-41,715	-41,715	104,665	114,141	130,893	132,827	74,367	75,454	121,366	117,573	67,710	55,710

	DEAD LOAD REACTIONS (KIPS)			
	UNIV. OF CAL.		DIV. OF B.T.C.	
	VERTICAL	HORIZONTAL	VERTICAL	HORIZONTAL
ROCKER BRG	1276.3	0	1274.0	0
HINGED BRG	1273.6	37.34	1276.0	37.34
SUM	2549.9	37.34	2550.0	37.34

COMPARISON OF GIRDER MOMENTS AND BEARING REACTIONS

FIG. 5.2

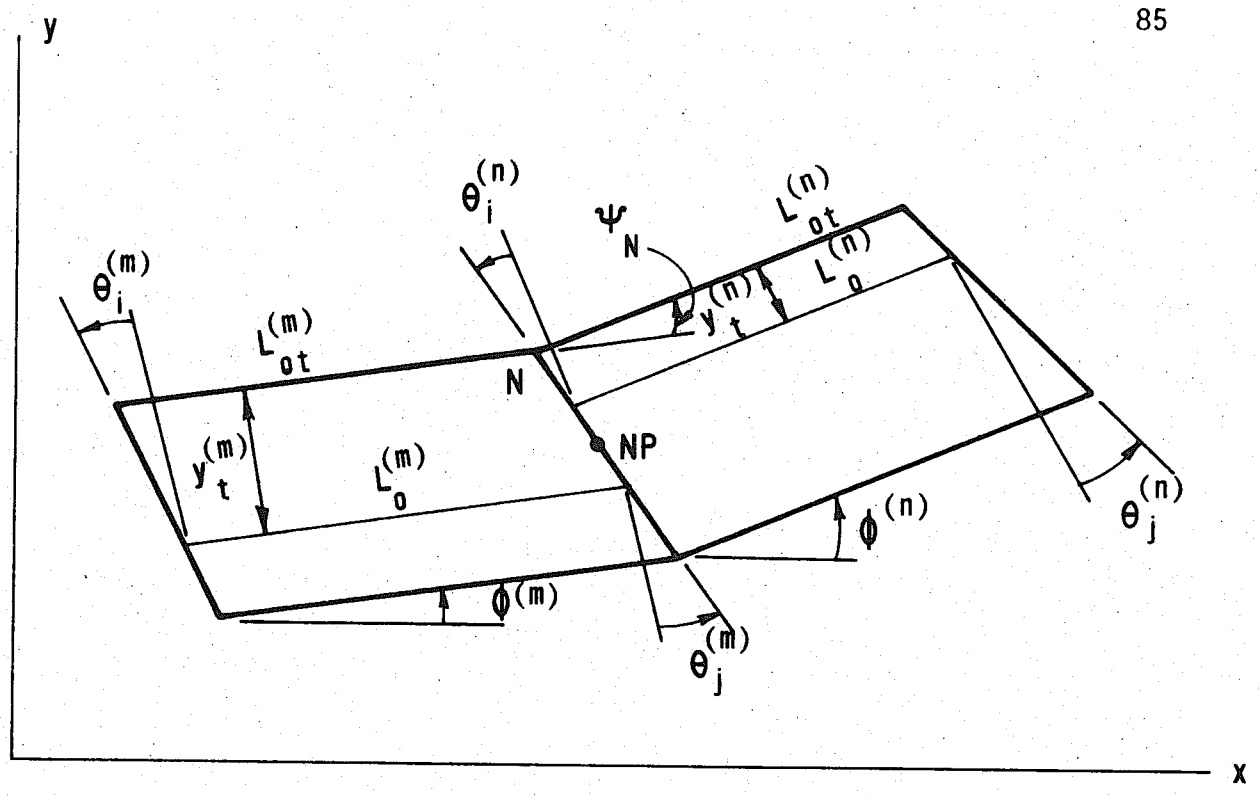

GEOMETRY OF TWO ADJACENT MEMBERS OF THE UNSTRESSED GIRDER

FIG. 5.3

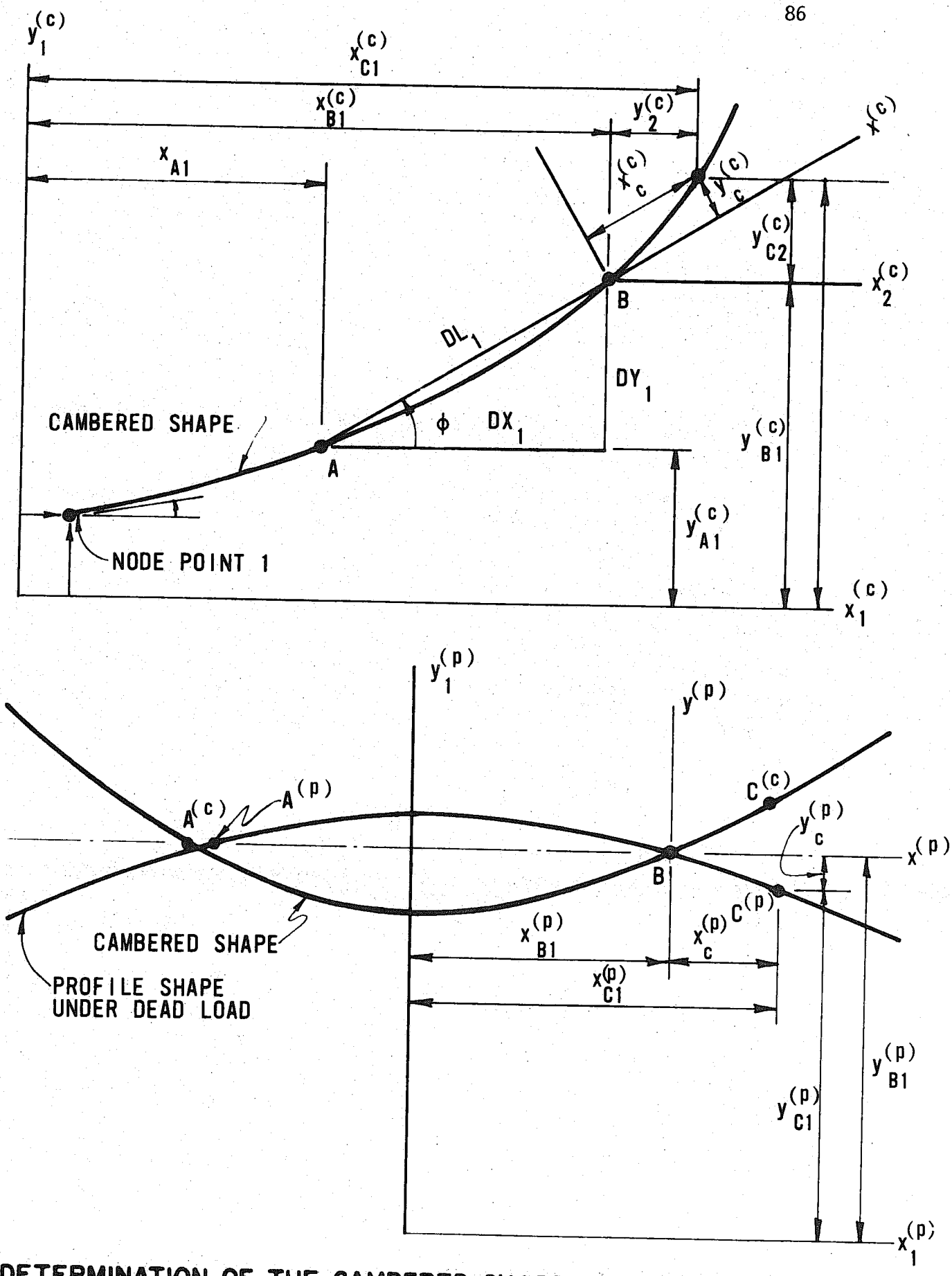

DETERMINATION OF THE CAMBERED SHAPE OF THE GIRDER

FIG. 5.4

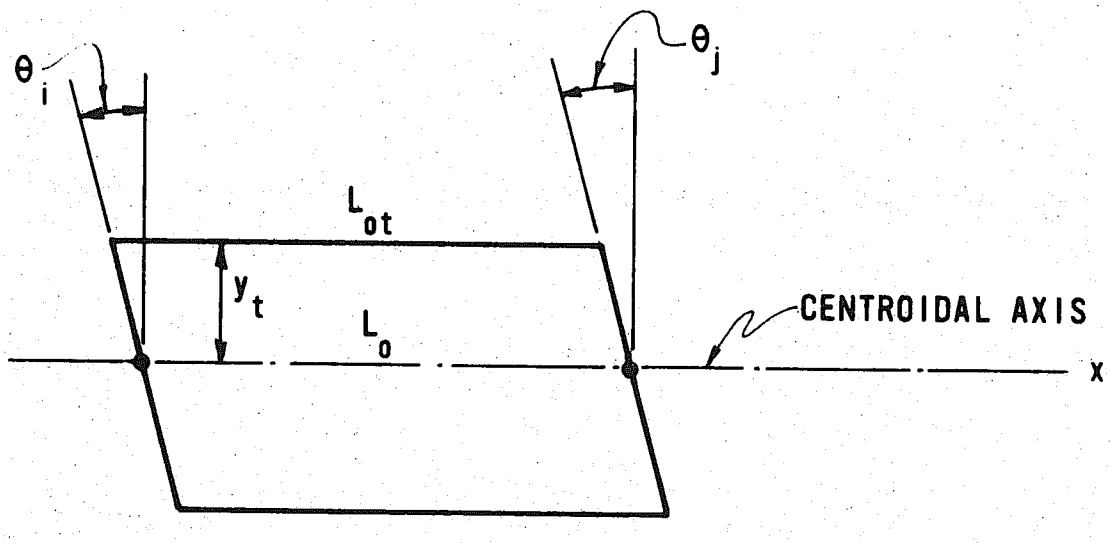

LENGTHS AND ANGLES OF UNSTRESSED MEMBER

FIG. 5.5

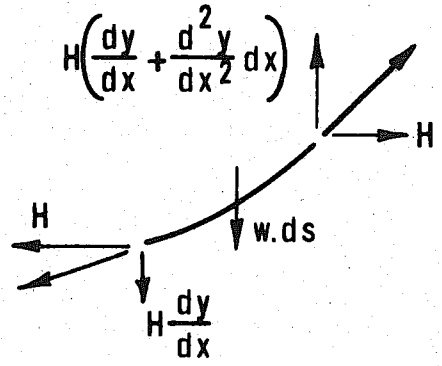

(a) DIFFERENTIAL ELEMENT

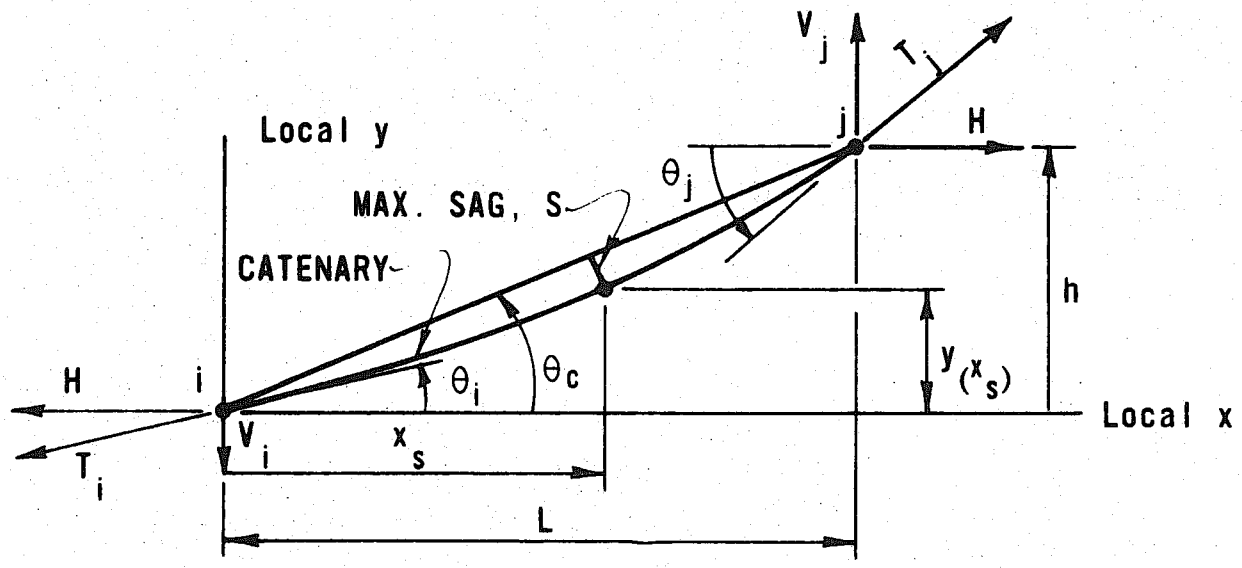

(b) TRUE ELEVATION OF CATENARY

TRUE VIEW OF CATENARY

FIG. 5.6

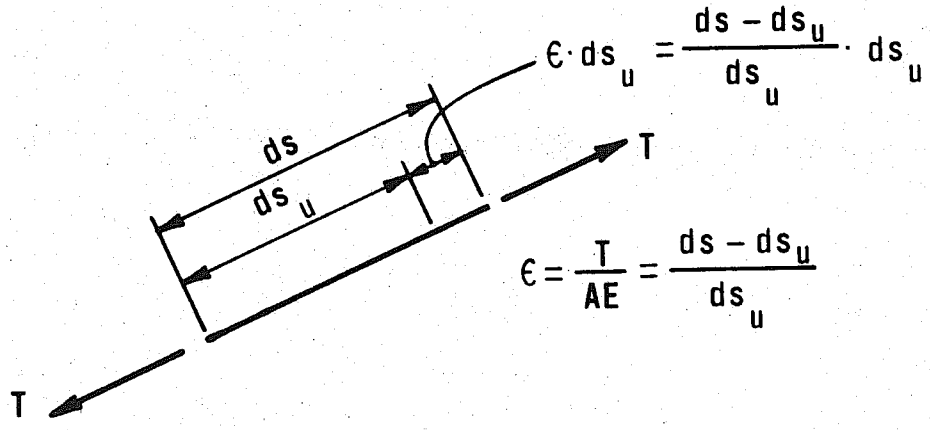

DIFFERENTIAL ELEMENTS OF CABLE

FIG. 5.7

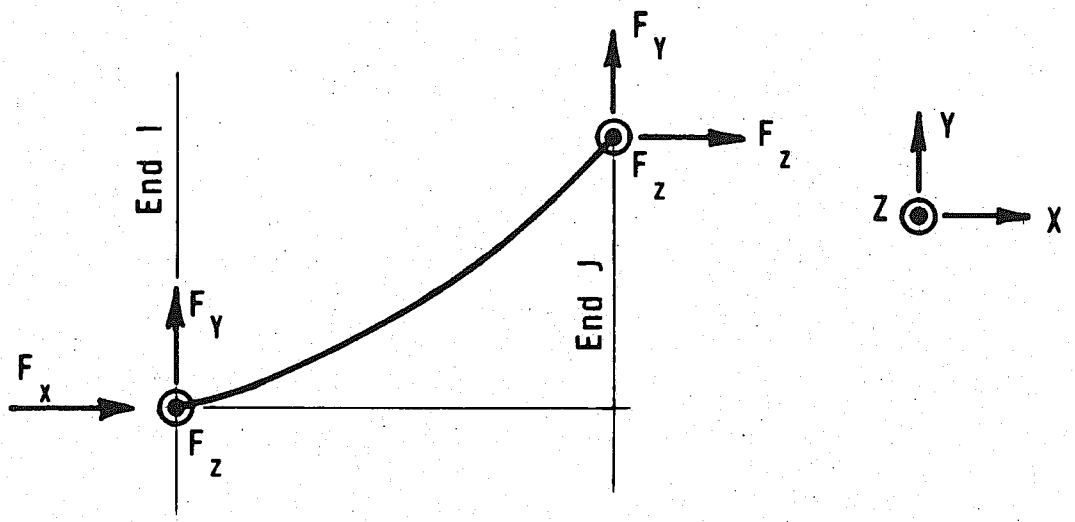

a) Elevation: Projection on global XY plane

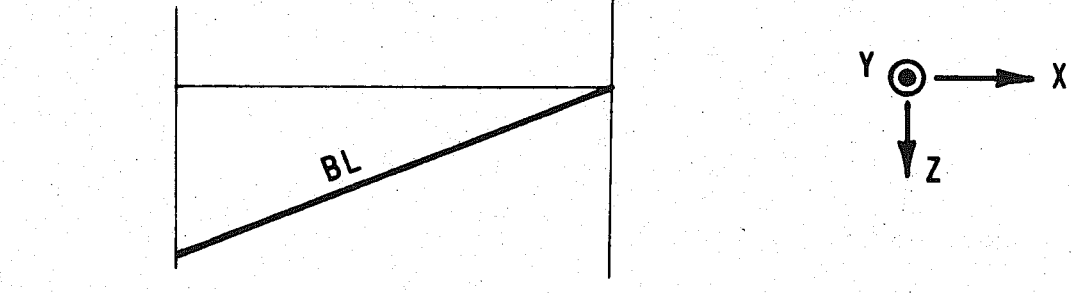

b) Plan: Projection on global XZ plane

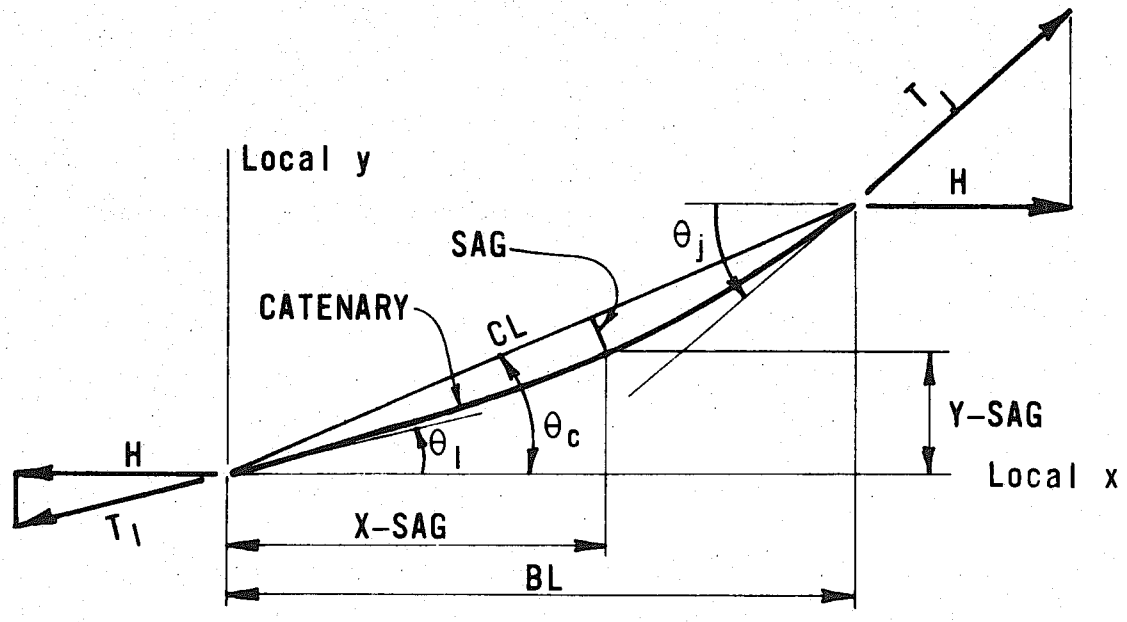

c) True Elevation: Projection of cable on the true vertical plane of Cable.

STATIC AND GEOMETRIC TERMS OF CABLES

FIG. 5.8

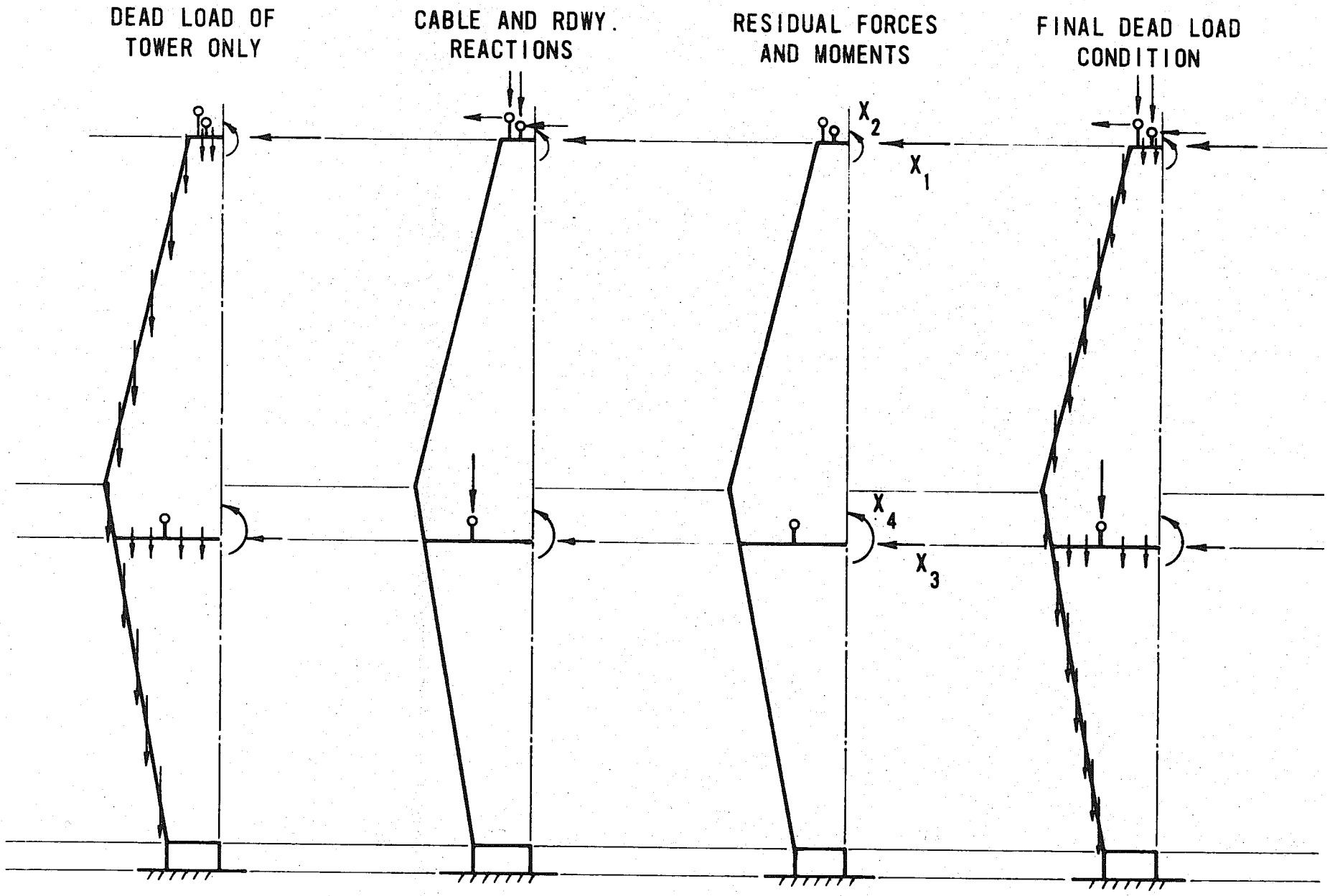

INSTALLMENTS AND FINAL CONDITION OF TOWER AT DEAD LOAD

FIG. 5.9

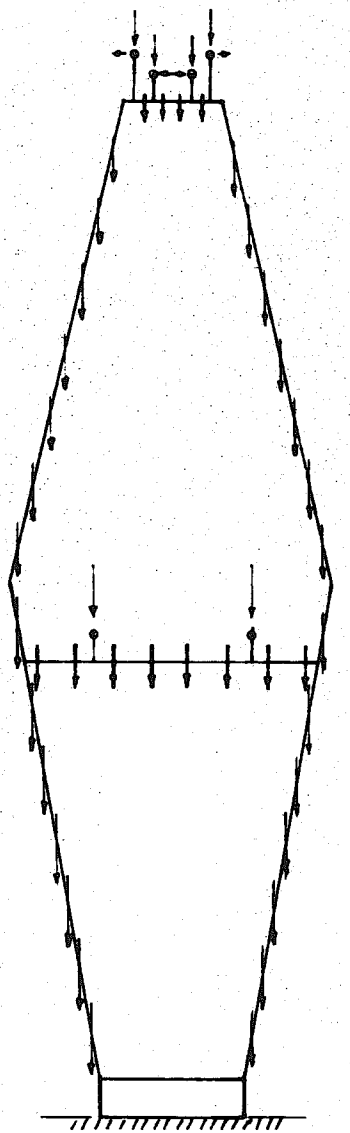

FULL DEAD LOAD CONDITION
STAGE B

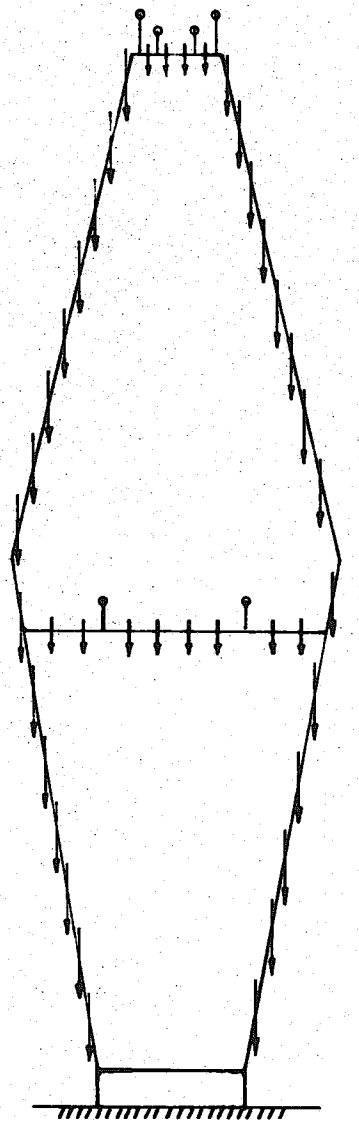

PARTIAL DEAD LOAD CONDITION
STAGE T

STAGES B AND T OF TOWER

FIG. 5.10

6. EFFECTS OF LIVE LOADS, TEMPERATURE CHANGES, AND DIFFERENTIAL MOVEMENTS

Results are given in this Chapter of the maximum effects caused by live loads, temperature changes, and differential movements. Ordinarily, the effects of these conditions and of dead load are of primary concern in conducting a review of the design of a bridge.

In this Chapter, the maximum effects caused by live loads are obtained for selected members of the Southern Crossing Bridge. The selected members are listed in Fig. 6.1 and are most likely to control the proportions and dimensions of the bridge. Influence lines, based on the linear theory of elastic structures, are used to obtain the maximum effects caused by live loads. The results for temperature changes and differential movements also are based on the linear theory of elastic structures.

6.1 Influence Lines

Influence lines for different functions of a structure can be obtained in several ways. They can be obtained by computing the desired functions for various positions of a unit load on a structure. However, the latter procedure at times is inefficient for obtaining a selected group of influence lines. In this investigation, the influence lines are obtained by direct application of Müller-Breslau's principle. This principle may be stated as follows:

> If an influence line for any function is desired, introduce a unit discontinuity at the section on which the function acts and the displacements of the load line represent the

influence line. The unit discontinuity must correspond to the function and the displacement to the unit load, by definition of work.

For the application of this principle, the writers developed a general procedure for obtaining influence lines of any linearly elastic structure composed of finite elements. The procedure extends the use of the direct stiffness matrix approach for the analysis of such structures. A subroutine, called MULLER, was written and incorporated into the general computer program employed for the bridge. The output of MULLER yields the following information for each influence line: (1) the complete shape of the influence line, (2) the maximum positive and negative ordinates and their locations, (3) the length and area of each positive and each negative segment, and (4) the total load lengths and areas of the positive and of the negative segments. This information is required to obtain the maximum positive and negative values of the functions for the various positions of the live load.

In this report, influence lines are given for forces or moments at various sections of the bridge. Because of the combined states of stress that exist at a section, it may be desired to obtain the maximum value of a force and the accompanying moment at the section, or the maximum value of a moment and the accompanying force. In either case, the focus is on the strength or stability of the entire section. The calculations then need be slightly modified but can be obtained through influence lines. For other purposes, it may be desired to obtain influence lines for stresses at a point. In the latter case, the focus is on the strength or stability of the region in the immediate vicinity of the point. Such influence lines can be obtained through MULLER.

For the Southern Crossing Bridge, influence lines are given in Figs. 6.2 (II) to 6.19 (II) for selected force and moment components in the various members of the bridge. Included among the members are those of the roadway, cables, saddles, reactions, and towers. The selected force and moment components are considered to be essential in the preliminary phases of design. See Figs. 6.1 and 6.1 (II) for a listing of the force and moment components that are considered, and of the corresponding Figures of Volume II in which the influence lines are assembled.

In Figs. 6.2 (II) to 6.13 (II), each influence line shows the effect of a vertical load, P_y equal to one unit, moving along the top of the roadway on the magnitude and sign of the parameter considered. The information given for each influence line is that obtained by means of MULLER. Thirty nine of such kinds of influence lines are given.

The effects of a horizontal traction load, P_x equal to one unit, moving along the top of the roadway on the values of various parameters are shown in Figs. 6.15 (II) to 6.19 (II). For each of these influence lines, only the shapes and the values of the maximum positive and negative ordinates are given.

It has been mentioned that depending on the speed of application of load, the bearing at Tower 1 is designed to act either as a rocker or as a hinge. The influence lines obtained in this study are based on the assumption that the bearing at Tower 1 acts as a hinge. The effects of the kind of bearing at Tower 1 on the properties of influence lines is indicated in Table 6.1. In the Table, the properties of the influence line for the tension force in Cable C are summarized for the bearing acting as a hinge or as a rocker. The differences in

results for the two influence lines are small. Based on this and other studies for vertical loads P_Y, the influence lines for the various force and moment components of the bridge are practically the same for either condition of the bearing at Tower 1.

For horizontal traction loads P_X, the influence lines for the various functions of the bridge can differ appreciably, however, depending on the condition of the bearing at Tower 1. For the latter kinds of loads (and for wind and seismic effects) it is assumed that the bearing at Tower 1 acts as a hinged bearing.

Further, the results of the linear theory of structures given in this report are based on assumed values of E for the cables as given in Table 2.1. Because the latter values of E depend on the conditions of the curved cables in their stressed stages, a comparison is given in Table 6.2 of the effects of different values of E for Cables A and C on the properties of selected influence lines. The selected influence lines are for the axial forces of the two cables. For Cables A and C respectively, the differences between the corresponding maximum ordinates of the two sets of influence lines are 8.2 percent and 0.08 percent. The differences between the corresponding positive areas of the two sets of influence lines are 11.7 percent and 0.08 percent.

6.2 Maxima Caused By Live Loads

Maximum values for selected force and moment components caused by live loads are given in Table 6.4. The selected components are the same as those for which influence lines are reported. The maximum values are calculated in accordance with the basic requirements of AASHO but reduced as recommended in a paper by Ivy et al (6). The

recommended reductions are intended for long-span bridges and are based on loaded lengths. A summary of the recommended live loads is given in Table 6.3.

For each component of force or moment, the maximum values are calculated by means of the areas and ordinates of the respective influence line. Questions however arise in the determination of the maximum values because of the various shapes of the influence lines, the different loaded lengths, and the accompanying values of the live loads. The questions arise because of the probabilistic distributions of live loads across and along the roadway of a long-span bridge. A probabilistic approach to the determination of maxima caused by live loads is being pursued by the senior writer. The results of the latter approach will be reported later.

In this report, the load lengths considered are the full lengths of each positive or negative segment of an influence line, or any combination of the full segments. Partial lengths of a segment are not considered although the latter consideration can at times yield a greater value of a maximum than that based on full lengths. For the loaded lengths obtained in this way, the values of maxima reported in Table 6.4 are in accordance with the specified values of live load as given in Table 6.3. Sample calculations for determining the maximum positive and negative values of a moment component and of a shear component are given in Figs. 6.2 and 6.3, respectively. The moment component is p_6 of member 42, and the shear component is p_8 of member 24. All values of maxima and minima reported in Table 6.4 are calculated in this way. It is observed that the effects of live loads in the simple spans which flank the cable-stayed girder bridge are not

included in the values of Table 6.4. If desired, the latter values can easily be adjusted to take into account the effects of live loads in the flanking spans. For this purpose, reinspect the influence lines.

6.3 Effects of Temperature Changes

Four cases of temperature changes, specified by the designers, are considered for the bridge. The four cases are for the bridge when erected and are as follows:

Case T1: A ± 40° F change in temperature from the ambient condition for all members of the bridge including the end-bents. The coefficients of thermal expansion are 0.0000055/°F/unit length for the concrete members and 0.0000065/°F/unit length for the steel members.

Case T2: A ± 20 °F difference between the temperatures of the cables and of the other members of the bridge.

Case T3: A linear distribution of temperature changes through the depth of the roadway girder only; with a ± 20 °F difference in the temperature between the top and bottom of the girder.

Case T4: The same as Case T3, but accompanied by a linear distribution of temperature changes through the global X-thicknesses of the towers. A 20 °F difference in temperature exists between the respective X-faces of each tower.

Summaries are given in Fig. 6.20 (II) to 6.23 (II) for the effects of the different cases of temperature changes considered. For each case, the summary includes the magnitudes of the Y-displacements along the roadway girder, and the magnitudes of the force and moment components for the various members of the bridge. The general computer program employed herein was modified to include the effects of thermal

changes. It is based on the analysis of linearly elastic structures. Because of a possible confusion with signs, the results given herein are for but one kind of a change in temperature for each case. The results are for the following kinds:

Case T1: The change of 40 °F in temperature is an increase.

Case T2: The temperature of the cables is 20 °F greater than that of the other members.

Case T3: The temperature at the top of the girder is 20 °F greater than at the bottom.

Case T4: The temperature through the X-thickness of a tower decreases with an increase in the value of X.

An inspection of Figs. 6.20 (II) to 6.23 (II) shows that in general the effects of Case T1 on the forces and moments in the various members of the bridge are less severe than those of the other cases. The effects of Case T4 are more severe than those of the other cases.

6.4 Effects of Differential Movements

The effects of possible differential movements of the supports on the forces and moments in the bridge are inspected for three cases, designated by S1 to S3. In Case S1, a vertical settlement of one foot at the base of the end-bent located at X=1150 ft. is considered. The results for this case are summarized in Fig. 6.24 (II). A vertical settlement of one foot at the base of Tower 2 is considered in Case S2, and a rotation of 0.001 radians about the global Z-axis at the base of the same Tower in Case S3. The results for the latter two cases are respectively summarized in Figs. 6.25 (II) and 6.26 (II).

6.5 Summary of Results for Selected Members

A summary of the forces and moments in selected members of the bridge is given in Table 6.4. The summary is for the effects of dead load, live loads, temperature changes, and differential movements. The selected members and the components are the same as those for which influence lines are reported.

An inspection of Table 6.4 readily shows the relative magnitudes of the internal forces and moments that are caused in the bridge by the various sources of stress or strain.

TABLE 6.1

EFFECTS OF THE CONDITION OF THE BEARING AT TOWER 1 ON THE PROPERTIES OF INFLUENCE LINES.

PROPERTIES OF INFLUENCE LINES FOR COMPONENT p_1 OF CABLE C: MEMBER 161			
BEARING AT TOWER 1	ACTS AS A HINGE	Value of E	23,000 K/in.^{2}
		Positive area	341.03 Ft.
		Length of positive segments	1,324.3 Ft.
		Maximum ordinate	0.87163
		At node point	60
		Negative area	-60.948
		Length of negative segments	980.69 Ft.
		Minimum ordinate	-0.19924
		At node point	32
	ACTS AS A ROLLER	Value of E	23,000 K/in.^{2}
		Positive area	351.85 Ft.
		Length of positive segments	1385.0 Ft.
		Maximum ordinate	0.88496
		At node point	60
		Negative area	-59.479 Ft.
		Length of negative segments	920.02 Ft.
		Minimum ordinate	-0.20650
		At node point	32

TABLE 6.2

EFFECTS OF DIFFERENT VALUES OF E OF THE CABLES ON THE PROPERTIES OF INFLUENCE LINES.

PROPERTIES OF INFLUENCE LINES FOR COMPONENTS p_1 OF CABLES A AND C.			
CABLE A: MEM. 151	Value of E	22000 K/in^2	20486 K/in^2
	Positive area	742.73 Ft	655.65 Ft
	Length of positive segments	1405.2 Ft	1345.3 Ft
	Maximum ordinate	1.2244	1.1240
	At Node pt.	74	72
	Negative area	-166.90 Ft	-142.65 Ft
	Length of negative segments	899.80 Ft	959.69 Ft
	Minimum ordinate	-0.52972	-0.48653
	At Node pt.	24	24
CABLE C: MEM. 161	Value of E	23000 K/in^2	22708 K/in^2
	Positive area	341.03 Ft	346.53 Ft
	Length of positive segments	1324.3 Ft	1346.9 Ft
	Maximum ordinate	0.87163	0.87233
	At Node pt.	60	60
	Negative area	-60.948 Ft	-59.768 Ft
	Length of negative segments	980.69 Ft	958.06 Ft
	Minimum ordinate	-0.19924	-0.19814
	At Node pt.	32	32

Table 6.3

EQUIVALENT LANE LOADING IN RELATION TO LOADED LENGTH

LOADED LENGTH (FT.)	UNIFORM LL PER LANE (K/FT.)	CONCENTRATED LL PER LANE		IMPACT FACTOR	LL FOR 8 LANE DESIGN **		
		MOM. (K)	SHEAR (K)		UNIFORM LL(K/FT.)	CONCENTRATED LL	
						MOMENT (K)	SHEAR (K)
0–600	0.64	18	26	7%	4.1088	115.56	166.92
601–800	0.64	9	13	6%	4.0704	57.24	82.68
801–1000	0.64	0	0	5%	4.032	—	—
1001–1200	0.60	0	0	4%	3.744	—	—
1201 & Over	0.56	0	0	4%	3.4944	—	—

** Impact factor and reduction in load intensity for multi-lane loading are included.

TABLE 6.4

SUMMARY OF FORCES AND MOMENTS IN SELECTED MEMBERS OF THE BRIDGE FOR DEAD LOADS, LIVE LOADS, TEMPERATURE CHANGES, AND DIFFERENTIAL MOVEMENTS.
(FORCE COMPONENTS IN KIPS: MOMENT COMPONENTS IN KIP-FT.)

	MEMBER NO.	COM-PO-NENT	DEAD LOAD	LIVE LOAD MAXIMA		TEMPERATURE CASES				MOVEMENT OF SUPPORTS		
				POS.	NEG.	T1	T2	T3	T4	S1 DEFL. 1 FT.	S2 DEFL. 1 FT.	S3 ROT. 0.001R
GIRDER AND END BENT	2	P_1	-111.00	638.2	-695.4	-27.86	11.71	27.52	19.96	96.52	-168.23	-18.85
	7	P_1	4179.6	1037.5	-296.24	49.17	-28.87	65.22	77.79	-158.17	275.39	31.32
		P_2	506.86	392.0	-124.2	-1.92	-2.65	60.06	58.80	17.46	-30.71	-2.98
	14	P_3	1068.7	245.9	-96.81	1.82	2.71	-60.20	-58.96	-17.14	30.14	2.92
	16	P_1	6632.2	1235.0	-24.98	46.32	-50.18	22.71	38.02	-196.95	345.28	37.10
		P_2	1091.8	217.23	-115.25	-4.39	-21.97	21.77	23.01	-17.93	33.06	2.32
		P_6	120410.0	25821.9	-19888.7	483.57	446.96	-11934.0	-11653.0	-3855.2	6775.4	666.92
	24	P_3	695.98	461.31	-92.03	4.32	22.05	-21.80	-23.07	18.24	-33.61	-2.38
	25	P_1	6616.0	1863.39	-230.05	46.31	-50.17	22.71	38.02	-196.94	345.27	37.10
		P_2	564.17	396.18	-95.60	9.78	24.93	-10.76	-12.44	26.48	-51.64	-0.58
		P_6	73493.0	32270.7	-1072.4	1464.6	6067.4	-17434.0	-17502.0	1128.9	-2368.0	-7.50
	32	P_3	1130.8	219.15	-135.01	-100.41	-24.65	10.63	12.23	-25.37	49.71	0.38

TABLE 6.4 (Continued)

SUMMARY OF FORCES AND MOMENTS IN SELECTED MEMBERS OF THE BRIDGE FOR DEAD LOADS, LIVE LOADS, TEMPERATURE CHANGES, AND DIFFERENTIAL MOVEMENTS.
(FORCE COMPONENTS IN KIPS: MOMENT COMPONENTS IN KIP-FT.)

MEMBER NO.		COM-PO-NENT	DEAD LOAD	LIVE LOAD MAXIMA		TEMPERATURE CASES				MOVEMENT OF SUPPORTS		
				POS.	NEG.	T1	T2	T3	T4	S1 DEFL. 1 FT.	S2 DEFL. 1 FT.	S3 ROT.0.001R
GIRDER	34	P_1	4489.4	1451.45	-156.30	52.59	-42.97	28.60	43.77	-198.67	357.84	35.64
		P_2	915.18	368.2	-56.87	3.86	17.59	-16.41	-17.87	27.10	-62.06	1.04
		P_6	132250.0	27248.3	-9252.1	-718.04	267.83	-14924.0	-14584.0	-5233.9	9994.0	176.96
	40	P_8	705.74	220.17	-463.95	-4.11	-17.38	16.27	17.67	-26.18	60.41	-1.21
	42	P_1	312.22	459.90	-166.86	69.46	-9.33	-2.73	1.77	-14.44	4.86	36.07
		P_2	1508.7	466.97	-51.12	-4.59	0.02	-11.89	3.99	-68.82	121.60	0.98
		P_6	105140.0	25239.2	-15937.8	-1368.1	-3232.7	-11675.0	-11046.0	-10507.0	22091.0	25.26
	48	P_2	-0.48	218.81	-218.69	-4.16	-0.04	-0.14	4.00	-68.90	121.63	1.20
		P_6	-43681.0	664.2	-38672.9	-424.50	-3228.5	-11646.0	-11925.0	4646.3	-4666.4	-224.93
CABLES	151(A)	P_1	-4674.4	355.88	-1297.7	-57.15	32.58	-73.83	-88.13	179.35	-311.98	-35.99
	157(B)	P_1	-3326.8	53.2	-591.9	3.91	29.25	58.35	54.59	53.25	-95.96	-7.95
	161(C)	P_1	-2964.7	132.7	-703.6	8.86	10.13	8.29	8.10	-2.47	17.73	-2.03
	165(D)	P_1	-4989.8	47.6	-1180.1	19.03	37.94	-35.34	-47.37	207.79	-398.13	0.49

TABLE 6.4 (Continued)

SUMMARY OF FORCES AND MOMENTS IN SELECTED MEMBERS OF THE BRIDGE FOR DEAD LOADS, LIVE LOADS, TEMPERATURE CHANGES, AND DIFFERENTIAL MOVEMENTS.

(FORCE COMPONENTS IN KIPS: MOMENT COMPONENTS IN KIP-FT.)

	MEMBER NO.	COM-PO-NENT	DEAD LOAD	LIVE LOAD MAXIMA		TEMPERATURE CASES				MOVEMENTS OF SUPPORTS		
				POS.	NEG.	T1	T2	T3	T4	S1 DEFL. 1 FT.	S2 DEFL. 1 FT.	S3 ROT. 0.001R
TOWER MEMBERS	95	P1	27430.0	2206.5	-41.04	22.66	-11.72	-27.65	-15.95	-165.43	289.88	20.04
		P5	-10754.0	20458.0	-49917.5	-31504.0	4140.3	1274.2	-761.20	6650.0	-2460.7	-16275.0
		P6	31167.0	1697.7	1687.9	2425.9	211.86	-107.0	-133.02	381.33	-697.52	-35.81
	96	P1	27722.0	2244.6	-37.58	12.43	-13.53	-27.31	-15.21	-171.17	300.15	20.65
		P3	23.13	459.53	-169.95	71.13	-9.29	-2.72	1.86	-14.84	5.20	36.74
		P5	-10449.0	16399.2	-38768.2	-29629.0	3895.2	1202.0	-727.84	6258.3	-2322.4	-1530.7
	100	P10	1064.1	1516.31	-1412.62	3035.9	-399.9	-125.1	-13.33	-643.39	242.42	1568.5
		P11	6450.3	10311.6	-34542.1	18237.0	-2407.4	-766.3	429.1	-3880.9	1489.1	9423.4
	103	P5	-5857.6	42832.6	-13279.0	-16393.0	2166.2	694.57	-442.58	3494.8	-1351.5	-8471.2

TABLE 6.4 (Continued)

SUMMARY OF FORCES AND MOMENTS IN SELECTED MEMBERS OF THE BRIDGE FOR DEAD LOADS, LIVE LOADS, TEMPERATURE CHANGES, AND DIFFERENTIAL MOVEMENTS.

(FORCE COMPONENTS IN KIPS: MOMENT COMPONENTS IN KIP-FT.)

	MEMBER NO.	COM-PO-NENT	DEAD LOAD	LIVE LOAD MAXIMA		TEMPERATURE CASES				MOVEMENT OF SUPPORTS		
				POS.	NEG.	T1	T2	T3	T4	S1 DEFL. 1 FT.	S2 DEFL. 1 FT.	S3 ROT. 0.001R
TOWER MEMBERS	110	P1	10174.0	1710.3	-36.64	7.42	-59.79	4.88	19.86	-214.86	383.50	23.54
		P3	23.23	55.12	-184.4	71.13	-9.29	-2.72	1.86	-14.84	5.20	36.74
	112	P1	4376.3	715.9	-10.12	-8.75	-26.64	-44.93	-42.27	-34.09	52.29	6.74
		P3	315.57	390.4	-423.3	3.46	-14.10	-36.61	-34.00	-40.54	82.50	4.35
	113	P1	4599.6	1044.3	-129.9	17.61	-32.10	49.87	61.87	-176.27	323.20	16.30
		P3	-292.42	319.4	435.8	67.36	4.85	33.90	35.86	25.76	-77.32	32.23
	114	P1	1276.4	859.0	-178.03	14.03	47.03	-32.59	-35.55	44.93	-85.62	-3.00
		P3	0.00	638.2	-221.9	-0.0004	0.00	0.00	0.00	0.00	-0.00	-0.00

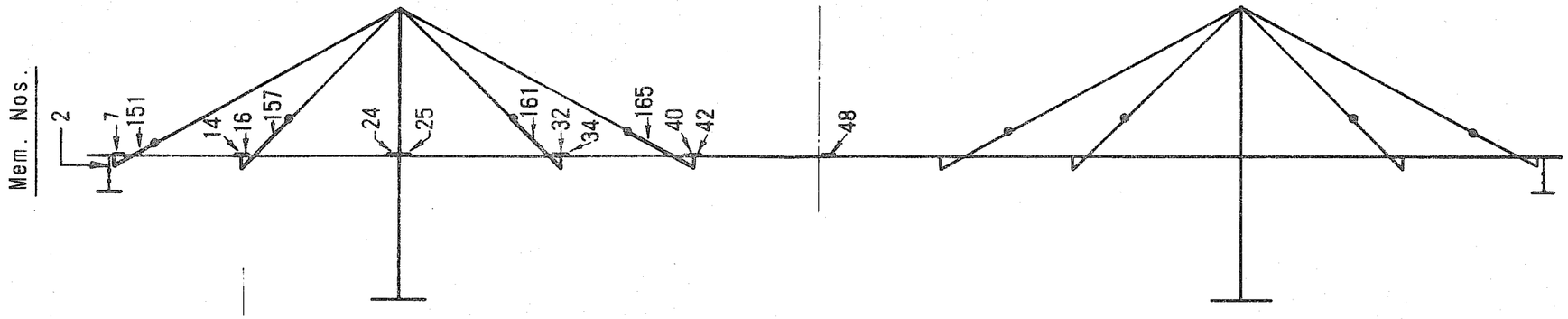

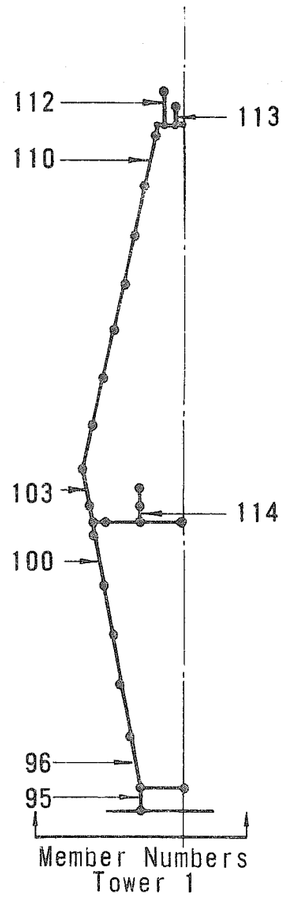

MEMBER NUMBERS		FOR LOADS P_Y ALONG THE GIRDER FORCE COMPONETS												FOR LOADS P_X ALONG THE GIRDER FORCE COMPONETS											
		P_1	P_2	P_3	P_4	P_5	P_6	P_7	P_8	P_9	P_{10}	P_{11}	P_{12}	P_1	P_2	P_3	P_4	P_5	P_6	P_7	P_8	P_9	P_{10}	P_{11}	P_{12}
		FIGURE NUMBERS REFER TO FIGURES IN VOLUME II																							
GIRDER AND END BENT	2	6.3																							
	7	6.8	6.5											6.17	6.16										
	14								6.5												6.16				
	16	6.9	6.6				6.3							6.17	6.16				6.15						
	24								6.6												6.16				
	25	6.9	6.6				6.4							6.17	6.16				6.15						
	32								6.7												6.16				
	34	6.9	6.7				6.4							6.17	6.16				6.15						
	40								6.7												6.16				
	42	6.10	6.8				6.4							6.17	6.16				6.16						
	48		6.8				6.5																		
TOWER 1	95	6.10												6.17				6.19							
	96			6.12		6.13								6.17		6.18		6.19							
	100										6.14	6.14												6.19	
	103					6.14												6.9							
	110	6.10		6.12										6.18		6.18							6.19		
	112	6.11		6.12										6.18		6.18									
	113	6.11		6.13										6.18		6.19									
	114	6.11		6.13										6.18		6.19									
CABLES	151	6.2												6.15											
	157	6.2												6.15											
	161	6.2												6.15											
	165	6.3												6.15											

LISTING OF INFLUENCE LINES AND CORRESPONDING FIGURE NUMBERS OF VOLUME II

FIG. 6.1

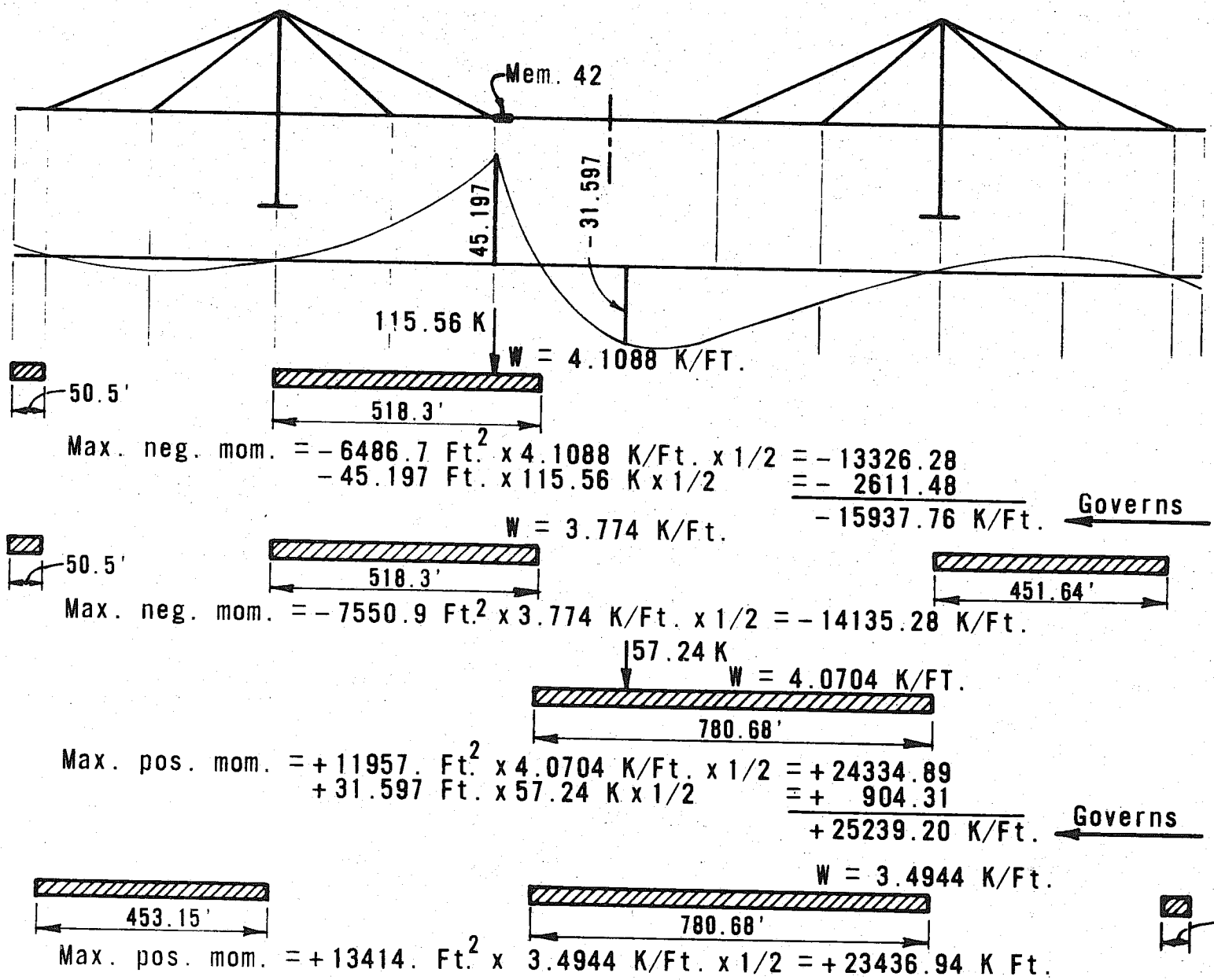

MAXIMUM POSITIVE AND NEGATIVE VALUES OF LL MOMENT FOR COMPONENT P_6 OF MEMBER 42

FIG. 6.2

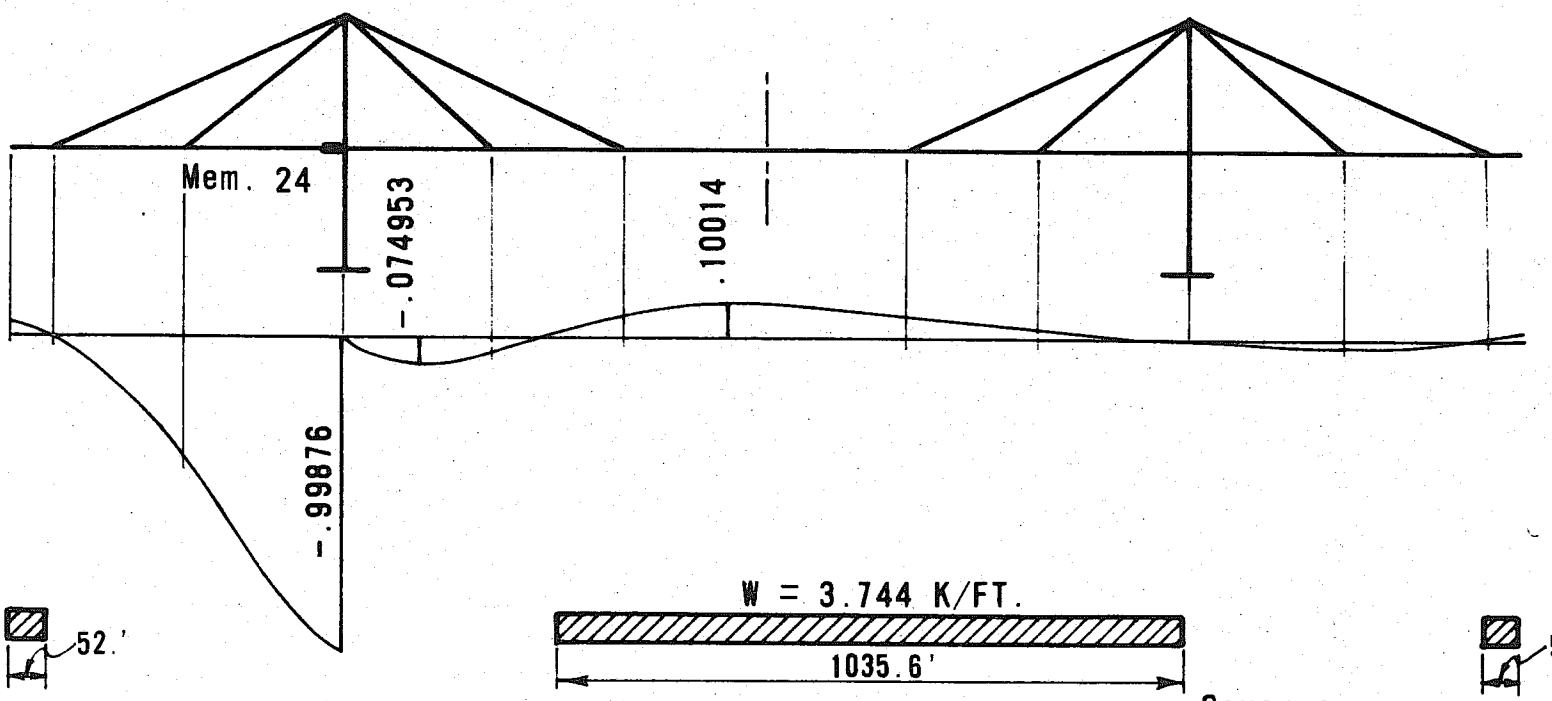

Max. neg. shear = −49.161 Ft. x 3.744 K/Ft. x 1/2 = −92.03 K ← Governs

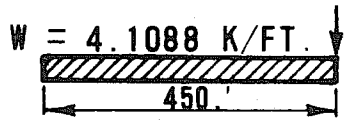

Max. pos. shear = +183.97 Ft. x 4.1088 K/Ft. x 1/2 = +377.95
+ .99876 x 166.92 K x 1/2 = + 83.36
+461.31 K ← Governs

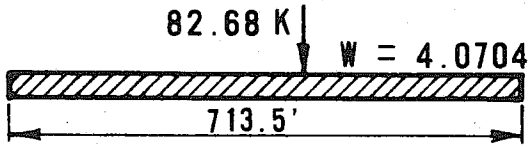

Max. pos. shear = +196.78 Ft. x 4.0704 K/Ft. x 1/2 = +400.49
+ .99876 x 82.68 K x 1/2 = + 41.29
+441.78 K

MAXIMUM POSITIVE AND NEGATIVE LL. SHEARS FOR COMPONENT P_8 OF MEMBER 24

FIG. 6.3

7. OVERALL INFLUENCES OF DIFFERENT LIVE LOAD DISTRIBUTIONS

In this Chapter, ten different distributions of live load are considered to obtain a more complete description of the overall behavior of the bridge. Influence lines, although useful in obtaining the maximum values of selected parameters, do not readily yield the complete states of stress that accompany the maximum values. The complete states of stress are useful in studies of initial or local failures and of subsequent modes of failure that might lead to the total collapse of the bridge. They are useful in assessing the consequences of different kinds of failure, and in determining factors of safety for the different components of the bridge. Further, they are useful in indicating the kinds of nonlinear studies required to determine actual load factors or the reserve strength of the bridge beyond the specified live loads.

From an inspection of the influence lines given in Figs. 6.1 (II) to 6.14 (II), it is observed that approximately 26 different cases of live load distributions yield the maximum values of the selected parameters. A summary is given in Fig. 7.1 of 26 distributions of live loads which approximate those actually considered in obtaining the values of maxima. Several of the latter distributions differ but slightly from each other and their effects on values of maxima are almost identical. Based on this observation, 10 different cases of live load distributions are selected for obtaining a more complete description of the overall behavior of the bridge. The 10 cases are shown in Fig. 7.2. The effects of these cases are calculated by means of the general program for linearly elastic structures and are summarized in Figs. 7.1 (II) to 7.10 (II). For each case, a summary

is given in a separate Figure of the displacements and of the distributions of forces and moments along the various members of the bridge.

The total state of stress for dead load and a given case of live load is obtained by adding the effects of both loadings. The addition can be performed by the simple expedient of inverting the diagrams obtained for dead load and superposing them on the corresponding diagrams for live load. Obviously, the latter addition is possible provided that corresponding diagrams are drawn to the same scale.

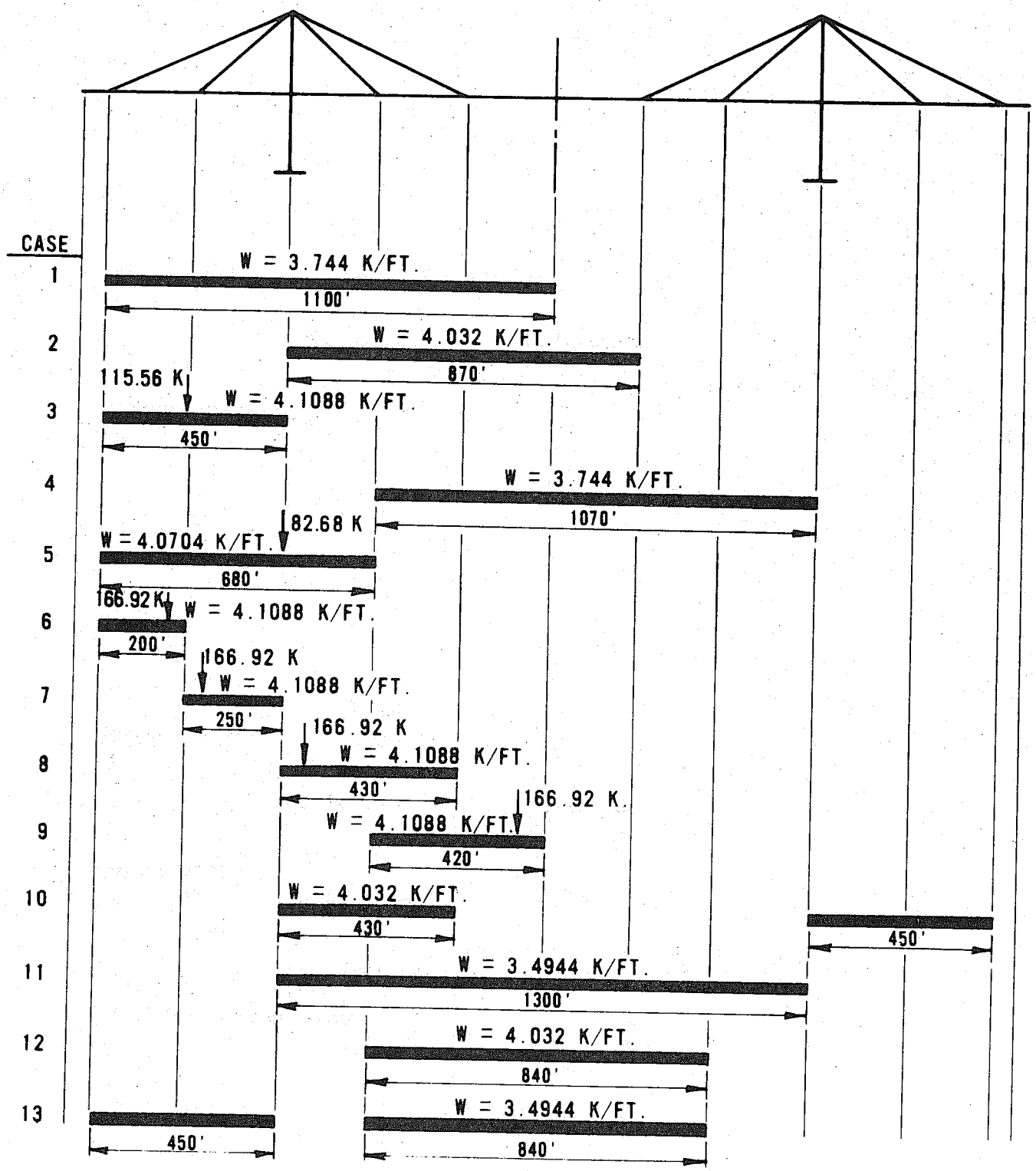

LOAD CASES APPROXIMATE TO THOSE USED IN DETERMINING MAXIMUM FORCES AND MOMENTS

FIG. 7.1
SHEET 1 OF 2

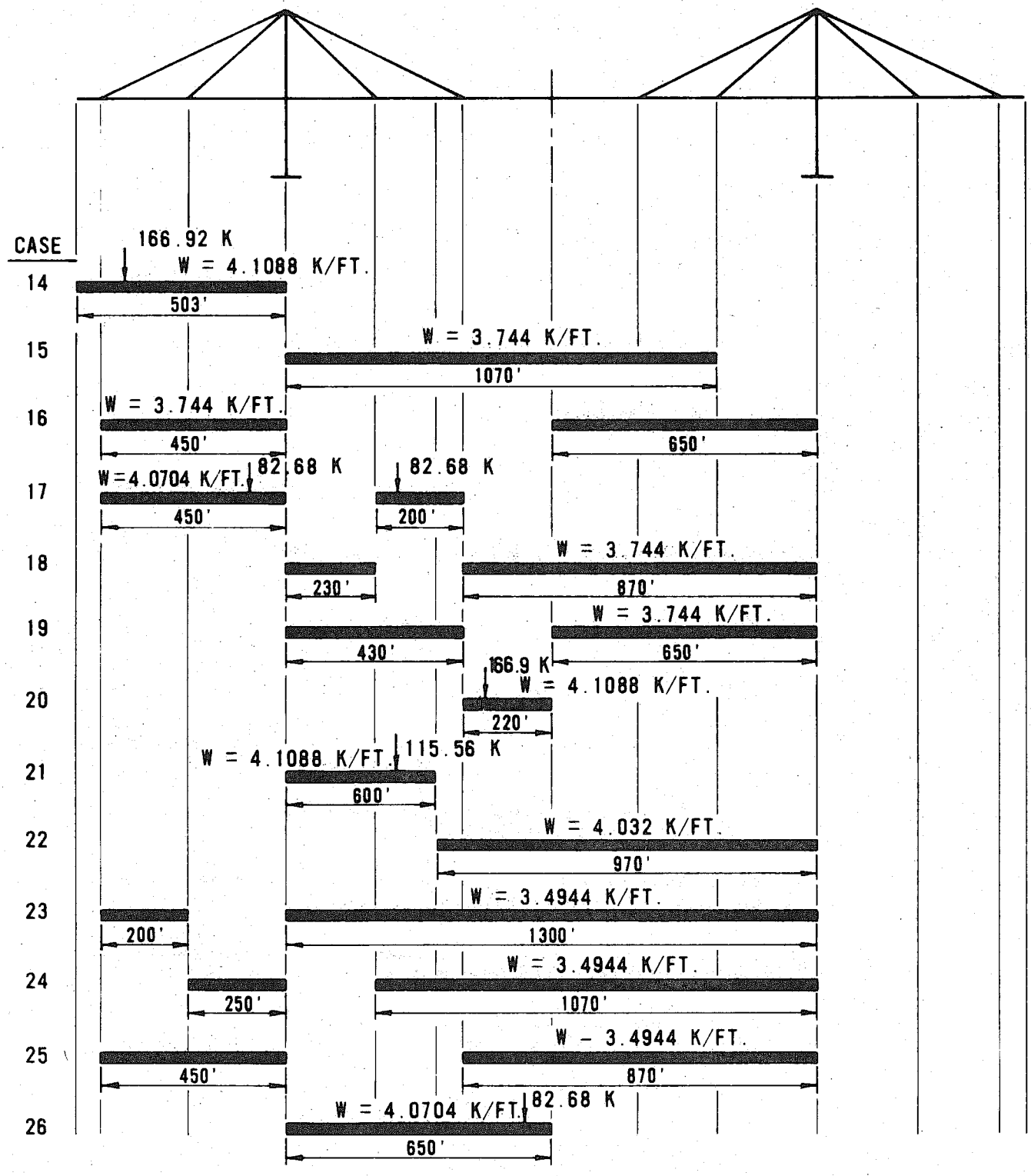

LOAD CASES APPROXIMATE TO THOSE USED IN DETERMINING MAXIMUM FORCES AND MOMENTS

FIG. 7.1
SHEET 2 OF 2

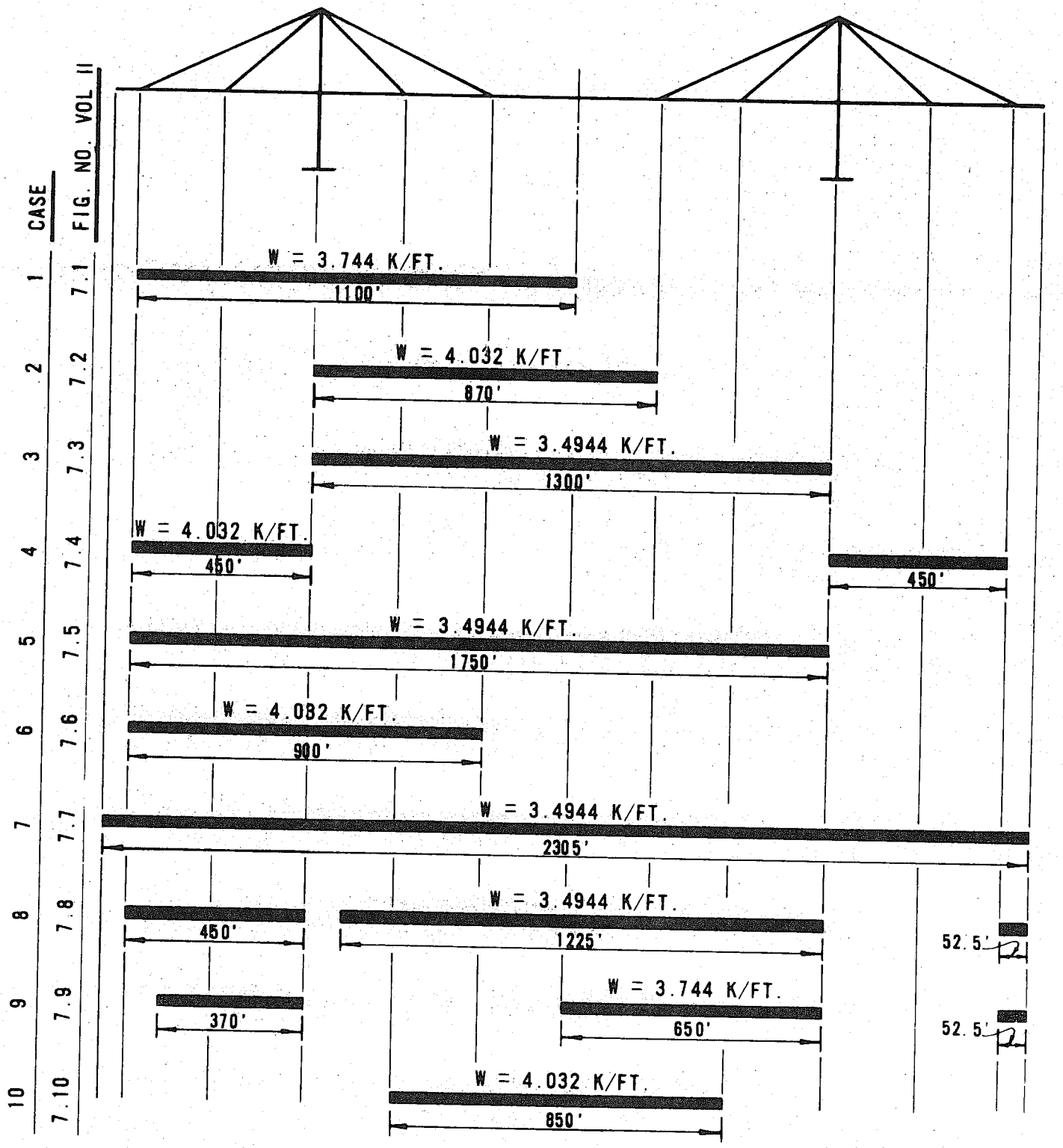

LIST OF LIVE LOAD DISTRIBUTIONS CONSIDERED FOR OVERALL EFFECTS

FIG. 7.2

8. NONLINEAR BEHAVIOR OF THE BRIDGE

Four kinds of studies are presented in the report concerning the nonlinear behavior of the bridge. The first two kinds are given in Chapter 5 and deal with the determination of (1) the dimensions of each member of the bridge when the member has no stress, and (2) the camber of the roadway girder. The last two kinds are given in this Chapter and deal with the determination of (3) joint displacements and member forces for various stages of erection, and (4) the nonlinear response of the bridge to a selected overload of vehicular traffic.

8.1 Description Of The Erection Procedure

A critical aspect in the design of any major structure is the selection of a suitable erection procedure. In design, what may be but a concept becomes a reality only when erected. Also, if a structure can be built, in general, it will remain standing. The preceding statements are intended merely to indicate the necessity and importance of conducting a close review of the erection procedure to be selected for the Southern Crossing Bridge. The final procedure will be selected by the contractor, subject to the approval of the designers. In this study, the procedure selected by the Division of Bay Toll Crossings as a base for determining the feasibility of design is considered. In selecting the procedure, the Division assumed that temporary erection bents may be used in the side spans but would not be allowed in the 1200 foot navigation channel.

The erection procedure considered by the Division of Bay Toll Crossings is described in the design drawings and in Ref. 10. The assumed erection sequence is shown in Fig. 8.1 and 8.1 (II). It consists of six stages and is as follows:

In Stage I, temporary erection bents are installed between the main towers and the anchor piers at the ends of the cable stayed girder bridge. For example, consider Tower 1 and the anchor pier closest to it. A bent is installed near Tower 1, and another at the transverse anchorage beam associated with cable B. The girder sections are cantilevered in both directions from the main tower using a balanced cantilever method. The rocker bearing at Tower 1 is blocked temporarily during this phase. The cantilevering proceeds until the girder lands on the bent associated with the position of cable B.

In Stage II, the bent near the main tower is removed. The girder sections in the center span are extended to the transverse anchorage beam associated with the position of cable C, while the side span is completed to the anchor pier but still supported by the temporary bent at cable B. At this stage, the tapered girder in the flanking span is erected, with an erection bent in the flanking span being optional. Temporary catwalks are then installed, and the saddle assemblies on top of the main tower are placed and bolted in final position

In Stage III, the catwalks provide access to the top of the tower and can be used to help support cables B and C during their placement. Cables B and C are continuous over their respective saddle and are clamped firmly in the saddle after being tensioned to an initial load of about 1450 kips each, as indicated by the designers. The tensioning is performed by jacking at both ends of the short cable simultaneously. In Stage III, the flanking span is connected to the end of the cable stayed girder.

During Stage IV, the center span is advanced by cantilevering to the next cable anchorage beam; that is, the anchorage beam associated

with cable D. The temporary erection bent in the side span can be removed when the dead load reaction during erection reduces to zero. Catwalks are placed for aid in installing the long cables.

In Stage V, cables A and D which are continuous over their respective saddle are clamped firmly in the saddle after being tensioned to an initial load of 2200 kips. The procedure for tensioning the long cables is the same as for the short cables. After the long cables are clamped at the saddle, an additional load of 250 kips, indicated by the designers, is applied to the shoreward side of the long cable. At this point, the top of the tower is expected to be deflected approximately 14 inches shoreward from the original vertical position.

In Stage VI, the remaining portion of the center span is then cantilevered, section by section, until the position of a central closing section is reached.

The entire procedure is repeated for the other half of the bridge, and then the closing section of about 60 feet in length is installed to form a continuous girder.

Thrust buffers are installed and the blocking at the rocker removed to allow the structure to move with temperature changes. The railing, median barrier and wearing surface are placed on the continuous structure. The tops of the towers which were deflected a maximum amount at one point in the erection procedure should return to their permanent position under dead load, and the forces on both sides of each long cable should now be approximately equalized.

8.2 Sequence Of Erection Calculations

From the viewpoint of analysis, the only state of a given structure completely known for erection purposes is the dead load state desired by the designers. In general, the desired conditions are within

the control of the designers provided that other conditions of loading, including those of erection, do not warrant changes in design. Obviously the desired conditions at dead load depend on the objectives in design, and on the establishment of suitable criteria for checking the design. Among the latter criteria are suitable factors of safety and load factors for other conditions of load beside dead load.

For the dead load state of the Southern Crossing Bridge, the distributions of forces and moments, the materials and sizes of members, and the geometry of the bridge are prescribed. The geometry is prescribed by specifying the profile and section of the roadway, the articulation of the bridge, and the coordinates of all work-points. The writers consider the dead load state as the reference state in the subsequent calculations concerning the erection procedure of the bridge. Also, for each stage of erection, only the dead load of the bridge at the given stage is considered. The effects of erection equipment, temperature changes, residual strains, and other conditions of loading that may be associated with the given stage are not considered. It is assumed for each stage that the camber shape and the dimensions of the unstressed members are based on the conditions at the dead load state of the bridge. For each stage of erection, the additional objectives of the designers (see Fig. 8.1) are considered.

It need be recognized that the sequence of calculations for a given structure need not be the same as that selected for the erection scheme. At first glance, it may seem preferable or even necessary to employ the same sequence in the calculations as in the erection scheme. It will be shown that in certain instances, depending on the erection sequence and on the need of the calculations, a sequence reverse to that of the erection scheme is preferable. In other instances, a combination

of both sequences is preferable. Of course, whatever sequence is selected for the analysis, the analysis must readily permit the conditions at any stage of erection to be completely described. The theory and the computer program developed by the writers permit either a forward or a reverse sequence to be employed in the calculations of an erection scheme. For the calculations reported herein, the writers employed a sequence that is reverse to the erection sequence shown in Fig. 8.1. The writers' preferences in selecting a reverse sequence are explained after the results are presented and the conduct of the calculations is described.

The sequence of calculations and the various states of the bridge for which the calculations are made are given in Figs. 8.2 and 8.2 (II). With reference to the dead load state, eight erection states of the bridge and Stage T of Tower 1 are considered. The eight states encompass the six stages of erection defined by the designers. Any other state that may be of interest during actual construction can be studied in the same way.

8.3 Results Of The Erection Calculations

Summaries are given in Figs. 8.3 (II) to 8.8 (II) and in Tables 8.1 to 8.8 of the results obtained for the eight states and for Stage T of Tower 1.

For reference, a summary is given in Fig. 8.3 (II) of the member forces for the dead load state of the bridge. Because of the changes that kept occuring in design, the analytical model used in the nonlinear studies of camber, erection, and overload conditions of the bridge differs from that used for the linear studies. The node point and member designations of the analytical model used for the non-linear

studies are shown in Fig. 8.3 (II). The latter designations are important to note when referring to Tables 8.1 to 8.3.

In Figs. 8.4 (II) to 8.8 (II), joint displacements and member forces are given for the eight erection states and for Stage T of Tower 1. A summary of the deflected structures for the eight states is given in Fig. 8.3. For each state, the deflections are referred to the dead load state of the bridge; that is, the dead load state serves as a reference from which the displacements are measured. For the dead load state, the horizontal displacements at the tops of Towers 1 and 2 respectively are -0.1076 feet and -0.0191 feet. To obtain the absolute displacement at the top of a tower for each erection state, the latter values and those recorded in Figs. 8.4 (II) to 8.8 (II) need be taken into account.

Summaries are given in Tables 8.1 to 8.7 of joint displacements and member forces for each erection state. In Table 8.1 (5 sheets), the summary is for forces and moments in selected members of the bridge. The selected members and the force and moment components are essentially the same as those considered in Table 6.4. Note, however, the differences in the member and node designations because of the two analytical models used in this study.

Total displacements of selected nodes for each state are given in Table 8.2. The latter displacements are with reference to the dead load state of the bridge. Relative displacements between different states also are given. They are given in Table 8.3. The relative displacements are between states as considered in the sequence of calculations.

Summaries are given in Tables 8.4 to 8.7 of selected parameters of the cables. The selected parameters are force components and slopes at the two ends of each cable. The magnitudes of the parameters are for each erection state.

8.4 Conduct Of The Erection Calculations

The results presented in Section 8.3 are based on the nonlinear theory of elastic structures. They are obtained by means of the general computer program called NONLIN. Note in the theory

$$P_{in} = K_{in} U_{in} \tag{8.1}$$

is in terms of the difference between two states of a structure; namely, states i and n. Consequently, an unknown state n can be obtained from any known state i by solving Eq. 8.1 for the difference between States i and n. In Eq. 8.1, subscripts i and n merely serve as index numbers for identifying known and unknown states of a structure. No restrictions are imposed on the values of i and n. This implies that many kinds of sequences can be followed in studying the erection stages of a structure. Included are sequences of calculations that are forward or backward to the sequence of construction. Also included are sequences of calculations that combine forward and backward sequences. In fact, the calculations need not be sequential.

The sequence of calculations followed in obtaining the results summarized in Section 8.3 is shown in Table 8.8. It is observed in processing the calculations that the output for a known State i serves as the input for a sought State n. For example, State 3 is obtained by considering the results of State 2 as input and solving Eq. 8.1 for the difference between States 2 and 3. The sequence selected herein is one of convenience and of preference rather than one of necessity. As stated before, the only state completely known for erection purposes is the dead load state desired by the designers. For this reason, the writers prefer to select the dead load state as the reference state for

the calculations of erection. In addition, the dead load state furnishes the initial data. Then, for reasons of accuracy, the writers prefer to select a sequence in which the difference between each State i and its associated State n is small.

In general, no special provision need be made in the solution technique described in Chapter 4 for determining the difference between two States. Program NONLIN is written to accommodate either specified displacements or external loads and reactions for any State n. In the erection procedure shown in Fig. 8.1, other requirements than those of external loads, displacements, and reactions are indicated for Stages 2, 3 and 4. The program also is written to accommodate other requirements than those of external loads, displacements, and selected reactions for any State n. For example, for State 6 of the erection calculations it is specified that no unbalanced horizontal force is to exist at the top of Tower 1. The results shown in Fig. 8.7 (II) are compatible with this requirement. They are obtained by means of an iterative procedure in which each estimate of State 6 is successively adjusted until the global X-components of the forces in Cables B and C are balanced, and the residual force vectors at the nodes are sufficiently small. For another example, for State 8 it is specified that the reaction and the displacement of the girder at the end bent are simultaneously zero. The results shown in Fig. 8.8 (II) are compatible with this dual requirement. For this example, the results are obtained by means of another iterative procedure in which each estimate of Step 8 is successively adjusted until the dual requirement is fulfilled, and the residual force vectors at the nodes are sufficiently small. In each iteration, a rigid body rotation of the girder about a global Z-axis at the bearing support at Tower 1 is incorporated.

For purposes of efficiency, particular attention is given in organizing suitable and flexible formats of input and output data for the various computer runs. The output of each run consists of (1) a printed record and listing of the results, and (2) punched cards which serve as input for a subsequent run. The following items are included in the printout: (1) total displacements of State n with reference to the dead load state, (2) relative displacements between States i and n, (3) member forces, (4) applied loads and reactions, and (5) the residual load vectors which may remain at the end of a specified number of iterations. The following items are punched on cards: (1) member data such as forces, or deformations, unstressed lengths, direction cosines of local axes, eccentricities of rigid arms, and (2) node data such as coordinates, total displacements with reference to the dead load state, and specified loadings or displacements. The punched data serve either for the calculation of the next erection state or for the further iteration of the same state if convergence is unsatisfactory. The number of iterations used for obtaining the results of each state is given in Table 8.8.

Some difficulties arise in the processing of data for the various states because each state differs from the others. Consequently, a different set of node and member designations need be used for the solution system of each state. For efficient processing, the writers devised a solution system of node and member designations for each state and a single master system for all states. Matrix arrays are defined and are used in the input data by means of which the solution system of a State i is transformed to that of a State n. For output, the solution system of State n is transformed to the single master system.

In the program NONLIN, either member forces or deformations are used as input data. For the calculations of erection, it is preferable to input member deformations. This is because from Eq. 8.2,

$$p = k(u) \cdot u \tag{8.2}$$

the calculation of member forces from deformations is performed directly; whereas, the calculation of deformations from member forces involves an iterative scheme (see Section 5.1). Note, deformations associated with temperature changes or misfits are easily taken into account.

8.5 Overload of Vehicular Traffic

As stated before, several innovations in design are introduced for the Southern Crossing Bridge. The central span length is greater than that of any other bridge of the same kind constructed elsewhere. Also, an orthotropic deck is incorporated with a cable system and with uniquely shaped towers. For these and the reasons given in Chapter 1, a study is made of the nonlinear behavior of the bridge when the bridge is subjected to an overload of vehicular traffic.

The distribution of live load for the overload case is the same as that of Fig. 7.3 (II). The live load is distributed uniformly between the two towers. The intensity of the overload is 3.4944k/ft. for one-half bridge, which is twice the live load specified for design purposes.

The results for the overload case are summarized in Figs. 8.4 and 8.9 (II), in Tables 8.1 to 8.7, and in Table 8.9. Forces, moments, and displacements for the total bridge are summarized in Fig. 8.9 (II). The summaries in Tables 8.1 to 8.7 are of the same kind as those given

for the erection calculations. A comparison is given in Fig. 8.4 of the deflected structures obtained by means of the linear and nonlinear theories. Also, a comparison is given in Table 8.9 of the influences of nonlinearity on different parameters of the bridge. Four groups of parameters are considered in the Table. The four groups are (1) forces in the cables, (2) shears, P_χ, at the saddles, (3) displacements, and (4) moments in the girder and at the base of Tower 1. For the loading case considered, the percentage differences between the results of the two theories are smallest for the values of forces in the cables. They are biggest for the values of shears in the saddles at the top of Tower 1.

TABLE 8.1 (SHEET 1 OF 5)

SUMMARY OF FORCES AND MOMENTS IN SELECTED MEMBERS OF THE BRIDGE FOR THE ERECTION SEQUENCE AND FOR DEAD LOAD PLUS TWICE LIVE LOAD. (FORCE COMPONENTS IN KIPS, MOMENT COMPONENTS IN KIP-FT.)

Member		Com-po-nent	Dead Load	States In The Erection Calculations								Stage T	Overload DL+2.0×LL
	No.			1	2	3	4	5	6	7	8		
GIRDER AND END BENT	2	p_1	-111.00	-191.18	742.09	985.39	780.30	695.64	577.78	132.07	—	—	-1320.8
	7	p_1	4179.6	3139.1	1725.9	27.734	19.55	8.00	2.69	-4.21	-11.856	—	6120.2
		p_2	506.86	316.24	549.36	34.748	-170.22	-254.57	-372.36	-234.73	-366.88	—	229.97
	15	p_8	1068.7	875.78	652.66	1167.5	1372.7	1457.3	1575.2	1437.2	1566.5	—	1315.7
	17	p_1	6632.2	5163.9	3247.2	2611.2	2568.4	1090.8	1066.0	15.98	15.167	—	8998.2
		p_2	1091.8	901.77	685.03	1090.8	1299.7	1597.6	1719.1	608.40	715.71	—	1207.3
		p_6	120410	100430.	52031.	154730.	195690.	210740.	234300	175050	201360	—	176260
	26	p_8	695.98	412.23	644.18	223.56	10.55	-270.04	-392.37	496.06	621.93	—	527.20
	27	p_1	6616.0	5147.4	2937.0	2690.4	2734.4	994.33	1020.5	5.77	3.6882	—	10376.
		p_2	564.17	303.37	658.87	101.26	55.19	527.83	500.99	1459.8	1459.8	—	939.40
		p_6	73493.	44440	52924	57549	46708	-10649	-16897	204690	204710	—	104680
	35	p_8	1130.8	95 01	611.45	1158.9	1204.1	753.18	783.84	-181.02	-180.98	—	1531.3

TABLE 8.1 (SHEET 2 OF 5)

SUMMARY OF FORCES AND MOMENTS IN SELECTED MEMBERS OF THE BRIDGE FOR THE ERECTION SEQUENCE AND FOR DEAD LOAD PLUS TWICE LIVE LOAD. (FORCE COMPONENTS IN KIPS, MOMENT COMPONENTS IN KIP-FT.)

Member	No.	Com-po-nent	Dead Load	States In The Erection Calculations								Stage T	Overload DL+2.0×LL
				1	2	3	4	5	6	7	8		
GIRDER	37	p_1	4489.4	3463.8	1448.8	10.71	9.20	3.58	3.46	-0.22	-0.502	—	7393.5
		p_2	915.18	651.34	788.12	1440.7	1440.6	180.87	180.95	180.94	181.26	—	1378.9
		p_6	132250	111200	36170	165710	165680	994.06	995.29	994.29	998.49	—	170260
	44	p_8	707.74	583.38	365.72	-191.31	-191.38	—	—	—	—	—	923.17
	46	p_1	31.22	68.61	4.491	.8877	.6877	—	—	—	—	—	1028.9
		p_2	1508.7	1078.2	189.48	191.90	190.97	—	—	—	—	—	2278.0
		p_6	105140	99498	1031.5	1058.2	1048.0	—	—	—	—	—	117120
	53	p_2	-0.48	1.82	—	—	—	—	—	—	—	—	-11.81
		p_6	-43681	-2230.9	—	—	—	—	—	—	—	—	-116390
CABLES	161 (A)	p_1	-4674.4	-3505.5	-1886.5	—	—	—	—	—	—	—	-6892.8
	167(B)	p_1	-3326.8	-2739.3	-2063.9	-3485.3	-3420.0	-1404.3	-1367.5	—	—	—	-3893.4
	171 (C)	p_1	-2964.7	-2333.4	-2041.7	-3769.9	-3837.4	-1363.2	-1402.1	—	—	—	-4199.0
	175(D)	p_1	-4989.8	-377[illegible].0	-1559.9	—	—	—	—	—	—	—	-7173.4

TABLE 8.1 (SHEET 3 OF 5)

SUMMARY OF FORCES AND MOMENTS IN SELECTED MEMBERS OF THE BRIDGE FOR THE ERECTION SEQUENCE AND FOR DEAD LOAD PLUS TWICE LIVE LOAD. (FORCE COMPONENTS IN KIPS, MOMENT COMPONENTS IN KIP-FT.)

Member	No.	Com-po-nent	Dead Load	States In The Erection Calculations 1	2	3	4	5	6	7	8	Stage T	Overload DL+2.0×LL
TOWER MEMBERS	105	p_1	27430	24969	23149	22562	22307	19436	19290	19385	19279	17178	30921
		p_3	32.43	73.29	15.35	-32.69	-29.917	-19.42	-17.79	-6.19	-2.872	0.0	1007.6
		p_5	-10754	-36589	-86143	43105	66481	-8195.3	5073.1	978.41	382.65	0.0	-108020
		p_6	31167	29389	27714	27595	27480	25116	25053	24372	24325	23090	33891
	106	p_1	27722	25218	23345	22766	22511	19573	19427	19479	19374	17254	31285
		p_3	23.13	75.63	101.66	-55.63	-11.680	15.38	-25.98	1.14	-19.77	0.0	1008.9
		p_5	-10449	-35656	-87030	42895	65438	-8492.0	4920.3	835.63	684.18	0.0	-97055
		p_6	-17960	-18864	-27985	-21035	-19391	-27363	-26419	-43981	-43332	-36747	-11920
	108	p_1	24250	21375	19862	19283	19028	16089	15943	15996	15890	13770	27801
		p_3	33.16	79.42	86.25	-54.99	-27.006	-16.34	-24.76	-0.64	-14.18	0.0	1013.2
		p_{11}	8144.4	27731	82637	-38525	-62379	10623	-2515.4	-682.06	-133.65	0.0	-8065.2
		p_{12}	-18040	-1910[illegible]	-23740	-20658	-19964	-24350	-23950	-31844	-31577	-29931	-14425

TABLE 8.1 (SHEET 4 OF 5)

SUMMARY OF FORCES AND MOMENTS IN SELECTED MEMBERS OF THE BRIDGE FOR THE ERECTION SEQUENCE AND FOR DEAD LOAD PLUS TWICE LIVE LOAD. (FORCE COMPONENTS IN KIPS, MOMENT COMPONENTS IN KIP-FT.)

	Member No.	Component	Dead Load	States In The Erection Calculations 1	2	3	4	5	6	7	8	Stage T	Overload DL+2.0*LL
TOWER MEMBERS	110	p_{10}	1064.1	3679.6	10533	-4987.8	-7918.3	1246.5	-412.21	-222.50	-177.68	0.0	1201.5
		p_{11}	6450.3	22174	80728	-35572	-59083	12147	-955.64	-383.20	-116.74	0.0	-78178
		p_{12}	1975.3	-358.93	-14048	-4453.6	-2241.5	-14735	-13461	-38248	-37374	-30270	11989
	113	p_5	-5857.6	-20113	-80554	34336	56119	-12090	601.03	-202.60	214.47	0.0	95925
		p_6	-55226	-40880	-26470	-26067	-25370	-5992.7	-5993.7	1512.7	1851.4	3020.6	-77664
		p_{11}	4609.7	18226	69995	-30342	-51456	11042	-401.02	65.19	445.63	0.0	-86977
		p_{12}	-57090	-54221	-47621	-50983	-51611	-44148	-44509	-34957	-35243	-36268	-63579
	117	p_1	12030	10054	7595.1	7985.0	7986.5	4853.7	4855.0	2832.6	2832.1	2830.5	15372
		p_3	18.19	85.71	380.66	-157.78	-241.66	56.86	-3.93	1.67	-6.953	0.0	-428.60
		p_{11}	2792.9	9696.8	35960	-15501	-26161	-5732.3	-112.60	15.12	132.56	0.0	-45529
		p_{12}	-4037.0	-2973.3	-951.49	-1498.3	-1637.3	406.49	327.93	2702.6	2650.0	2359.6	-6252.3

TABLE 8.1 (SHEET 5 OF 5)

SUMMARY OF FORCES AND MOMENTS IN SELECTED MEMBERS OF THE BRIDGE FOR THE ERECTION SEQUENCE AND FOR DEAD LOAD PLUS TWICE LIVE LOAD. (FORCE COMPONENTS IN KIPS, MOMENT COMPONENTS IN KIP-FT.)

	Member No.	Component	Dead Load	States In The Erection Calculations 1	2	3	4	5	6	7	8	Stage T	Overload DL+2.0×LL
TOWER MEMBERS	120	P_1	10174	8206.6	5747.0	6137.2	6138.6	3005.8	3007.2	984.67	984.17	982.65	13524
		P_9	-18.58	-85.33	-363.52	152.45	242.04	-53.45	2.27	-0.84	3.967	0.0	440.37
		P_{11}	1208.9	2421.4	6524.4	-2828.9	-4972.5	1160.0	56.27	-10.81	57.04	0.0	-8342.5
		P_{12}	-10853	-11180	-12640	-11074	-10850	-12862	-12729	-15732	-15604	-15340	-9772.2
	122	P_1	4376.3	3546.1	2891.1	5039.6	5042.2	1981.2	1983.2	0.0	0.0	0.0	5612.5
		P_3	315.57	343.61	62.36	-137.82	-235.81	58.22	3.05	0.0	0.0	0.0	-147.84
	123	P_1	4599.6	3511.2	1761.7	0.	0.0	0.0	0.0	0.0	0.0	0.0	6634.7
		P_3	-292.42	-242.88	294.36	0.	0.0	0.0	0.0	0.0	0.0	0.0	-265.00
	125	P_1	1276.4	733.75	1312.5	346.29	90.206	275.35	127.89	2205.7	2100.5	—	1520.6
		P_3	0.0	0.0	-315.75	95.77	191.54	-76.08	-19.35	-59.89	-57.01	—	1361.3

TABLE 8.2

SUMMARY OF TOTAL DISPLACEMENTS AT SELECTED NODES FOR THE ERECTION SEQUENCE AND FOR DEAD LOAD PLUS TWICE LIVE LOAD. (DISPLACEMENTS IN FEET WITH REFERENCE TO DEAD LOAD STATE).

	NODE NO.	U-COMPONENT	STATES IN THE ERECTION CALCULATIONS 1	2	3	4	5	6	7	8	STAGE T	OVERLOAD DL+2.0×LL
GIRDER	1	U_Y	.0887	.2361	−.0871	−.2115	−.2226	−.2938	−.1534	−.2376	—	−.1911
	5	U_Y	−.0008	.0139	−.0064	−.0073	−.0022	−.0026	.0000	0.0	—	.0053
	13	U_Y	−.1232	−.4078	.2229	.4069	.4881	.6247	.6616	.6607	—	.3792
	23	U_Y	−.1579	−.5244	.3182	.6273	.6272	.8046	.8046	1.0214	—	.5059
	33	U_Y	−.1414	−.4350	.2736	.5172	.4398	.5794	.8880	1.0691	—	.4493
	43	U_X	.1282	.0504	.3040	.3701	.2549	.2925	.2834	.3060	—	.0009
		U_Y	.0029	.0036	.0046	.0047	.0072	.0073	.0021	.0018	—	−.0034
	51	U_Y	.2032	.5856	−.2275	−.4001	.1518	.0532	−1.6386	−1.8198	—	−.5904
	61	U_X	.1242	.0406	.3417	.4126	.2698	.3111	.3657	.3906	—	−.0023
		U_Y	.6243	1.3657	−.5446	−.8302	.8596	.6965	−3.0630	−3.3963	—	−1.1790
	69	U_Y	.9019	2.1530	−.8590	−1.2225	—	—	—	—	—	−1.6647
	77	U_X	.1159	−.0126	.3741	.4474	—	—	—	—	—	−.0011
		U_Y	1.4008	4.0489	−1.2430	−1.7360	—	—	—	—	—	−2.5388
	91	U_Y	1.9924	—	—	—	—	—	—	—	—	−3.5908
TOWER	204	U_X	−.2456	−.9243	.6039	.9273	.0488	.2324	−.0033	.0084	0.0	.6950
		U_Y	.0082	.0162	.0178	.0173	.0311	.0312	.0381	.0380	.0406	−.0146
	205	U_X	−.2455	.9149	.5984	.9188	.0495	.2314	−.0042	.0075	0.0	.6856
		U_Y	.0083	.[illegible]4	.0179	.0174	.0313	.0315	.0384	.0383	.0409	−.0147
	207	U_X	−.0352	−.0732	.0801	.1206	.0495	.0723	−.0322	−.0265	0.0	−.0465
		U_Y	.0026	.0028	.0049	.0055	.0072	.0076	.0039	.0042	.0068	−.0027

TABLE 8.3

SUMMARY OF RELATIVE DISPLACEMENTS AT SELECTED NODES FOR THE ERECTION SEQUENCE. (RELATIVE DISPLACEMENTS IN FEET BETWEEN SUCCESSIVE STATES IN THE ERECTION CALCULATIONS).

	NODE NO.	ΔU-COMPONENTS	INCREMENTAL STEPS IN THE ERECTION CALCULATIONS							
			0 TO 1	1 TO 2	2 TO 3	3 TO 8	3 TO 4	4 TO 5	5 TO 6	6 TO 7
GIRDER	1	ΔU_Y	.0887	.1474	-.3232	-.1505	-.1244	-.0111	-.0712	.1404
	5	ΔU_Y	-.0008	-.0025	-.0031	-.0064	-.0009	.0050	-.0004	.0026
	13	ΔU_Y	-.1232	-.2845	.6306	-.4379	.2331	.0272	.1366	-.1278
	23	ΔU_Y	-.1579	-.3665	.8425	.7032	.3091	0.0	.1773	0.0
	33	ΔU_Y	-.1404	-.2946	.7086	.7955	.2436	-.0561	.1396	.3085
	43	ΔU_X	.1282	-.0778	.2535	-.0021	.0661	-.1152	.0376	-.0091
		ΔU_Y	.0029	.0007	.0009	-.0028	.0002	.0025	.0001	-.0052
	51	ΔU_Y	.2932	.2923	-.8130	-1.5924	-.1726	.5519	-.0986	-1.6918
	61	ΔU_X	.1242	-.0835	.3010	.0489	.0709	-.1428	.0412	.0547
		ΔU_Y	.6243	.7413	-1.9101	-2.8519	-.2858	1.6898	-.1632	-3.7595
	69	ΔU_Y	.9019	1.2510	-3.0119	—	-.3636	—	—	—
	77	ΔU_X	.1159	-.1285	.3867	—	.0733	—	—	—
		ΔU_Y	1.4008	2.6480	-5.2919	—	-.4930	—	—	—
	91	ΔU_Y	1.9924	—	—	—	—	—	—	—
TOWER	204	ΔU_X	-.2456	-.6787	1.5282	-.5955	.3234	-.8784	.1836	-.2357
		ΔU_Y	.0082	.0079	.0016	.0202	-.0005	.0139	.0001	.0068
	205	ΔU_X	-.2435	-.6714	1.5133	-.5909	.3204	-.8694	.1819	-.2356
		ΔU_Y	.0083	.0081	.0016	.0203	-.0005	.0139	.0001	.0069
	207	ΔU_X	-.0352	-.0380	.1534	-.1066	.0404	-.0711	.0229	-.1045
		ΔU_Y	.0026	.0002	.0021	-.0007	.0006	.0017	.0003	-.0036

TABLE 8.4

SUMMARY OF FORCE COMPONENTS AND END-SLOPES OF CABLE A FOR THE ERECTION SEQUENCE AND FOR DEAD LOAD PLUS TWICE LIVE LOAD. (FORCE COMPONENTS IN KIPS)

CABLE A PARAMETERS		DEAD LOAD	STEPS OF ERECTION CALCULATIONS 1	2	3	4	5	6	OVERLOAD DL+2.0*LL
END I	H	4189.3	3149.8	1709.9	—	—	—	—	6163.9
	F_{XI}	-4166.0	-3132.3	-1700.3	—	—	—	—	-6129.7
	F_{YI}	-2072.8	-1538.5	-797.01	—	—	—	—	-3085.0
	F_{ZI}	441.13	331.90	180.36	—	—	—	—	648.3
	T_I	4674.0	3505.5	1886.5	—	—	—	—	6892.8
	TAN θ_I	0.4948	0.4885	0.4661	—	—	—	—	0.5005
END J	H	4189.3	3149.8	1709.9	—	—	—	—	6163.9
	F_{XJ}	4166.0	3132.3	1700.3	—	—	—	—	6129.7
	F_{YJ}	2248.6	1713.7	971.60	—	—	—	—	3263.2
	F_{ZJ}	-441.13	-331.90	-180.36	—	—	—	—	-648.3
	T_J	4754.6	3585.8	1966.6	—	—	—	—	6974.4
	TAN θ_J	0.5368	0.5440	0.5682	—	—	—	—	0.5295

TABLE 8.5

SUMMARY OF FORCE COMPONENTS AND END-SLOPES OF CABLE B FOR THE ERECTION SEQUENCE AND FOR DEAD LOAD PLUS TWICE LIVE LOAD. (FORCE COMPONENTS IN KIPS)

				DEAD LOAD	STEPS OF ERECTION CALCULATIONS						OVERLOAD
					1	2	3	4	5	6	DL+2.0xLL
CABLE B	PARAMETERS	END I	H	2483.2	2045.7	1542.9	2603.4	2557.6	1059.3	1032.6	2909.2
			F_{XI}	-2442.6	-2012.1	-1517.5	-2561.0	-2516.0	-1041.9	-1015.7	-2861.9
			F_{YI}	-2214.4	-1821.9	-1370.8	-2317.2	-2270.4	-922.06	-896.52	-2587.4
			F_{ZI}	447.18	368.88	278.84	468.21	459.50	190.81	185.94	522.57
			T_I	3327.1	2739.3	2063.9	3485.3	3420.0	1404.3	1367.5	3893.4
			TAN θ_I	0.8918	0.8906	0.8884	0.8901	0.8877	0.8705	0.8682	0.8894
		END J	H	2483.2	2045.7	1542.9	2603.4	2557.6	1059.3	1032.6	2909.2
			F_{XJ}	2442.6	2012.1	1517.5	2561.0	2516.0	1041.9	1015.7	2861.9
			F_{YJ}	2287.8	1895.2	1443.9	2390.7	2343.8	995.13	969.78	2661.2
			F_{ZJ}	-447.18	-368.88	-278.84	-468.21	-459.50	-190.81	-185.94	-522.57
			T_J	3376.4	2788.6	2113.2	3534.6	3469.1	1453.4	1416.6	3942.8
			TAN θ_J	0.9213	0.9264	0.9357	0.9183	0.9164	0.9393	0.9392	0.9148

TABLE 8.6

SUMMARY OF FORCE COMPONENTS AND END-SLOPES OF CABLE C FOR THE ERECTION SEQUENCE AND FOR DEAD LOAD PLUS TWICE LIVE LOAD. (FORCE COMPONENTS IN KIPS)

CABLE C PARAMETERS		DEAD LOAD	STEPS OF ERECTION CALCULATIONS 1	2	3	4	5	6	OVERLOAD DL+2.0×LL
END I	H	2171.4	1714.2	1506.0	2748.9	2794.7	1008.6	1036.3	3053.5
	F_{XI}	2129.8	1681.4	1477.4	2696.0	1740.8	989.27	1016.5	2994.6
	F_{YI}	-2023.2	-1583.1	-1378.5	-2579.9	-2629.7	-917.14	-944.33	-2882.2
	F_{ZI}	423.33	333.64	292.38	536.49	546.00	196.37	201.95	597.16
	T_I	2967.9	2333.4	2041.7	3769.9	3837.4	1363.2	1402.1	4199.0
	TAN Θ_I	0.9317	0.9235	0.9153	0.9385	0.9410	0.9094	0.9112	0.9439
END J	H	2171.4	1714.2	1506.0	2748.9	2794.7	1008.6	1036.3	3053.5
	F_{XJ}	-2129.8	-1681.4	-1477.4	-2696.0	-2740.8	-989.27	-1016.5	-2994.6
	F_{YJ}	2092.4	1652.1	1447.4	2649.1	2698.9	986.01	1013.5	2952.1
	F_{ZJ}	-423.33	-333.64	-292.38	-536.49	-546.00	-196.37	-201.95	-597.16
	T_J	3015.5	2380.7	2088.8	3817.6	3885.1	1410.5	1449.6	4247.2
	TAN Θ_J	0.9636	0.9637	0.9610	0.9637	0.9657	0.9774	0.9780	0.9669

TABLE 8.7

SUMMARY OF FORCE COMPONENTS AND END-SLOPES OF CABLE D FOR THE ERECTION SEQUENCE AND FOR DEAD LOAD PLUS TWICE LIVE LOAD. (FORCE COMPONENTS IN KIPS)

CABLE D PARAMETERS		DEAD LOAD	STEPS OF ERECTION CALCULATIONS 1	2	3	4	5	6	OVERLOAD DL+2.0×LL
END I	H	4491.1	3409.8	1428.9	—	—	—	—	6417.9
	F_{XI}	4463.7	3389.1	1420.3	—	—	—	—	6378.7
	F_{YI}	-2188.2	-1629.2	-625.72	—	—	—	—	-3204.4
	F_{ZI}	494.59	375.16	156.95	—	—	—	—	708.04
	T_I	4995.7	3779.0	1554.9	—	—	—	—	7173.4
	TAN θ_I	0.4872	0.4778	0.4379	—	—	—	—	0.4993
END J	H	4491.1	3409.8	1428.9	—	—	—	—	6417.9
	F_{XJ}	-4463.7	-3389.1	-1420.3	—	—	—	—	-6378.7
	F_{YJ}	2355.6	1796.1	791.51	—	—	—	—	3373.9
	F_{ZJ}	-494.59	-375.16	-156.95	—	—	—	—	-708.04
	T_J	5071.3	3853.9	1633.5	—	—	—	—	7250.7
	TAN θ_J	0.5245	0.5267	0.5539	—	—	—	—	0.5257

TABLE 8.8

SEQUENCE OF CALCULATIONS FOR THE ERECTION STATES

INDEX NUMBERS	STATE 1	2	3	4	5	6	7	8	STAGE T
i	0*	1	2	3	4	5	6	3	7
n	1	2	3	4	5	6	7	8	T
in	01	12	23	34	45	56	67	38	7T
NUMBER OF ITERATIONS	8	6	8	6	7	7	7	6	3

*0 IS THE DEAD LOAD REFERENCE STATE

TABLE 8.9

A COMPARISON OF RESULTS FOR THE LINEAR AND NONLINEAR THEORIES

FOR	PARAMETERS							
DL + 2.0 x LL	p_1 OF MEM 175	p_3 OF MEM 122	p_3 OF MEM 123	m_y OF MEM 106	U_Y OF NODE 91	U_X OF NODE 204	m_z OF MEM 46	m_z OF MEM 53
NONLINEAR	7173.4	-147.84	-265.00	-97055	-3.5908	0.6950	117120	-116390
LINEAR	7237.7	-123.63	-219.22	-88689	-3.1716	0.6104	124559	-108681
NONLIN.— LIN.	-64.3	-24.21	-45.78	-8366	-0.4192	0.0846	-7439	-7709
$\frac{\text{NONLIN-LIN}}{\text{LIN.}} \times 100$	-0.889	19.6	20.9	9.43	13.4	13.85	-5.98	7.10

TEMPORARY ERECTION BENTS ARE INSTALLED. GIRDER SECTIONS ARE CANTILEVERED IN BOTH DIRECTIONS FROM THE MAIN TOWER. TEMPORARY BLOCKING IS INSTALLED AT TOWER BEARING.

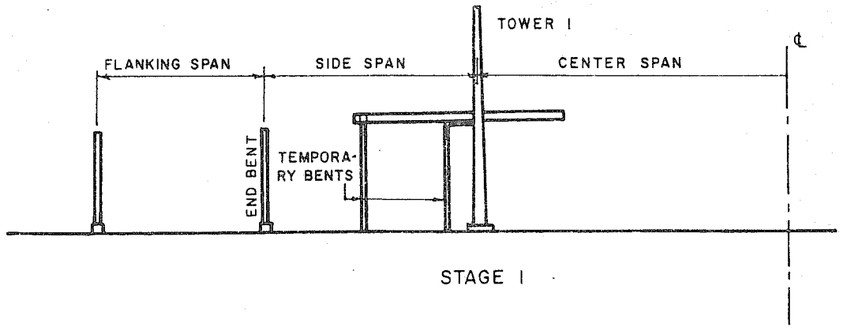

STAGE I

GIRDER SECTIONS ARE EXTENDED TO ANCHORAGE BEAM OF CABLE C, AND TO THE END BENT. TEMPORARY BENT AT CABLE B IS STILL IN PLACE. CATWALKS ARE INSTALLED.

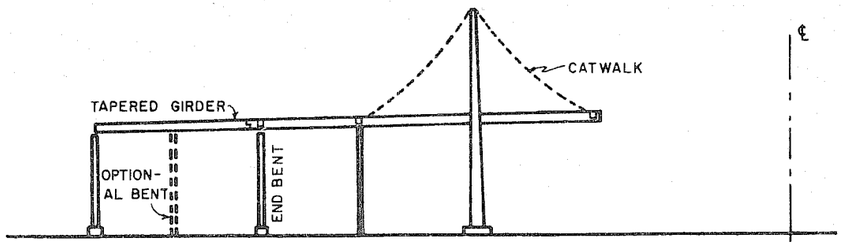

STAGE 2

CABLES B AND C ARE CLAMPED FIRMLY IN THE SADDLE AND ARE TENSIONED SIMULTANEOUSLY TO SPECIFIED LOADS AT THE ANCHORAGE ENDS OF THE CABLES. TOWER IS REQUIRED TO BE IN ITS ORIGINAL PLUMB POSITION AFTER COMPLETION OF JACKING.

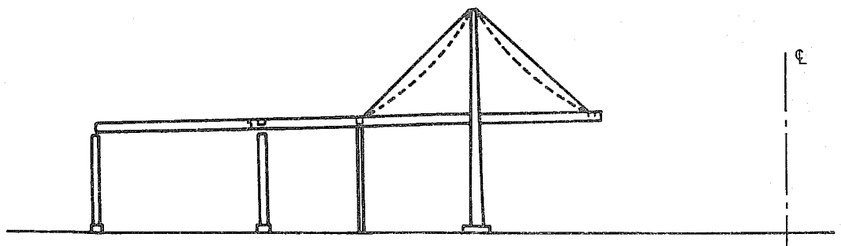

STAGE 3

GIRDER SECTIONS OF CENTER SPAN ARE ADVANCED BY CANTILEVERING TO ANCHORAGE BEAM OF CABLE D. TEMPORARY ERECTION BENT IN SIDE SPAN CAN BE REMOVED ONLY WHEN THE DEAD LOAD REACTION DURING ERECTION IS REGISTERED TO BE ZERO. CATWALKS ARE INSTALLED.

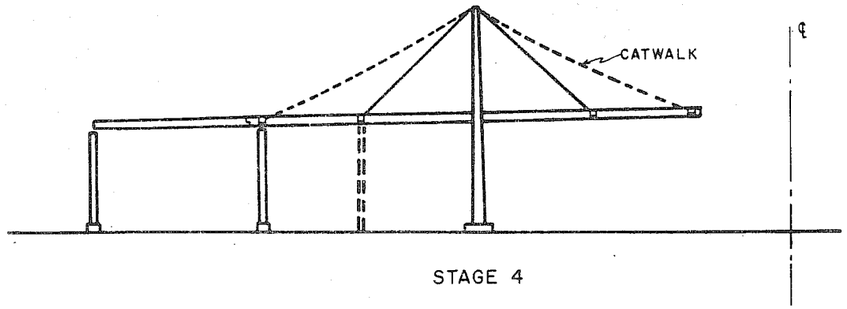

STAGE 4

CABLES A AND D ARE INSTALLED AND TENSIONED TO PRESCRIBED LOADS AT THE ANCHORAGE ENDS OF THE CABLES.

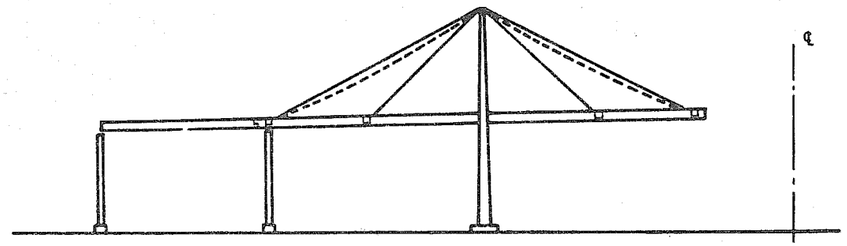

STAGE 5

REMAINING PORTION OF CENTER SPAN IS ERECTED BY CANTILEVERING TO CENTRAL SECTION. CENTRAL SECTION OF 60'± IS INSTALLED TO FORM A CONTINUOUS GIRDER. BLOCKING AT TOWER IS RELEASED. THRUST BUFFERS ARE INSTALLED. WEARING SURFACE, RAILING, AND MEDIAN BARRIER ARE PLACED.

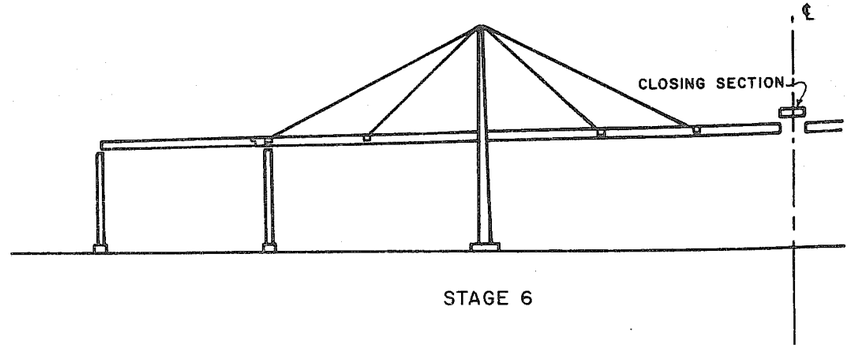

STAGE 6

SIX STAGES OF THE ERECTION SEQUENCE
FIG. 8.1

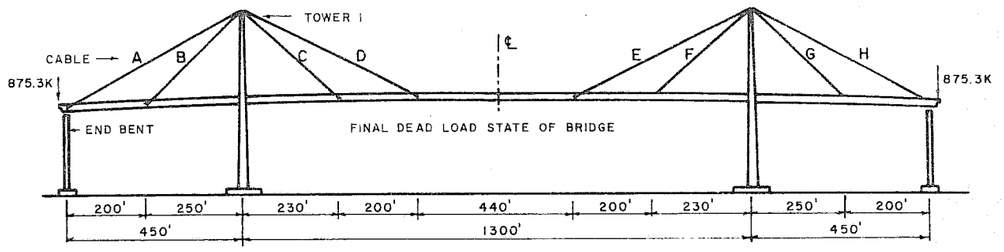

DEAD LOAD REFERENCE STATE

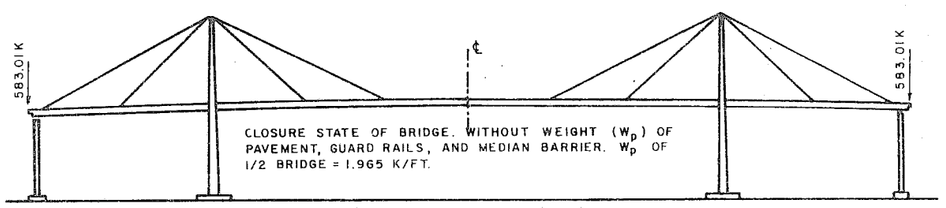

STATE 1

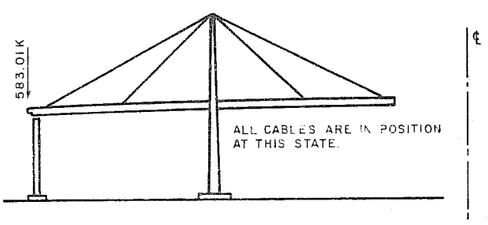

STATE 2

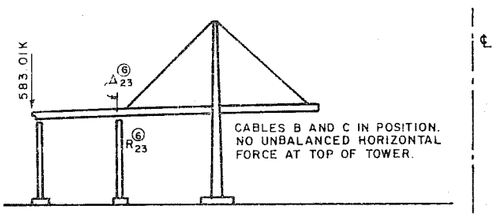

STATE 6

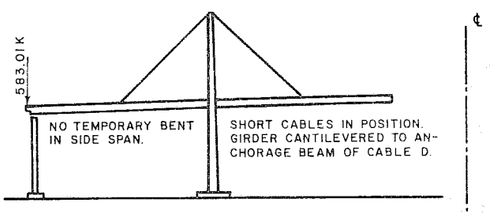

STATE 3

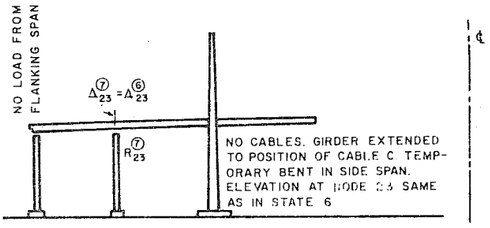

STATE 7

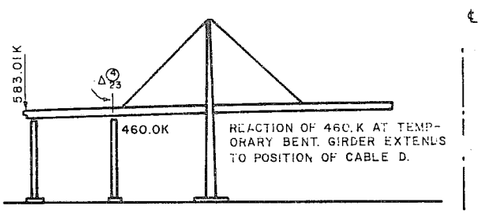

STATE 4

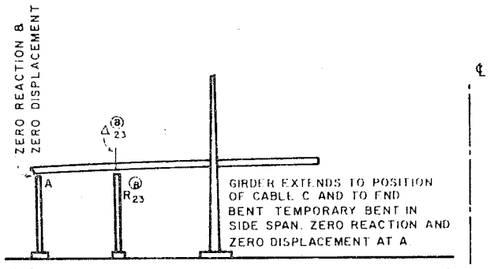

STATE 8

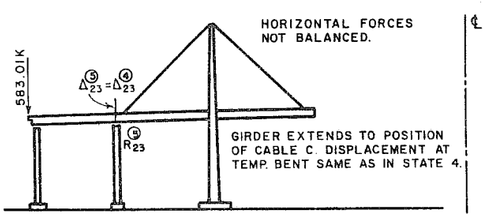

STATE 5

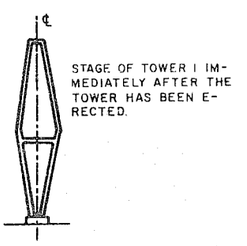

STAGE T

THE STATES USED IN THE ERECTION CALCULATIONS

FIG. 8.2

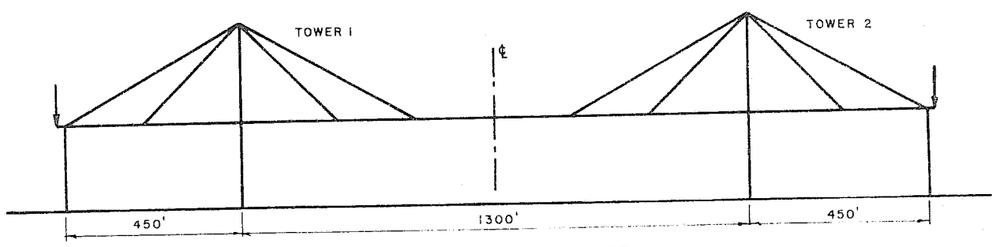

DEAD LOAD REFERENCE STATE

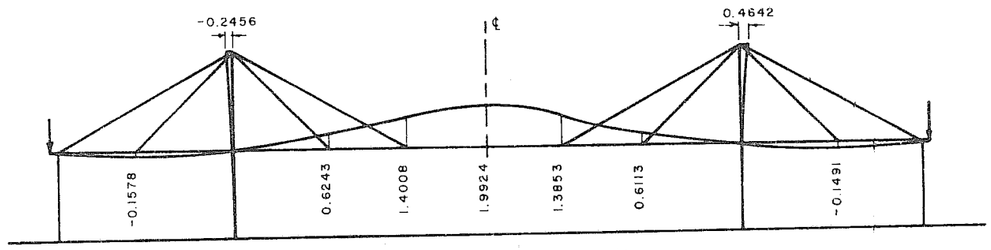

STATE 1

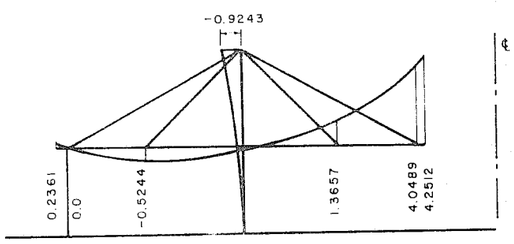

STATE 2

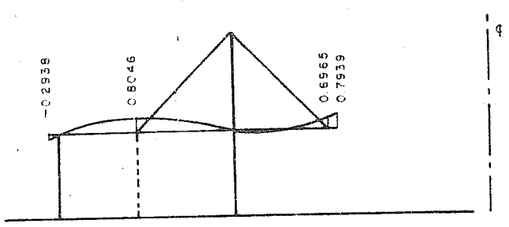

STATE 6

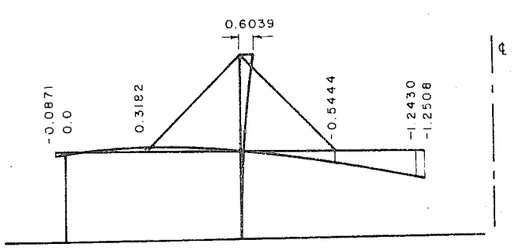

STATE 3

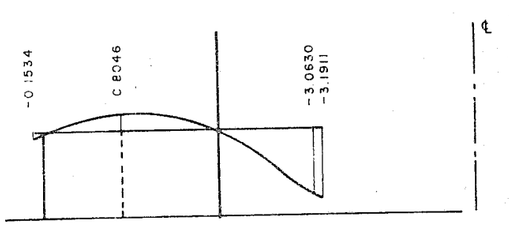

STATE 7

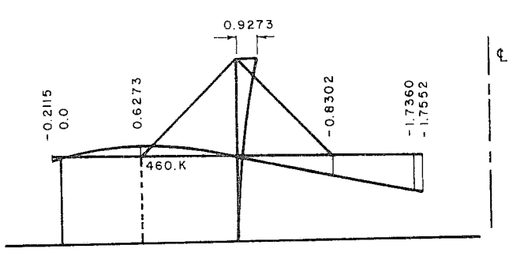

STATE 4

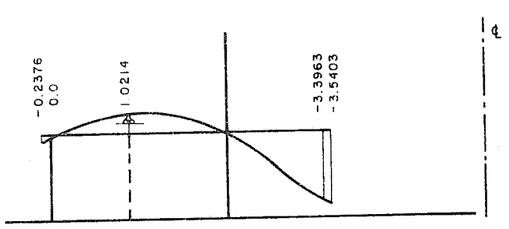

STATE 8

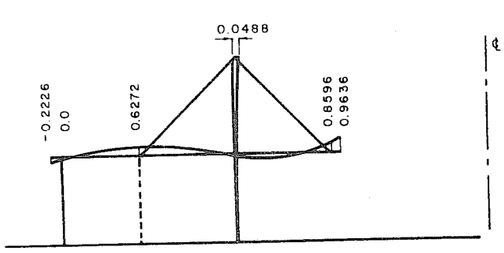

STATE 5

THE DEFLECTIONS FOR EACH STATE ARE IN FEET AND ARE REFERRED TO THE DEAD LOAD STATE. FOR THE DEAD LOAD STATE, THE HORIZONTAL DISPLACEMENTS AT THE TOPS OF TOWERS 1 AND 2 RESPECTIVELY ARE -0.1076 FEET AND 0.01912 FEET.

DEFLECTED STRUCTURES FOR THE VARIOUS STATES IN THE ERECTION CALCULATIONS

FIG. 8.3

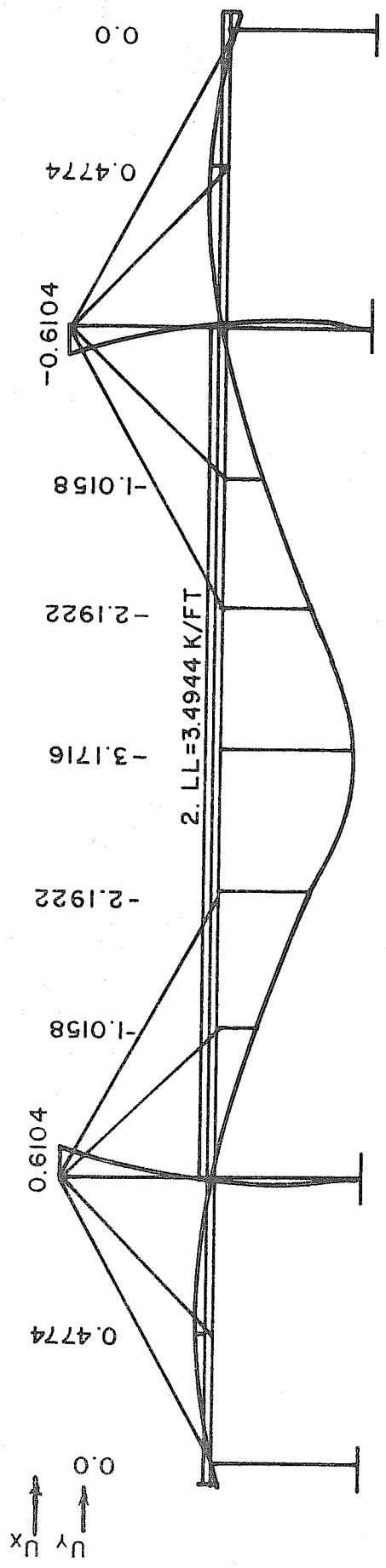

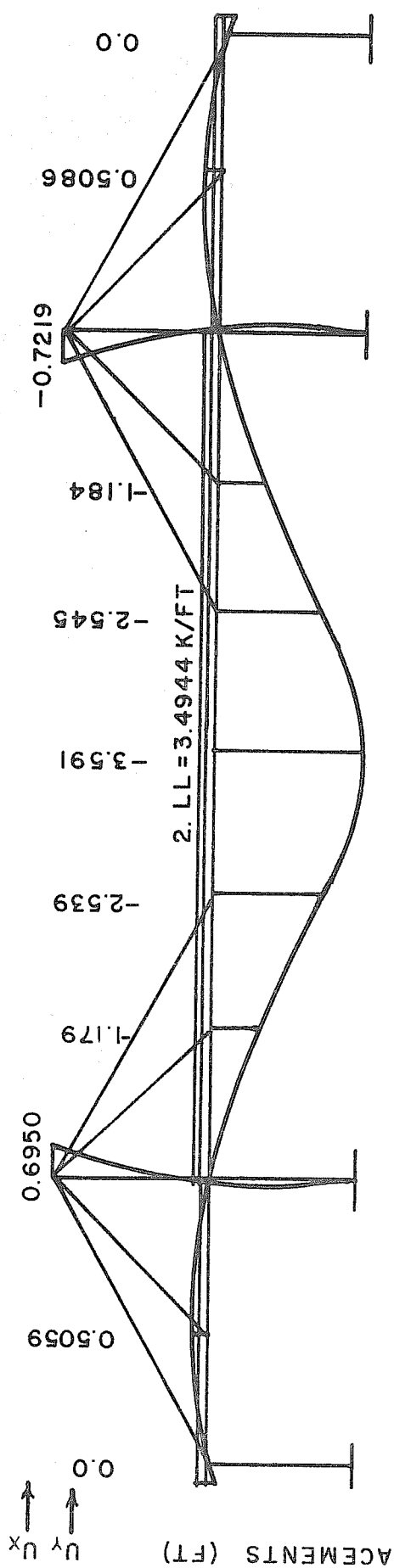

DEFLECTED STRUCTURE FOR DL PLUS TWICE LL

FIG. 8.4

9. SUMMARY AND CONCLUDING REMARKS

The report deals with the linear and nonlinear behavior of the Southern Crossing Bridge subjected to static loads. The bridge consists of an orthotropic deck girder stayed by cables which radiate to the girder from the tops of two diamond shaped towers. The loads are symmetrical with respect to the central longitudinal axis of the bridge and are those usually associated with the dimensioning phase of a bridge. Particular consideration is given to the determination of influence lines, and of maxima caused by dead loads, live loads, temperature changes, and foundation movements. Special attention is given to the nonlinear problems associated with camber, the erection procedure, and an overload of vehicular traffic. The behavior although planar necessitates the use of a theory which takes into account the nonlinear characteristics of cables and axial-flexural members lying in space. Results are given for the bridge, based on the use of a computer program applicable to space structures.

The report completes the first phase of a comprehensive study being pursued by the writers.

The uses of cable stayed girders and of orthotropic deck constructions for bridges are of more recent origin than other kinds of articulations. Consequently, additional research is needed in regard to the design and analysis of cable stayed girders before their full capacities can be realized. Mention is made of a few topics in this area that need further research. They are as follows:

(1) Three dimensional aspects of orthotropic deck constructions.

(2) Effects of spatial distributions of vehicular and of wind loads on the torsional, flexural, and axial characteristics of cable stayed girder bridges.

(3) Relationship of integral and local modes of failure to the selection of suitable factors of safety and load factors.

(4) Uses of prestressing in the girders and towers of cable stayed girder bridges.

(5) A probabilistic approach to the effects of live loads, and of wind loads, on long span bridges.

(6) The dynamic response of cable stayed girder bridges to seismic disturbances.

Several of the above topics are being pursued by graduate students at the University of California, Berkeley as part of their research and educational programs. Their researches are at various stages of progress. It is expected that some will be completed soon.

REFERENCES

1. Baron, F., and Venkatesan, M. S., "Nonlinear Analysis of Cable and Truss Structures," Journal of the Structural Division, ASCE, Vol. 97, No. ST2, Proc. Paper 7937, February, 1971, pp. 679-710.

2. Baron, F., and Venkatesan, M. S., "Nonlinear Formulations of Beam-Column Effects," Journal of the Structural Division, ASCE, Vol. 97, No. ST4, Proc. Paper 8080, April, 1971, pp. 1305-1340.

3. Connor Jr., J. J., Logcher, R. D., and Chan, S. C., "Nonlinear Analysis of Elastic Frame Structures," Journal of the Structural Division, ASCE, Vol. 94, No. ST6, Proc. Paper 6011, June, 1968.

4. Dean, D. L., "Static and Dynamic Analysis of Guy Cables," Journal of the Structural Division, ASCE, Vol. 87, No. ST1, Proc. Paper 2703, January, 1961, pp. 1-21.

5. Hadley, G., "Linear Programming," Addison-Wesley, Inc., 1961.

6. Ivy, R. J., Lin, T. Y., Mitchell, S., Raab, N. C., Richey, V. J. and Scheffey, J. M., "Live Loading for Long-Span Highway Bridges," Transactions, ASCE, Vol. 119, Paper No. 2708, 1954, pp. 981-994.

7. Livesley, R. K., "Matrix Methods of Structural Analysis," Pergamon Press, London, England, 1964.

8. Martin, H. C., "On the Derivation of Stiffness Matrices for the Analysis of Large Deflection and Stability Problems," Proc. of the Conf. on Matrix Methods in Structural Mechanics, Wright Patterson Air Force Base, Ohio, October, 1965, pp. 697-716.

9. Przemienicki, J. S., "Theory of Matrix Structural Analysis," McGraw-Hill Book Co., New York, N.Y., 1968.

10. Seim, C., Larsen, S., and Dang, A., "Design of the Southern Crossing Cable Stayed Girder," Preprint 1352, Paper presented at the ASCE National Meeting, Phoenix, Arizona, January, 1970.

11. Seim, C., Larsen, S., and Dang, A., "Analysis of the Southern Crossing Cable Stayed Girder," Preprint 1402, Paper presented at the ASCE National Meeting, Baltimore, Maryland, April, 1971.

12. Turner, M. J., Dill, E. H., Martin, H. C., and Melosh, R. J., "Large Deflections of Structures to Heating and External Loads," Journal of Aerospace Sciences, Vol. 27, 1960, pp. 97-102.

APPENDIX

CABLE STAYED BRIDGE

NUMBER OF ELEMENTS = 271
NUMBER OF NODAL POINTS = 264
NUMBER OF MATERIALS = 4
NUMBER OF ELEMENT TYPES = 33
NUMBER OF ELASTIC SUPPORT TYPES = -0
NUMBER OF FIXED END FORCE TYPES = -0
DEGREE OF TEMPERATURE CHANGE = -0.
DEGREE OF DIFFERENTIONAL TEMPERATURE CHANGE = -0.

MATERIAL	YOUNG S MODULUS	POISSON S RATIO	EXPANSION COEFFICIENT
1	4170000.	.30000	.65000E-05
2	524000.	.20000	.55000E-05
3	3170000.	.30000	.65000E-05
4	3310000.	.30000	.65000E-05

ELEMENT TYPE	AREA X	AREA Y	AREA Z	INERTIA X	INERTIA Y	INERTIA Z
1	.1000E+09	.1000E+09	.1000E+09	.1000E+09	.1000E+09	.1000E+09
2	.7403E+00	-0.	-0.	.1000E-03	.1000E-03	.1000E-03
3	.6886E+01	-0.	-0.	.1000E+09	.1000E+09	.3396E+03
4	.1316E+02	-0.	-0.	.1000E+09	.1000E+09	.6828E+03
5	.7150E+01	-0.	-0.	.1000E+09	.1000E+09	.3790E+03
6	.7420E+01	-0.	-0.	.1000E+09	.1000E+09	.4154E+03
7	.7780E+01	-0.	-0.	.1000E+09	.1000E+09	.4564E+03
8	.8060E+01	-0.	-0.	.1000E+09	.1000E+09	.4873E+03
9	.8410E+01	-0.	-0.	.1000E+09	.1000E+09	.5221E+03
10	.1158E+02	-0.	-0.	.1000E+09	.1000E+09	.7115E+03
11	.8650E+01	-0.	-0.	.1000E+09	.1000E+09	.5486E+03
12	.9360E+01	-0.	-0.	.1000E+09	.1000E+09	.5834E+03
13	.1187E+02	-0.	-0.	.1000E+09	.1000E+09	.7473E+03
14	.1096E+02	-0.	-0.	.1000E+09	.1000E+09	.6944E+03
15	.6140E+01	-0.	-0.	.1000E+09	.1000E+09	.2929E+03
16	.3224E+03	.1979E+03	.1559E+03	.2743E+05	.1853E+05	.1909E+05
17	.3008E+03	.1852E+03	.1440E+03	.2339E+05	.1654E+05	.1655E+05
18	.2748E+03	.1700E+03	.1298E+03	.1969E+05	.1412E+05	.1394E+05
19	.2582E+03	.1610E+03	.1218E+03	.1699E+05	.1205E+05	.1187E+05
20	.2449E+03	.1542E+03	.1152E+03	.1441E+05	.1026E+05	.1007E+05
21	.2277E+03	.1450E+03	.1085E+03	.1109E+05	.8010E+04	.7934E+04
22	.2113E+03	.1368E+03	.1007E+03	.9563E+04	.6865E+04	.6787E+04
23	.1904E+03	.1244E+03	.9020E+02	.7905E+04	.5768E+04	.5621E+04
24	.1778E+03	.1166E+03	.8320E+02	.6551E+04	.4900E+04	.4705E+04
25	.1681E+03	.1107E+03	.7770E+02	.5439E+04	.3995E+04	.3959E+04
26	.1581E+03	.1050E+03	.7220E+02	.4138E+04	.3268E+04	.3306E+04
27	.1477E+03	.1045E+03	.6730E+02	.3115E+04	.2666E+04	.2708E+04
28	.1397E+03	.9530E+02	.6410E+02	.2807E+04	.2234E+04	.2295E+04
29	.1120E+03	.6300E+02	.7500E+02	.3820E+04	.3612E+04	.2446E+04
30	.2365E+03	.9700E+02	.1490E+03	.1330E+05	.9616E+04	.9972E+04
31	.7740E+00	-0.	-0.	.1000E-03	.1000E-03	.1000E-03
32	.4440E+00	-0.	-0.	.1000E-03	.1000E-03	.1000E-03
33	.1000E+09	.1000E+09	.1000E+09	.1000E+09	.1000E+09	.1000E+09

PROPERTIES AND DIMENSIONS OF THE ANALYTICAL MODEL

TABLE 2.1 A

(SHEET 1 OF 11)

NODE	CODE	NODAL COORDINATES X	Y	Z	LINEAR BOUNDARY CONDITIONS X	Y	Z	ANGULAR BOUNDARY CONDITIONS X	Y	Z	ELASTIC SUPPORT TYPE
1	-0	-1152.500	225.999	30.000	-0.	-0.	-0.	-0.	-0.	-0.	-0
2	1110	-1152.500	225.999	-0.	-0.	-0.	-0.	-0.	-0.	-0.	-0
3	-0	-1111.000	227.389	30.000	-0.	-0.	-0.	-0.	-0.	-0.	-0
4	1110	-1111.000	227.389	-0.	-0.	-0.	-0.	-0.	-0.	-0.	-0
5	-0	-1100.000	228.143	30.000	-0.	-0.	-0.	-0.	-0.	-0.	-0
6	1110	-1100.000	228.143	-0.	-0.	-0.	-0.	-0.	-0.	-0.	-0
7	-0	-1089.000	227.591	30.000	-0.	-0.	-0.	-0.	-0.	-0.	-0
8	1110	-1089.000	227.591	-0.	-0.	-0.	-0.	-0.	-0.	-0.	-0
9	-0	-1037.250	228.663	30.000	-0.	-0.	-0.	-0.	-0.	-0.	-0
10	1110	-1037.250	228.663	-0.	-0.	-0.	-0.	-0.	-0.	-0.	-0
11	-0	-985.500	227.930	30.000	-0.	-0.	-0.	-0.	-0.	-0.	-0
12	1110	-985.500	227.930	-0.	-0.	-0.	-0.	-0.	-0.	-0.	-0
13	-0	-965.500	228.547	30.000	-0.	-0.	-0.	-0.	-0.	-0.	-0
14	1110	-965.500	228.547	-0.	-0.	-0.	-0.	-0.	-0.	-0.	-0
15	-0	-945.500	228.471	30.000	-0.	-0.	-0.	-0.	-0.	-0.	-0
16	1110	-945.500	228.471	-0.	-0.	-0.	-0.	-0.	-0.	-0.	-0
17	-0	-925.500	228.425	30.000	-0.	-0.	-0.	-0.	-0.	-0.	-0
18	1110	-925.500	228.425	-0.	-0.	-0.	-0.	-0.	-0.	-0.	-0
19	-0	-911.000	229.272	30.000	-0.	-0.	-0.	-0.	-0.	-0.	-0
20	1110	-911.000	229.272	-0.	-0.	-0.	-0.	-0.	-0.	-0.	-0
21	-0	-900.000	230.277	30.000	-0.	-0.	-0.	-0.	-0.	-0.	-0
22	1110	-900.000	230.277	-0.	-0.	-0.	-0.	-0.	-0.	-0.	-0
23	-0	-889.000	229.514	30.000	-0.	-0.	-0.	-0.	-0.	-0.	-0
24	1110	-889.000	229.514	-0.	-0.	-0.	-0.	-0.	-0.	-0.	-0
25	-0	-865.400	229.127	30.000	-0.	-0.	-0.	-0.	-0.	-0.	-0
26	1110	-865.400	229.127	-0.	-0.	-0.	-0.	-0.	-0.	-0.	-0
27	-0	-845.000	229.931	30.000	-0.	-0.	-0.	-0.	-0.	-0.	-0
28	1110	-845.000	229.931	-0.	-0.	-0.	-0.	-0.	-0.	-0.	-0
29	-0	-824.600	230.721	30.000	-0.	-0.	-0.	-0.	-0.	-0.	-0
30	1110	-824.600	230.721	-0.	-0.	-0.	-0.	-0.	-0.	-0.	-0
31	-0	-769.800	231.884	30.000	-0.	-0.	-0.	-0.	-0.	-0.	-0
32	1110	-769.800	231.884	-0.	-0.	-0.	-0.	-0.	-0.	-0.	-0
33	-0	-715.000	232.457	30.000	-0.	-0.	-0.	-0.	-0.	-0.	-0
34	1110	-715.000	232.457	-0.	-0.	-0.	-0.	-0.	-0.	-0.	-0
35	-0	-695.000	232.306	30.000	-0.	-0.	-0.	-0.	-0.	-0.	-0
36	1110	-695.000	232.306	-0.	-0.	-0.	-0.	-0.	-0.	-0.	-0
37	-0	-671.000	232.365	30.000	-0.	-0.	-0.	-0.	-0.	-0.	-0
38	1110	-671.000	232.365	-0.	-0.	-0.	-0.	-0.	-0.	-0.	-0
39	-0	-650.000	232.353	30.000	-0.	-0.	-0.	-0.	-0.	-0.	-0
40	1110	-650.000	232.393	-0.	-0.	-0.	-0.	-0.	-0.	-0.	-0
41	-0	-629.000	232.854	30.000	-0.	-0.	-0.	-0.	-0.	-0.	-0
42	1110	-629.000	232.854	-0.	-0.	-0.	-0.	-0.	-0.	-0.	-0
43	-0	-605.400	233.593	30.000	-0.	-0.	-0.	-0.	-0.	-0.	-0
44	1110	-605.400	233.593	-0.	-0.	-0.	-0.	-0.	-0.	-0.	-0
45	-0	-575.000	234.435	30.000	-0.	-0.	-0.	-0.	-0.	-0.	-0
46	1110	-575.000	234.435	-0.	-0.	-0.	-0.	-0.	-0.	-0.	-0
47	-0	-525.000	235.123	30.000	-0.	-0.	-0.	-0.	-0.	-0.	-0
48	1110	-525.000	235.123	-0.	-0.	-0.	-0.	-0.	-0.	-0.	-0
49	-0	-485.000	235.233	30.000	-0.	-0.	-0.	-0.	-0.	-0.	-0
50	1110	-485.000	235.233	-0.	-0.	-0.	-0.	-0.	-0.	-0.	-0
51	-0	-465.000	235.132	30.000	-0.	-0.	-0.	-0.	-0.	-0.	-0
52	1110	-465.000	235.132	-0.	-0.	-0.	-0.	-0.	-0.	-0.	-0

PROPERTIES AND DIMENSIONS OF THE ANALYTICAL MODEL

TABLE 2.1 A

(SHEET 2 OF 11)

NODE	CODE	NODAL COORDINATES X	Y	Z	LINEAR BOUNDARY CONDITIONS X	Y	Z	ANGULAR BOUNDARY CONDITIONS X	Y	Z	ELASTIC SUPPORT TYPE
53	-0	-431.200	236.343	30.000	-0.	-0.	-0.	-0.	-0.	-0.	-0
54	1110	-431.200	236.343	-0.	-0.	-0.	-0.	-0.	-0.	-0.	-0
55	-0	-420.000	237.448	30.000	-0.	-0.	-0.	-0.	-0.	-0.	-0
56	1110	-420.000	237.448	-0.	-0.	-0.	-0.	-0.	-0.	-0.	-0
57	-0	-408.800	236.741	30.000	-0.	-0.	-0.	-0.	-0.	-0.	-0
58	1110	-408.800	236.741	-0.	-0.	-0.	-0.	-0.	-0.	-0.	-0
59	-0	-385.600	236.319	30.000	-0.	-0.	-0.	-0.	-0.	-0.	-0
60	1110	-385.600	236.319	-0.	-0.	-0.	-0.	-0.	-0.	-0.	-0
61	-0	-355.600	236.998	30.000	-0.	-0.	-0.	-0.	-0.	-0.	-0
62	1110	-355.600	236.998	-0.	-0.	-0.	-0.	-0.	-0.	-0.	-0
63	-0	-335.600	237.593	30.000	-0.	-0.	-0.	-0.	-0.	-0.	-0
64	1110	-335.600	237.593	-0.	-0.	-0.	-0.	-0.	-0.	-0.	-0
65	-0	-283.400	238.184	30.000	-0.	-0.	-0.	-0.	-0.	-0.	-0
66	1110	-283.400	238.184	-0.	-0.	-0.	-0.	-0.	-0.	-0.	-0
67	-0	-231.200	239.767	30.000	-0.	-0.	-0.	-0.	-0.	-0.	-0
68	1110	-231.200	239.767	-0.	-0.	-0.	-0.	-0.	-0.	-0.	-0
69	-0	-220.000	241.076	30.000	-0.	-0.	-0.	-0.	-0.	-0.	-0
70	1110	-220.000	241.076	-0.	-0.	-0.	-0.	-0.	-0.	-0.	-0
71	-0	-208.800	240.398	30.000	-0.	-0.	-0.	-0.	-0.	-0.	-0
72	1110	-208.800	240.398	-0.	-0.	-0.	-0.	-0.	-0.	-0.	-0
73	-0	-165.200	240.105	30.000	-0.	-0.	-0.	-0.	-0.	-0.	-0
74	1110	-165.200	240.105	-0.	-0.	-0.	-0.	-0.	-0.	-0.	-0
75	-0	-125.200	240.498	30.000	-0.	-0.	-0.	-0.	-0.	-0.	-0
76	1110	-125.200	240.498	-0.	-0.	-0.	-0.	-0.	-0.	-0.	-0
77	-0	-85.200	240.937	30.000	-0.	-0.	-0.	-0.	-0.	-0.	-0
78	1110	-85.200	240.937	-0.	-0.	-0.	-0.	-0.	-0.	-0.	-0
79	-0	-42.600	241.355	30.000	-0.	-0.	-0.	-0.	-0.	-0.	-0
80	1110	-42.600	241.355	-0.	-0.	-0.	-0.	-0.	-0.	-0.	-0
81	-0	-0.	241.373	30.000	-0.	-0.	-0.	-0.	-0.	-0.	-0
82	1110	-0.	241.373	-0.	-0.	-0.	-0.	-0.	-0.	-0.	-0
83	-0	42.600	241.355	30.000	-0.	-0.	-0.	-0.	-0.	-0.	-0
84	1110	42.600	241.355	-0.	-0.	-0.	-0.	-0.	-0.	-0.	-0
85	-0	85.200	240.937	30.000	-0.	-0.	-0.	-0.	-0.	-0.	-0
86	1110	85.200	240.937	-0.	-0.	-0.	-0.	-0.	-0.	-0.	-0
87	-0	125.200	240.498	30.000	-0.	-0.	-0.	-0.	-0.	-0.	-0
88	1110	125.200	240.498	-0.	-0.	-0.	-0.	-0.	-0.	-0.	-0
89	-0	165.200	240.105	30.000	-0.	-0.	-0.	-0.	-0.	-0.	-0
90	1110	165.200	240.105	-0.	-0.	-0.	-0.	-0.	-0.	-0.	-0
91	-0	208.800	240.398	30.000	-0.	-0.	-0.	-0.	-0.	-0.	-0
92	1110	208.800	240.398	-0.	-0.	-0.	-0.	-0.	-0.	-0.	-0
93	-0	220.000	241.076	30.000	-0.	-0.	-0.	-0.	-0.	-0.	-0
94	1110	220.000	241.076	-0.	-0.	-0.	-0.	-0.	-0.	-0.	-0
95	-0	231.200	239.767	30.000	-0.	-0.	-0.	-0.	-0.	-0.	-0
96	1110	231.200	239.767	-0.	-0.	-0.	-0.	-0.	-0.	-0.	-0
97	-0	283.400	238.184	30.000	-0.	-0.	-0.	-0.	-0.	-0.	-0
98	1110	283.400	238.184	-0.	-0.	-0.	-0.	-0.	-0.	-0.	-0
99	-0	335.600	237.593	30.000	-0.	-0.	-0.	-0.	-0.	-0.	-0
100	1110	335.600	237.593	-0.	-0.	-0.	-0.	-0.	-0.	-0.	-0
101	-0	355.600	236.998	30.000	-0.	-0.	-0.	-0.	-0.	-0.	-0
102	1110	355.600	236.998	-0.	-0.	-0.	-0.	-0.	-0.	-0.	-0
103	-0	385.600	236.319	30.000	-0.	-0.	-0.	-0.	-0.	-0.	-0
104	1110	385.600	236.319	-0.	-0.	-0.	-0.	-0.	-0.	-0.	-0
105	-0	408.800	236.741	30.000	-0.	-0.	-0.	-0.	-0.	-0.	-0
106	1110	408.800	236.741	-0.	-0.	-0.	-0.	-0.	-0.	-0.	-0
107	-0	420.000	237.448	30.000	-0.	-0.	-0.	-0.	-0.	-0.	-0
108	1110	420.000	237.448	-0.	-0.	-0.	-0.	-0.	-0.	-0.	-0

PROPERTIES AND DIMENSIONS OF THE ANALYTICAL MODEL

TABLE 2.1 A

(SHEET 3 OF 11)

NODE	CODE	NODAL COORDINATES X	Y	Z	LINEAR BOUNDARY CONDITIONS X	Y	Z	ANGULAR BOUNDARY CONDITIONS X	Y	Z	ELASTIC SUPPORT TYPE
109	-0	431.200	236.343	30.000	-0.	-0.	-0.	-0.	-0.	-0.	-0
110	1110	431.200	236.343	-0.	-0.	-0.	-0.	-0.	-0.	-0.	-0
111	-0	465.000	235.132	30.000	-0.	-0.	-0.	-0.	-0.	-0.	-0
112	1110	465.000	235.132	-0.	-0.	-0.	-0.	-0.	-0.	-0.	-0
113	-0	485.000	235.233	30.000	-0.	-0.	-0.	-0.	-0.	-0.	-0
114	1110	485.000	235.233	-0.	-0.	-0.	-0.	-0.	-0.	-0.	-0
115	-0	525.000	235.123	30.000	-0.	-0.	-0.	-0.	-0.	-0.	-0
116	1110	525.000	235.123	-0.	-0.	-0.	-0.	-0.	-0.	-0.	-0
117	-0	575.000	234.435	30.000	-0.	-0.	-0.	-0.	-0.	-0.	-0
118	1110	575.000	234.435	-0.	-0.	-0.	-0.	-0.	-0.	-0.	-0
119	-0	605.400	233.593	30.000	-0.	-0.	-0.	-0.	-0.	-0.	-0
120	1110	605.400	233.593	-0.	-0.	-0.	-0.	-0.	-0.	-0.	-0
121	-0	629.000	232.894	30.000	-0.	-0.	-0.	-0.	-0.	-0.	-0
122	1110	629.000	232.894	-0.	-0.	-0.	-0.	-0.	-0.	-0.	-0
123	-0	650.000	232.393	30.000	-0.	-0.	-0.	-0.	-0.	-0.	-0
124	1110	650.000	232.393	-0.	-0.	-0.	-0.	-0.	-0.	-0.	-0
125	-0	671.000	232.369	30.000	-0.	-0.	-0.	-0.	-0.	-0.	-0
126	1110	671.000	232.369	-0.	-0.	-0.	-0.	-0.	-0.	-0.	-0
127	-0	695.000	232.306	30.000	-0.	-0.	-0.	-0.	-0.	-0.	-0
128	1110	695.000	232.306	-0.	-0.	-0.	-0.	-0.	-0.	-0.	-0
129	-0	715.000	232.457	30.000	-0.	-0.	-0.	-0.	-0.	-0.	-0
130	1110	715.000	232.457	-0.	-0.	-0.	-0.	-0.	-0.	-0.	-0
131	-0	769.800	231.864	30.000	-0.	-0.	-0.	-0.	-0.	-0.	-0
132	1110	769.800	231.864	-0.	-0.	-0.	-0.	-0.	-0.	-0.	-0
133	-0	824.600	230.721	30.000	-0.	-0.	-0.	-0.	-0.	-0.	-0
134	1110	824.600	230.721	-0.	-0.	-0.	-0.	-0.	-0.	-0.	-0
135	-0	845.000	229.931	30.000	-0.	-0.	-0.	-0.	-0.	-0.	-0
136	1110	845.000	229.931	-0.	-0.	-0.	-0.	-0.	-0.	-0.	-0
137	-0	865.400	229.127	30.000	-0.	-0.	-0.	-0.	-0.	-0.	-0
138	1110	865.400	229.127	-0.	-0.	-0.	-0.	-0.	-0.	-0.	-0
139	-0	889.000	229.514	30.000	-0.	-0.	-0.	-0.	-0.	-0.	-0
140	1110	889.000	229.514	-0.	-0.	-0.	-0.	-0.	-0.	-0.	-0
141	-0	900.000	230.277	30.000	-0.	-0.	-0.	-0.	-0.	-0.	-0
142	1110	900.000	230.277	-0.	-0.	-0.	-0.	-0.	-0.	-0.	-0
143	-0	911.000	229.272	30.000	-0.	-0.	-0.	-0.	-0.	-0.	-0
144	1110	911.000	229.272	-0.	-0.	-0.	-0.	-0.	-0.	-0.	-0
145	-0	925.500	228.425	30.000	-0.	-0.	-0.	-0.	-0.	-0.	-0
146	1110	925.500	228.425	-0.	-0.	-0.	-0.	-0.	-0.	-0.	-0
147	-0	945.500	228.471	30.000	-0.	-0.	-0.	-0.	-0.	-0.	-0
148	1110	945.500	228.471	-0.	-0.	-0.	-0.	-0.	-0.	-0.	-0
149	-0	965.500	228.547	30.000	-0.	-0.	-0.	-0.	-0.	-0.	-0
150	1110	965.500	228.547	-0.	-0.	-0.	-0.	-0.	-0.	-0.	-0
151	-0	985.500	227.930	30.000	-0.	-0.	-0.	-0.	-0.	-0.	-0
152	1110	985.500	227.930	-0.	-0.	-0.	-0.	-0.	-0.	-0.	-0
153	-0	1037.250	228.663	30.000	-0.	-0.	-0.	-0.	-0.	-0.	-0
154	1110	1037.250	228.663	-0.	-0.	-0.	-0.	-0.	-0.	-0.	-0
155	-0	1089.000	227.591	30.000	-0.	-0.	-0.	-0.	-0.	-0.	-0
156	1110	1089.000	227.591	-0.	-0.	-0.	-0.	-0.	-0.	-0.	-0
157	-0	1100.000	228.143	30.000	-0.	-0.	-0.	-0.	-0.	-0.	-0
158	1110	1100.000	228.143	-0.	-0.	-0.	-0.	-0.	-0.	-0.	-0
159	-0	1111.000	227.389	30.000	-0.	-0.	-0.	-0.	-0.	-0.	-0
160	1110	1111.000	227.389	-0.	-0.	-0.	-0.	-0.	-0.	-0.	-0
161	-0	1152.500	225.999	30.000	-0.	-0.	-0.	-0.	-0.	-0.	-0
162	1110	1152.500	225.999	-0.	-0.	-0.	-0.	-0.	-0.	-0.	-0
163	111111	-650.000	15.000	29.310	-0.	-0.	-0.	-0.	-0.	-0.	-0
164	-0	-650.000	40.400	29.310	-0.	-0.	-0.	-0.	-0.	-0.	-0

PROPERTIES AND DIMENSIONS OF THE ANALYTICAL MODEL

TABLE 2.1 A

(SHEET 4 OF 11)

NODE	CODE	NODAL COORDINATES X	Y	Z	LINEAR BOUNDARY CONDITIONS X	Y	Z	ANGULAR BOUNDARY CONDITIONS X	Y	Z	ELASTIC SUPPORT TYPE
165	-0	-650.000	70.200	34.710	-0.	-0.	-0.	-0.	-0.	-0.	-0
166	-0	-650.000	100.000	40.120	-0.	-0.	-0.	-0.	-0.	-0.	-0
167	-0	-650.000	132.670	46.040	-0.	-0.	-0.	-0.	-0.	-0.	-0
168	-0	-650.000	165.330	51.960	-0.	-0.	-0.	-0.	-0.	-0.	-0
169	-0	-650.000	198.000	57.870	-0.	-0.	-0.	-0.	-0.	-0.	-0
170	-0	-650.000	208.000	59.680	-0.	-0.	-0.	-0.	-0.	-0.	-0
171	-0	-650.000	218.000	61.490	-0.	-0.	-0.	-0.	-0.	-0.	-0
172	-0	-650.000	240.000	65.500	-0.	-0.	-0.	-0.	-0.	-0.	-0
173	-0	-650.000	270.000	58.540	-0.	-0.	-0.	-0.	-0.	-0.	-0
174	-0	-650.000	300.000	51.570	-0.	-0.	-0.	-0.	-0.	-0.	-0
175	-0	-650.000	330.000	44.600	-0.	-0.	-0.	-0.	-0.	-0.	-0
176	-0	-650.000	360.000	37.630	-0.	-0.	-0.	-0.	-0.	-0.	-0
177	-0	-650.000	390.000	30.670	-0.	-0.	-0.	-0.	-0.	-0.	-0
178	-0	-650.000	420.000	23.700	-0.	-0.	-0.	-0.	-0.	-0.	-0
179	-0	-650.000	436.000	20.000	-0.	-0.	-0.	-0.	-0.	-0.	-0
180	-0	-650.000	444.000	18.150	-0.	-0.	-0.	-0.	-0.	-0.	-0
181	-0	-650.000	444.000	12.250	-0.	-0.	-0.	-0.	-0.	-0.	-0
182	-0	-650.000	444.000	10.330	-0.	-0.	-0.	-0.	-0.	-0.	-0
183	1110	-650.000	444.000	-0.	-0.	-0.	-0.	-0.	-0.	-0.	-0
184	-0	-650.000	459.800	12.250	-0.	-0.	-0.	-0.	-0.	-0.	-0
185	-0	-650.000	457.900	10.330	-0.	-0.	-0.	-0.	-0.	-0.	-0
186	-0	-650.000	208.000	50.120	-0.	-0.	-0.	-0.	-0.	-0.	-0
187	-0	-650.000	208.000	30.000	-0.	-0.	-0.	-0.	-0.	-0.	-0
188	-0	-650.000	220.000	30.000	-0.	-0.	-0.	-0.	-0.	-0.	-0
189	1110	-650.000	208.000	-0.	-0.	-0.	-0.	-0.	-0.	-0.	-0
190	1110	-650.000	40.400	-0.	-0.	-0.	-0.	-0.	-0.	-0.	-0
191	111111	650.000	15.000	29.310	-0.	-0.	-0.	-0.	-0.	-0.	-0
192	-0	650.000	40.400	29.310	-0.	-0.	-0.	-0.	-0.	-0.	-0
193	-0	650.000	70.200	34.710	-0.	-0.	-0.	-0.	-0.	-0.	-0
194	-0	650.000	100.000	40.120	-0.	-0.	-0.	-0.	-0.	-0.	-0
195	-0	650.000	132.670	46.040	-0.	-0.	-0.	-0.	-0.	-0.	-0
196	-0	650.000	165.330	51.960	-0.	-0.	-0.	-0.	-0.	-0.	-0
197	-0	650.000	198.000	57.870	-0.	-0.	-0.	-0.	-0.	-0.	-0
198	-0	650.000	208.000	59.680	-0.	-0.	-0.	-0.	-0.	-0.	-0
199	-0	650.000	218.000	61.490	-0.	-0.	-0.	-0.	-0.	-0.	-0
200	-0	650.000	240.000	65.500	-0.	-0.	-0.	-0.	-0.	-0.	-0
201	-0	650.000	270.000	58.540	-0.	-0.	-0.	-0.	-0.	-0.	-0
202	-0	650.000	300.000	51.570	-0.	-0.	-0.	-0.	-0.	-0.	-0
203	-0	650.000	330.000	44.600	-0.	-0.	-0.	-0.	-0.	-0.	-0
204	-0	650.000	360.000	37.630	-0.	-0.	-0.	-0.	-0.	-0.	-0
205	-0	650.000	390.000	30.670	-0.	-0.	-0.	-0.	-0.	-0.	-0
206	-0	650.000	420.000	23.700	-0.	-0.	-0.	-0.	-0.	-0.	-0
207	-0	650.000	436.000	20.000	-0.	-0.	-0.	-0.	-0.	-0.	-0
208	-0	650.000	444.000	18.150	-0.	-0.	-0.	-0.	-0.	-0.	-0
209	-0	650.000	444.000	12.250	-0.	-0.	-0.	-0.	-0.	-0.	-0
210	-0	650.000	444.000	10.330	-0.	-0.	-0.	-0.	-0.	-0.	-0
211	1110	650.000	444.000	-0.	-0.	-0.	-0.	-0.	-0.	-0.	-0
212	-0	650.000	459.800	12.250	-0.	-0.	-0.	-0.	-0.	-0.	-0
213	-0	650.000	457.900	10.330	-0.	-0.	-0.	-0.	-0.	-0.	-0
214	-0	650.000	208.000	50.120	-0.	-0.	-0.	-0.	-0.	-0.	-0
215	-0	650.000	208.000	30.000	-0.	-0.	-0.	-0.	-0.	-0.	-0
216	-0	650.000	220.000	30.000	-0.	-0.	-0.	-0.	-0.	-0.	-0
217	1110	650.000	208.000	-0.	-0.	-0.	-0.	-0.	-0.	-0.	-0
218	1110	650.000	40.400	-0.	-0.	-0.	-0.	-0.	-0.	-0.	-0
219	-0	-1100.000	224.100	58.000	-0.	-0.	-0.	-0.	-0.	-0.	-0
220	-0	-1025.000	263.066	50.055	-0.	-0.	-0.	-0.	-0.	-0.	-0

PROPERTIES AND DIMENSIONS OF THE ANALYTICAL MODEL

TABLE 2.1 A

(SHEET 5 OF 11)

NODE	CODE	NODAL COORDINATES X	Y	Z	LINEAR BOUNDARY CONDITIONS X	Y	Z	ANGULAR BOUNDARY CONDITIONS X	Y	Z	ELASTIC SUPPORT TYPE
221	-0	-950.000	302.033	42.110	-0.	-0.	-0.	-0.	-0.	-0.	-0
222	-0	-875.000	341.000	34.165	-0.	-0.	-0.	-0.	-0.	-0.	-0
223	-0	-800.000	379.966	26.220	-0.	-0.	-0.	-0.	-0.	-0.	-0
224	-0	-725.000	418.933	18.275	-0.	-0.	-0.	-0.	-0.	-0.	-0
225	-0	-900.000	229.100	58.000	-0.	-0.	-0.	-0.	-0.	-0.	-0
226	-0	-837.500	286.775	46.562	-0.	-0.	-0.	-0.	-0.	-0.	-0
227	-0	-775.000	344.450	35.125	-0.	-0.	-0.	-0.	-0.	-0.	-0
228	-0	-712.500	402.125	23.687	-0.	-0.	-0.	-0.	-0.	-0.	-0
229	-0	-420.000	236.910	58.000	-0.	-0.	-0.	-0.	-0.	-0.	-0
230	-0	-477.500	292.632	46.562	-0.	-0.	-0.	-0.	-0.	-0.	-0
231	-0	-535.000	348.355	35.125	-0.	-0.	-0.	-0.	-0.	-0.	-0
232	-0	-592.500	404.077	23.687	-0.	-0.	-0.	-0.	-0.	-0.	-0
233	-0	-220.000	238.610	58.000	-0.	-0.	-0.	-0.	-0.	-0.	-0
234	-0	-291.667	275.158	50.055	-0.	-0.	-0.	-0.	-0.	-0.	-0
235	-0	-363.333	311.707	42.110	-0.	-0.	-0.	-0.	-0.	-0.	-0
236	-0	-435.000	348.255	34.165	-0.	-0.	-0.	-0.	-0.	-0.	-0
237	-0	-506.667	384.803	26.220	-0.	-0.	-0.	-0.	-0.	-0.	-0
238	-0	-578.333	421.352	18.275	-0.	-0.	-0.	-0.	-0.	-0.	-0
239	-0	220.000	238.610	58.000	-0.	-0.	-0.	-0.	-0.	-0.	-0
240	-0	291.667	275.158	50.055	-0.	-0.	-0.	-0.	-0.	-0.	-0
241	-0	363.333	311.707	42.110	-0.	-0.	-0.	-0.	-0.	-0.	-0
242	-0	435.000	348.255	34.165	-0.	-0.	-0.	-0.	-0.	-0.	-0
243	-0	506.667	384.803	26.220	-0.	-0.	-0.	-0.	-0.	-0.	-0
244	-0	578.333	421.352	18.275	-0.	-0.	-0.	-0.	-0.	-0.	-0
245	-0	420.000	236.910	58.000	-0.	-0.	-0.	-0.	-0.	-0.	-0
246	-0	477.500	292.632	46.562	-0.	-0.	-0.	-0.	-0.	-0.	-0
247	-0	535.000	348.355	35.125	-0.	-0.	-0.	-0.	-0.	-0.	-0
248	-0	592.500	404.077	23.687	-0.	-0.	-0.	-0.	-0.	-0.	-0
249	-0	900.000	229.100	58.000	-0.	-0.	-0.	-0.	-0.	-0.	-0
250	-0	837.500	286.775	46.562	-0.	-0.	-0.	-0.	-0.	-0.	-0
251	-0	775.000	344.450	35.125	-0.	-0.	-0.	-0.	-0.	-0.	-0
252	-0	712.500	402.125	23.687	-0.	-0.	-0.	-0.	-0.	-0.	-0
253	-0	1100.000	224.100	58.000	-0.	-0.	-0.	-0.	-0.	-0.	-0
254	-0	1025.000	263.066	50.055	-0.	-0.	-0.	-0.	-0.	-0.	-0
255	-0	950.000	302.033	42.110	-0.	-0.	-0.	-0.	-0.	-0.	-0
256	-0	875.000	341.000	34.165	-0.	-0.	-0.	-0.	-0.	-0.	-0
257	-0	800.000	379.966	26.220	-0.	-0.	-0.	-0.	-0.	-0.	-0
258	-0	725.000	418.933	18.275	-0.	-0.	-0.	-0.	-0.	-0.	-0
259	111111	-1100.000	210.500	30.000	-0.	-0.	-0.	-0.	-0.	-0.	-0
260	-0	-1100.000	213.433	30.000	-0.	-0.	-0.	-0.	-0.	-0.	-0
261	-0	-1100.000	227.433	30.000	-0.	-0.	-0.	-0.	-0.	-0.	-0
262	-0	1100.000	227.433	30.000	-0.	-0.	-0.	-0.	-0.	-0.	-0
263	-0	1100.000	213.433	30.000	-0.	-0.	-0.	-0.	-0.	-0.	-0
264	111111	1100.000	210.500	30.000	-0.	-0.	-0.	-0.	-0.	-0.	-0

PROPERTIES AND DIMENSIONS OF THE ANALYTICAL MODEL

TABLE 2.1 A

(SHEET 6 OF 11)

ELEMENT	NODE I	NODE J	MATERIAL TYPE	ELEMENT TYPE	DEAD LOAD	END RELEASE CODE I	END RELEASE CODE J	DIRN COSINES OF LOCAL Y AXIS X	Y	Z	ECCENTRICITY I	ECCENTRICITY J
1	259	260	2	1	-0.	-0	-0	-0.	-0.	1.00000	-0.	-0.
2	260	261	1	2	-0.	111	-0	-0.	-0.	1.00000	-0.	-0.
3	261	5	1	1	-0.	111	-0	-0.	-0.	1.00000	-0.	-0.
4	219	5	1	1	-0.	-0	-0	-0.	.98990	.14140	-0.	-0.
5	1	3	1	3	-0.	-0	-0	-0.	1.00000	-0.	-0.	-.52650
6	3	5	1	4	-0.	-0	-0	-0.	1.00000	-0.	.52650	-0.
7	5	7	1	4	-0.	-0	-0	-0.	1.00000	-0.	-0.	.78000
8	7	9	1	5	-0.	-0	-0	-0.	1.00000	-0.	-.78000	-0.
9	9	11	1	5	-0.	-0	-0	-0.	1.00000	-0.	-0.	.23350
10	11	13	1	6	-0.	-0	-0	-0.	1.00000	-0.	-.23350	.26850
11	13	15	1	7	-0.	-0	-0	-0.	1.00000	-0.	-.26850	.19750
12	15	17	1	8	-0.	-0	-0	-0.	1.00000	-0.	-.19750	.22650
13	17	19	1	9	-0.	-0	-0	-0.	1.00000	-0.	-.22650	-.80000
14	19	21	1	10	-0.	-0	-0	-0.	1.00000	-0.	.80000	-0.
15	225	21	1	1	-0.	-0	-0	-0.	.99910	.04200	-0.	-0.
16	21	23	1	10	-0.	-0	-0	-0.	1.00000	-0.	-0.	.96850
17	23	25	1	11	-0.	-0	-0	-0.	1.00000	-0.	-.96850	-.16850
18	25	27	1	9	-0.	-0	-0	-0.	1.00000	-0.	.16850	-.22650
19	27	29	1	8	-0.	-0	-0	-0.	1.00000	-0.	.22650	-.19750
20	29	31	1	7	-0.	-0	-0	-0.	1.00000	-0.	.19750	-0.
21	31	33	1	7	-0.	-0	-0	-0.	1.00000	-0.	-0.	.19750
22	33	35	1	8	-0.	-0	-0	-0.	1.00000	-0.	-.19750	.22650
23	35	37	1	9	-0.	-0	-0	-0.	1.00000	-0.	-.22650	.33400
24	37	39	1	12	-0.	-0	-0	-0.	1.00000	-0.	-.33400	-0.
25	39	41	1	12	-0.	-0	-0	-0.	1.00000	-0.	-0.	-.16550
26	41	43	1	11	-0.	-0	-0	-0.	1.00000	-0.	.16550	-.16850
27	43	45	1	9	-0.	-0	-0	-0.	1.00000	-0.	.16850	-.22650
28	45	47	1	8	-0.	-0	-0	-0.	1.00000	-0.	.22650	.22650
29	47	49	1	9	-0.	-0	-0	-0.	1.00000	-0.	-.22650	.16850
30	49	51	1	11	-0.	-0	-0	-0.	1.00000	-0.	-.16850	.33400
31	51	53	1	12	-0.	-0	-0	-0.	1.00000	-0.	-.33400	-.98850
32	53	55	1	13	-0.	-0	-0	-0.	1.00000	-0.	.98850	-0.
33	229	55	1	1	-0.	-0	-0	-0.	.99980	.01921	-0.	-0.
34	55	57	1	13	-0.	-0	-0	-0.	1.00000	-0.	-0.	.82300
35	57	59	1	11	-0.	-0	-0	-0.	1.00000	-0.	-.82300	-.16850
36	59	61	1	9	-0.	-0	-0	-0.	1.00000	-0.	.16850	-.22650
37	61	63	1	8	-0.	-0	-0	-0.	1.00000	-0.	.22650	-.19750
38	63	65	1	7	-0.	-0	-0	-0.	1.00000	-0.	.19750	-0.
39	65	67	1	7	-0.	-0	-0	-0.	1.00000	-0.	-0.	-1.24400
40	67	69	1	14	-0.	-0	-0	-0.	1.00000	-0.	1.24450	-0.
41	233	69	1	1	-0.	-0	-0	-0.	.99610	.08772	-0.	-0.
42	69	71	1	14	-0.	-0	-0	-0.	1.00000	-0.	-0.	.74250
43	71	73	1	5	-0.	-0	-0	-0.	1.00000	-0.	-.74250	-.25350
44	73	75	1	3	-0.	-0	-0	-0.	1.00000	-0.	.25350	-0.
45	75	77	1	3	-0.	-0	-0	-0.	1.00000	-0.	-0.	-.33650
46	77	79	1	15	-0.	-0	-0	-0.	1.00000	-0.	.33650	-0.
47	79	81	1	15	-0.	-0	-0	-0.	1.00000	-0.	-0.	-0.
48	81	83	1	15	-0.	-0	-0	-0.	1.00000	-0.	-0.	-0.
49	83	85	1	15	-0.	-0	-0	-0.	1.00000	-0.	-0.	.33650
50	85	87	1	3	-0.	-0	-0	-0.	1.00000	-0.	-.33650	-0.
51	87	89	1	3	-0.	-0	-0	-0.	1.00000	-0.	-0.	.25350
52	89	91	1	9	-0.	-0	-0	-0.	1.00000	-0.	-.25350	-.74250

PROPERTIES AND DIMENSIONS OF THE ANALYTICAL MODEL

TABLE 2.1 A

(SHEET 7 OF 11)

ELEMENT	NODE I	NODE J	MATERIAL TYPE	ELEMENT TYPE	DEAD LOAD	END RELEASE CODE I	END RELEASE CODE J	DIRN COSINES OF LOCAL Y AXIS X	DIRN COSINES OF LOCAL Y AXIS Y	DIRN COSINES OF LOCAL Y AXIS Z	ECCENTRICITY I	ECCENTRICITY J
53	91	93	1	14	-0.	-0	-0	-0.	1.00000	-0.	.74250	-0.
54	239	93	1	1	-0.	-0	-0	-0.	.99610	.08772	-0.	-0.
55	93	95	1	14	-0.	-0	-0	-0.	1.00000	-0.	-0.	1.24450
56	95	97	1	7	-0.	-0	-0	-0.	1.00000	-0.	-1.24400	-0.
57	97	99	1	7	-0.	-0	-0	-0.	1.00000	-0.	-0.	.19750
58	99	101	1	8	-0.	-0	-0	-0.	1.00000	-0.	-.19750	.22650
59	101	103	1	9	-0.	-0	-0	-0.	1.00000	-0.	-.22650	.16850
60	103	105	1	11	-0.	-0	-0	-0.	1.00000	-0.	-.16850	-.82300
61	105	107	1	13	-0.	-0	-0	-0.	1.00000	-0.	.82300	-0.
62	245	107	1	1	-0.	-0	-0	-0.	.99980	.01921	-0.	-0.
63	107	109	1	13	-0.	-0	-0	-0.	1.00000	-0.	-0.	.98850
64	109	111	1	12	-0.	-0	-0	-0.	1.00000	-0.	-.98850	-.33400
65	111	113	1	11	-0.	-0	-0	-0.	1.00000	-0.	.33400	-.16850
66	113	115	1	9	-0.	-0	-0	-0.	1.00000	-0.	.16850	-.22650
67	115	117	1	8	-0.	-0	-0	-0.	1.00000	-0.	.22650	.22650
68	117	119	1	9	-0.	-0	-0	-0.	1.00000	-0.	-.22650	.16850
69	119	121	1	11	-0.	-0	-0	-0.	1.00000	-0.	-.16850	.16550
70	121	123	1	12	-0.	-0	-0	-0.	1.00000	-0.	-.16550	-0.
71	123	125	1	12	-0.	-0	-0	-0.	1.00000	-0.	-0.	-.33400
72	125	127	1	9	-0.	-0	-0	-0.	1.00000	-0.	.33400	-.22650
73	127	129	1	8	-0.	-0	-0	-0.	1.00000	-0.	.22650	-.19750
74	129	131	1	7	-0.	-0	-0	-0.	1.00000	-0.	.19750	-0.
75	131	133	1	7	-0.	-0	-0	-0.	1.00000	-0.	-0.	.19750
76	133	135	1	8	-0.	-0	-0	-0.	1.00000	-0.	-.19750	.22650
77	135	137	1	9	-0.	-0	-0	-0.	1.00000	-0.	-.22650	.16850
78	137	139	1	11	-0.	-0	-0	-0.	1.00000	-0.	-.16850	-.96850
79	139	141	1	10	-0.	-0	-0	-0.	1.00000	-0.	.96850	-0.
80	249	141	1	1	-0.	-0	-0	-0.	.99910	.04200	-0.	-0.
81	141	143	1	10	-0.	-0	-0	-0.	1.00000	-0.	-0.	.80000
82	143	145	1	9	-0.	-0	-0	-0.	1.00000	-0.	-.80000	-.22650
83	145	147	1	8	-0.	-0	-0	-0.	1.00000	-0.	.22650	-.19750
84	147	149	1	7	-0.	-0	-0	-0.	1.00000	-0.	.19750	-.26850
85	149	151	1	6	-0.	-0	-0	-0.	1.00000	-0.	.26850	-.23350
86	151	153	1	6	-0.	-0	-0	-0.	1.00000	-0.	.23350	-0.
87	153	155	1	5	-0.	-0	-0	-0.	1.00000	-0.	-0.	-.78000
88	155	157	1	4	-0.	-0	-0	-0.	1.00000	-0.	.78000	-0.
89	157	159	1	4	-0.	-0	-0	-0.	1.00000	-0.	-0.	.52650
90	159	161	1	3	-0.	-0	-0	-0.	1.00000	-0.	-.52650	-0.
91	253	157	1	1	-0.	-0	-0	-0.	.98590	.14140	-0.	-0.
92	262	157	1	1	-0.	111	-0	-0.	-0.	1.00000	-0.	-0.
93	263	262	1	2	-0.	111	-0	-0.	-0.	1.00000	-0.	-0.
94	264	263	2	1	-0.	-0	-0	-0.	-0.	1.00000	-0.	-0.
95	163	164	2	1	-0.	-0	-0	-0.	-0.	1.00000	-0.	-0.
96	164	165	2	16	-0.	-0	-0	-0.	-.17800	.98402	-0.	-0.
97	165	166	2	17	-0.	-0	-0	-0.	-.17800	.98402	-0.	-0.
98	166	167	2	18	-0.	-0	-0	-0.	-.17800	.98402	-0.	-0.
99	167	168	2	19	-0.	-0	-0	-0.	-.17800	.98402	-0.	-0.
100	168	169	2	20	-0.	-0	-0	-0.	-.17800	.98402	-0.	-0.
101	169	170	2	1	-0.	-0	-0	-0.	-.17800	.98402	-0.	-0.
102	170	171	2	1	-0.	-0	-0	-0.	-.17800	.98402	-0.	-0.
103	171	172	2	21	-0.	-0	-0	-0.	-.17800	.98402	-0.	-0.
104	172	173	2	22	-0.	-0	-0	-0.	.22700	.97389	-0.	-0.
105	173	174	2	23	-0.	-0	-0	-0.	.22700	.97389	-0.	-0.
106	174	175	2	24	-0.	-0	-0	-0.	.22700	.97389	-0.	-0.
107	175	176	2	25	-0.	-0	-0	-0.	.22700	.97389	-0.	-0.
108	176	177	2	26	-0.	-0	-0	-0.	.22700	.97389	-0.	-0.

PROPERTIES AND DIMENSIONS OF THE ANALYTICAL MODEL

TABLE 2.1 A

(SHEET 8 OF 11)

ELEMENT	NODE I	NODE J	MATERIAL TYPE	ELEMENT TYPE	DEAD LOAD	END RELEASE CODE I	END RELEASE CODE J	DIRN COSINES OF LOCAL Y AXIS X	Y	Z	ECCENTRICITY I	ECCENTRICITY J
109	177	178	2	27	-0.	-0	-0	-0.	.22700	.97389	-0.	-0.
110	178	179	2	29	-0.	-0	-0	-0.	.22700	.97389	-0.	-0.
111	179	180	2	1	-0.	-0	-0	-0.	.22700	.97389	-0.	-0.
112	181	184	2	1	-0.	-0	-0	-0.	-0.	1.00000	-0.	-0.
113	182	185	2	1	-0.	-0	-0	-0.	-0.	1.00000	-0.	-0.
114	187	188	2	1	-0.	-0	111	-0.	-0.	1.00000	-0.	-0.
115	188	39	2	1	-0.	-0	111	-0.	-0.	1.00000	-0.	-0.
116	184	190	2	1	-0.	-0	-0	1.00000	-0.	-0.	-0.	-0.
117	173	186	2	1	-0.	-0	-0	1.00000	-0.	-0.	-0.	-0.
118	186	187	2	30	-0.	-0	-0	1.00000	-0.	-0.	-0.	-0.
119	187	189	2	30	-0.	-0	-0	1.00000	-0.	-0.	-0.	-0.
120	180	181	2	1	-0.	-0	-0	1.00000	-0.	-0.	-0.	-0.
121	181	182	2	1	-0.	-0	-0	1.00000	-0.	-0.	-0.	-0.
122	182	183	2	29	-0.	-0	-0	1.00000	-0.	-0.	-0.	-0.
123	191	192	2	1	-0.	-0	-0	-0.	-0.	1.00000	-0.	-0.
124	192	193	2	16	-0.	-0	-0	-0.	-.17800	.98402	-0.	-0.
125	193	194	2	17	-0.	-0	-0	-0.	-.17800	.98402	-0.	-0.
126	194	195	2	18	-0.	-0	-0	-0.	-.17800	.98402	-0.	-0.
127	195	196	2	19	-0.	-0	-0	-0.	-.17800	.98402	-0.	-0.
128	196	197	2	20	-0.	-0	-0	-0.	-.17800	.98402	-0.	-0.
129	197	198	2	1	-0.	-0	-0	-0.	-.17800	.98402	-0.	-0.
130	198	199	2	1	-0.	-0	-0	-0.	-.17800	.98402	-0.	-0.
131	199	200	2	21	-0.	-0	-0	-0.	-.17800	.98402	-0.	-0.
132	200	201	2	22	-0.	-0	-0	-0.	.22700	.97389	-0.	-0.
133	201	202	2	23	-0.	-0	-0	-0.	.22700	.97389	-0.	-0.
134	202	203	2	24	-0.	-0	-0	-0.	.22700	.97389	-0.	-0.
135	203	204	2	25	-0.	-0	-0	-0.	.22700	.97389	-0.	-0.
136	204	205	2	26	-0.	-0	-0	-0.	.22700	.97389	-0.	-0.
137	205	206	2	27	-0.	-0	-0	-0.	.22700	.97389	-0.	-0.
138	206	207	2	28	-0.	-0	-0	-0.	.22700	.97389	-0.	-0.
139	207	208	2	1	-0.	-0	-0	-0.	.22700	.97389	-0.	-0.
140	209	212	2	1	-0.	-0	-0	-0.	-0.	1.00000	-0.	-0.
141	210	213	2	1	-0.	-0	-0	-0.	-0.	1.00000	-0.	-0.
142	215	216	2	1	-0.	-0	111	-0.	-0.	1.00000	-0.	-0.
143	216	123	2	1	-0.	-0	-0	-0.	-0.	1.00000	-0.	-0.
144	192	218	2	1	-0.	-0	-0	1.00000	-0.	-0.	-0.	-0.
145	198	214	2	1	-0.	-0	-0	1.00000	-0.	-0.	-0.	-0.
146	214	215	2	30	-0.	-0	-0	1.00000	-0.	-0.	-0.	-0.
147	215	217	2	30	-0.	-0	-0	1.00000	-0.	-0.	-0.	-0.
148	208	209	2	1	-0.	-0	-0	1.00000	-0.	-0.	-0.	-0.
149	209	210	2	1	-0.	-0	-0	1.00000	-0.	-0.	-0.	-0.
150	210	211	2	29	-0.	-0	-0	1.00000	-0.	-0.	-0.	-0.
151	219	220	3	31	-0.	-0	-0	-0.	.19980	.97980	-0.	-0.
152	220	221	3	31	-0.	-0	-0	-0.	.19980	.97980	-0.	-0.
153	221	222	3	31	-0.	-0	-0	-0.	.19980	.97980	-0.	-0.
154	222	223	3	31	-0.	-0	-0	-0.	.19980	.97980	-0.	-0.
155	223	224	3	31	-0.	-0	-0	-0.	.19980	.97980	-0.	-0.
156	224	185	3	31	-0.	-0	-0	-0.	.19980	.97980	-0.	-0.
157	225	226	4	32	-0.	-0	-0	-0.	.19450	.98090	-0.	-0.
158	226	227	4	32	-0.	-0	-0	-0.	.19450	.98090	-0.	-0.
159	227	228	4	32	-0.	-0	-0	-0.	.19450	.98090	-0.	-0.
160	228	184	4	32	-0.	-0	-0	-0.	.19450	.98090	-0.	-0.
161	229	230	4	32	-0.	-0	-0	-0.	.20110	.97960	-0.	-0.
162	230	231	4	32	-0.	-0	-0	-0.	.20110	.97960	-0.	-0.
163	231	232	4	32	-0.	-0	-0	-0.	.20110	.97960	-0.	-0.
164	232	184	4	32	-0.	-0	-0	-0.	.20110	.97960	-0.	-0.

PROPERTIES AND DIMENSIONS OF THE ANALYTICAL MODEL

TABLE 2.1 A

(SHEET 9 OF 11)

ELEMENT	NODE I	NODE J	MATERIAL TYPE	ELEMENT TYPE	DEAD LOAD	END RELEASE CODE I	END RELEASE CODE J	DIRN COSINES OF LOCAL Y AXIS X	Y	Z	ECCENTRICITY I	ECCENTRICITY J
165	233	234	3	31	-0.	-0	-0	-0.	.21240	.97720	-0.	-0.
166	234	235	3	31	-0.	-0	-0	-0.	.21240	.97720	-0.	-0.
167	235	236	3	31	-0.	-0	-0	-0.	.21240	.97720	-0.	-0.
168	236	237	3	31	-0.	-0	-0	-0.	.21240	.97720	-0.	-0.
169	237	238	3	31	-0.	-0	-0	-0.	.21240	.97720	-0.	-0.
170	238	239	3	31	-0.	-0	-0	-0.	.21240	.97720	-0.	-0.
171	239	240	3	31	-0.	-0	-0	-0.	.21240	.97720	-0.	-0.
172	240	241	3	31	-0.	-0	-0	-0.	.21240	.97720	-0.	-0.
173	241	242	3	31	-0.	-0	-0	-0.	.21240	.97720	-0.	-0.
174	242	243	3	31	-0.	-0	-0	-0.	.21240	.97720	-0.	-0.
175	243	244	3	31	-0.	-0	-0	-0.	.21240	.97720	-0.	-0.
176	244	213	3	31	-0.	-0	-0	-0.	.21240	.97720	-0.	-0.
177	245	246	4	32	-0.	-0	-0	-0.	.20110	.97960	-0.	-0.
178	246	247	4	32	-0.	-0	-0	-0.	.20110	.97960	-0.	-0.
179	247	248	4	32	-0.	-0	-0	-0.	.20110	.97960	-0.	-0.
180	248	214	4	32	-0.	-0	-0	-0.	.20110	.97960	-0.	-0.
181	249	250	4	32	-0.	-0	-0	-0.	.19450	.98090	-0.	-0.
182	250	251	4	32	-0.	-0	-0	-0.	.19450	.98090	-0.	-0.
183	251	252	4	32	-0.	-0	-0	-0.	.19450	.98090	-0.	-0.
184	252	212	4	32	-0.	-0	-0	-0.	.19450	.98090	-0.	-0.
185	253	254	3	31	-0.	-0	-0	-0.	.19980	.97980	-0.	-0.
186	254	255	3	31	-0.	-0	-0	-0.	.19980	.97980	-0.	-0.
187	255	256	3	31	-0.	-0	-0	-0.	.19980	.97980	-0.	-0.
188	256	257	3	31	-0.	-0	-0	-0.	.19980	.97980	-0.	-0.
189	257	258	3	31	-0.	-0	-0	-0.	.19980	.97980	-0.	-0.
190	258	215	3	31	-0.	-0	-0	-0.	.19980	.97980	-0.	-0.
191	1	2	2	33	-0.	-0	-0	1.00000	-0.	-0.	-0.	-0.
192	3	4	2	33	-0.	-0	-0	1.00000	-0.	-0.	-0.	-0.
193	5	6	2	1	-0.	-0	-0	1.00000	-0.	-0.	-0.	-0.
194	7	8	2	33	-0.	-0	-0	1.00000	-0.	-0.	-0.	-0.
195	9	10	2	33	-0.	-0	-0	1.00000	-0.	-0.	-0.	-0.
196	11	12	2	33	-0.	-0	-0	1.00000	-0.	-0.	-0.	-0.
197	13	14	2	33	-0.	-0	-0	1.00000	-0.	-0.	-0.	-0.
198	15	16	2	33	-0.	-0	-0	1.00000	-0.	-0.	-0.	-0.
199	17	18	2	33	-0.	-0	-0	1.00000	-0.	-0.	-0.	-0.
200	19	20	2	33	-0.	-0	-0	1.00000	-0.	-0.	-0.	-0.
201	21	22	2	1	-0.	-0	-0	1.00000	-0.	-0.	-0.	-0.
202	23	24	2	33	-0.	-0	-0	1.00000	-0.	-0.	-0.	-0.
203	25	26	2	33	-0.	-0	-0	1.00000	-0.	-0.	-0.	-0.
204	27	28	2	33	-0.	-0	-0	1.00000	-0.	-0.	-0.	-0.
205	29	30	2	33	-0.	-0	-0	1.00000	-0.	-0.	-0.	-0.
206	31	32	2	33	-0.	-0	-0	1.00000	-0.	-0.	-0.	-0.
207	33	34	2	33	-0.	-0	-0	1.00000	-0.	-0.	-0.	-0.
208	35	36	2	33	-0.	-0	-0	1.00000	-0.	-0.	-0.	-0.
209	37	38	2	33	-0.	-0	-0	1.00000	-0.	-0.	-0.	-0.
210	39	40	2	33	-0.	-0	-0	1.00000	-0.	-0.	-0.	-0.
211	41	42	2	33	-0.	-0	-0	1.00000	-0.	-0.	-0.	-0.
212	43	44	2	33	-0.	-0	-0	1.00000	-0.	-0.	-0.	-0.
213	45	46	2	33	-0.	-0	-0	1.00000	-0.	-0.	-0.	-0.
214	47	48	2	33	-0.	-0	-0	1.00000	-0.	-0.	-0.	-0.
215	49	50	2	33	-0.	-0	-0	1.00000	-0.	-0.	-0.	-0.
216	51	52	2	33	-0.	-0	-0	1.00000	-0.	-0.	-0.	-0.
217	53	54	2	33	-0.	-0	-0	1.00000	-0.	-0.	-0.	-0.
218	55	56	2	1	-0.	-0	-0	1.00000	-0.	-0.	-0.	-0.
219	57	58	2	33	-0.	-0	-0	1.00000	-0.	-0.	-0.	-0.
220	59	60	2	33	-0.	-0	-0	1.00000	-0.	-0.	-0.	-0.

PROPERTIES AND DIMENSIONS OF THE ANALYTICAL MODEL

TABLE 2.1 A

(SHEET 10 OF 11)

ELEMENT	NODE I	NODE J	MATERIAL TYPE	ELEMENT TYPE	DEAD LOAD	END RELEASE CODE I	END RELEASE CODE J	DIRN COSINES OF LOCAL Y AXIS X	Y	Z	ECCENTRICITY I	ECCENTRICITY J
221	61	62	2	33	-0.	-0	-0	1.00000	-0.	-0.	-0.	-0.
222	63	64	2	33	-0.	-0	-0	1.00000	-0.	-0.	-0.	-0.
223	65	66	2	33	-0.	-0	-0	1.00000	-0.	-0.	-0.	-0.
224	67	68	2	33	-0.	-0	-0	1.00000	-0.	-0.	-0.	-0.
225	69	70	2	1	-0.	-0	-0	1.00000	-0.	-0.	-0.	-0.
226	71	72	2	33	-0.	-0	-0	1.00000	-0.	-0.	-0.	-0.
227	73	74	2	33	-0.	-0	-0	1.00000	-0.	-0.	-0.	-0.
228	75	76	2	33	-0.	-0	-0	1.00000	-0.	-0.	-0.	-0.
229	77	78	2	33	-0.	-0	-0	1.00000	-0.	-0.	-0.	-0.
230	79	80	2	33	-0.	-0	-0	1.00000	-0.	-0.	-0.	-0.
231	81	82	2	33	-0.	-0	-0	1.00000	-0.	-0.	-0.	-0.
232	83	84	2	33	-0.	-0	-0	1.00000	-0.	-0.	-0.	-0.
233	85	86	2	33	-0.	-0	-0	1.00000	-0.	-0.	-0.	-0.
234	87	88	2	33	-0.	-0	-0	1.00000	-0.	-0.	-0.	-0.
235	89	90	2	33	-0.	-0	-0	1.00000	-0.	-0.	-0.	-0.
236	91	92	2	33	-0.	-0	-0	1.00000	-0.	-0.	-0.	-0.
237	93	94	2	1	-0.	-0	-0	1.00000	-0.	-0.	-0.	-0.
238	95	96	2	33	-0.	-0	-0	1.00000	-0.	-0.	-0.	-0.
239	97	98	2	33	-0.	-0	-0	1.00000	-0.	-0.	-0.	-0.
240	99	100	2	33	-0.	-0	-0	1.00000	-0.	-0.	-0.	-0.
241	101	102	2	33	-0.	-0	-0	1.00000	-0.	-0.	-0.	-0.
242	103	104	2	33	-0.	-0	-0	1.00000	-0.	-0.	-0.	-0.
243	105	106	2	33	-0.	-0	-0	1.00000	-0.	-0.	-0.	-0.
244	107	108	2	1	-0.	-0	-0	1.00000	-0.	-0.	-0.	-0.
245	109	110	2	33	-0.	-0	-0	1.00000	-0.	-0.	-0.	-0.
246	111	112	2	33	-0.	-0	-0	1.00000	-0.	-0.	-0.	-0.
247	113	114	2	33	-0.	-0	-0	1.00000	-0.	-0.	-0.	-0.
248	115	116	2	33	-0.	-0	-0	1.00000	-0.	-0.	-0.	-0.
249	117	118	2	33	-0.	-0	-0	1.00000	-0.	-0.	-0.	-0.
250	119	120	2	33	-0.	-0	-0	1.00000	-0.	-0.	-0.	-0.
251	121	122	2	33	-0.	-0	-0	1.00000	-0.	-0.	-0.	-0.
252	123	124	2	33	-0.	-0	-0	1.00000	-0.	-0.	-0.	-0.
253	125	126	2	33	-0.	-0	-0	1.00000	-0.	-0.	-0.	-0.
254	127	128	2	33	-0.	-0	-0	1.00000	-0.	-0.	-0.	-0.
255	129	130	2	33	-0.	-0	-0	1.00000	-0.	-0.	-0.	-0.
256	131	132	2	33	-0.	-0	-0	1.00000	-0.	-0.	-0.	-0.
257	133	134	2	33	-0.	-0	-0	1.00000	-0.	-0.	-0.	-0.
258	135	136	2	33	-0.	-0	-0	1.00000	-0.	-0.	-0.	-0.
259	137	138	2	33	-0.	-0	-0	1.00000	-0.	-0.	-0.	-0.
260	139	140	2	33	-0.	-0	-0	1.00000	-0.	-0.	-0.	-0.
261	141	142	2	1	-0.	-0	-0	1.00000	-0.	-0.	-0.	-0.
262	143	144	2	33	-0.	-0	-0	1.00000	-0.	-0.	-0.	-0.
263	145	146	2	33	-0.	-0	-0	1.00000	-0.	-0.	-0.	-0.
264	147	148	2	33	-0.	-0	-0	1.00000	-0.	-0.	-0.	-0.
265	149	150	2	33	-0.	-0	-0	1.00000	-0.	-0.	-0.	-0.
266	151	152	2	33	-0.	-0	-0	1.00000	-0.	-0.	-0.	-0.
267	153	154	2	33	-0.	-0	-0	1.00000	-0.	-0.	-0.	-0.
268	155	156	2	33	-0.	-0	-0	1.00000	-0.	-0.	-0.	-0.
269	157	158	2	1	-0.	-0	-0	1.00000	-0.	-0.	-0.	-0.
270	159	160	2	33	-0.	-0	-0	1.00000	-0.	-0.	-0.	-0.
271	161	162	2	33	-0.	-0	-0	1.00000	-0.	-0.	-0.	-0.

PROPERTIES AND DIMENSIONS OF THE ANALYTICAL MODEL

TABLE 2.1 A

(SHEET 11 OF 11)